Optimization of Radially Heterogeneous 1000-MW(e) LMFBR Core Configurations

Volume 1: Design and Performance of Reference Cores

EPRI

EPRI NP-1000
Volume 1
Project 620-25
Interim Report
November 1979

MASTER

RECEIVED BY TIC APR 1 1980

Keywords:
LMFBR Core
HCDA
Heterogeneous Core
No Void Coefficient
Bull's-Eye Core

Prepared by
Argonne National Laboratory
Argonne, Illinois

DISTRIBUTION OF THIS DOCUMENT IS UNLIMITED

ELECTRIC POWER RESEARCH INSTITUTE

DISCLAIMER

This report was prepared as an account of work sponsored by an agency of the United States Government. Neither the United States Government nor any agency Thereof, nor any of their employees, makes any warranty, express or implied, or assumes any legal liability or responsibility for the accuracy, completeness, or usefulness of any information, apparatus, product, or process disclosed, or represents that its use would not infringe privately owned rights. Reference herein to any specific commercial product, process, or service by trade name, trademark, manufacturer, or otherwise does not necessarily constitute or imply its endorsement, recommendation, or favoring by the United States Government or any agency thereof. The views and opinions of authors expressed herein do not necessarily state or reflect those of the United States Government or any agency thereof.

DISCLAIMER

Portions of this document may be illegible in electronic image products. Images are produced from the best available original document.

Optimization of Radially Heterogeneous 1000-MW(e) LMFBR Core Configurations
Volume 1: Design and Performance of Reference Cores

NP-1000, Volume 1
Research Project 620-25

Interim Report, November 1979

Prepared by

ARGONNE NATIONAL LABORATORY
Applied Physics Division
EBR-II Division
9700 South Cass Avenue
Argonne, Illinois 60439

Principal Investigators
W. P. Barthold
Y. Orechwa
S. F. Su
E. Hutter
R. V. Batch
J. C. Beitel
R. B. Turski
P. S. K. Lam

DISCLAIMER

This book was prepared as an account of work sponsored by an agency of the United States Government. Neither the United States Government nor any agency thereof, nor any of their employees, makes any warranty, express or implied, or assumes any legal liability or responsibility for the accuracy, completeness, or usefulness of any information, apparatus, product, or process disclosed, or represents that its use would not infringe privately owned rights. Reference herein to any specific commercial product, process, or service by trade name, trademark, manufacturer, or otherwise, does not necessarily constitute or imply its endorsement, recommendation, or favoring by the United States Government or any agency thereof. The views and opinions of authors expressed herein do not necessarily state or reflect those of the United States Government or any agency thereof.

Prepared for

Electric Power Research Institute
3412 Hillview Avenue
Palo Alto, California 94304

EPRI Project Manager
Edward L. Fuller
Nuclear Power Division

DISTRIBUTION OF THIS DOCUMENT IS UNLIMITED

ORDERING INFORMATION

Requests for copies of this report should be directed to Research Reports Center (RRC) Box 50490, Palo Alto, CA 94303, (415) 961-9043 There is no charge for reports requested by EPRI member utilities and affiliates, contributing nonmembers, U S utility associations, U S government agencies (federal, state, and local), media, and foreign organizations with which EPRI has an information exchange agreement On request, RRC will send a catalog of EPRI reports

[redacted]

EPRI authorizes the reproduction and distribution of all or any portion of this report and the preparation of any derivative work based on this report in each case on the condition that any such reproduction distribution and preparation shall acknowledge this report and EPRI as the source

NOTICE

This report was prepared by the organization(s) named below as an account of work sponsored by the Electric Power Research Institute Inc (EPRI) Neither EPRI members of EPRI the organization(s) named below nor any person acting on their behalf (a) makes any warranty or representation express or implied with respect to the accuracy completeness or usefulness of the information contained in this report or that the use of any information apparatus method or process disclosed in this report may not infringe privately owned rights or (b) assumes any liabilities with respect to the use of or for damages resulting from the use of any information apparatus method or process disclosed in this report

Prepared by
Argonne National Laboratory
Argonne, Illinois

EPRI PERSPECTIVE

PROJECT DESCRIPTION

A hypothetical core disruptive accident (HCDA) and the impact it might cause, particularly on the underside of the head of a liquid metal fast breeder reactor (LMFBR) is a controversial issue. The debate is how much capability for safe absorption of impact energy must be designed into the reactor vessel and head. Neutronics and thermo-hydraulics analysts and core designers are the ones to whom this report is directed. Reactor vendors of early large-size LMFBRs can use this work as a sound starting base for improvements. The immediate application of this work is to provide the core design for the prototype large breeder reactor design studies conducted under EPRI Research Project 620.

This work, "Optimization of Radially Heterogeneous 1000-MW(e) LMFBR Core Configurations," is presented in four volumes. These are as follows:

- Volume 1: Design and Performance of Reference Cores
- Volume 2: Appendix A--Design Assumptions and Constraints
  Appendix B--Radially Heterogeneous Core Configurations
- Volume 3: Appendix C--Optimization of Core Performance Parameters
- Volume 4: Appendix D--Optimization of Core Configurations
  Appendix E--Component Designs

PROJECT OBJECTIVES

The objective of the work reported here is to make the characteristics of large cores such that the impact energy of an HCDA would approach zero. Without special provisions, an LMFBR vessel and head will have greater impact resistance than would be needed by such a core, thus relieving the controversy and assuring a safe design feature.

This report presents the results of the second of three phases of effort to optimize a radial heterogeneous 1000-MW(e) LMFBR core design that will minimize energetics in an HCDA and yet have highly desirable breeding gain and core performance. The final results of the three phases are intended to establish a reference core design that will be safe, licensable, reliable, and efficient.

PROJECT RESULTS

Although not reflected in the work reported, doubling time is not the simple figure of merit that it originally appeared to be. A minimum compound system doubling time is quite desirable when the U.S. utility industry is plutonium limited, i.e., all of the available Pu (owned by the utilities) is being fully utilized in breeder plants. However, this is not the case and probably will not be true until well after the year 2010. Emphasis will be shifted to maximize total net plutonium produced rather than doubling time. In-core inventory will optimize at a somewhat higher quantity of Pu.

As stated in the text there are too many uncertainties in the fuel costs to make them a figure of merit between designs. However, on a consistent basis of estimating, the promising core designs show only small differences in costs. It is highly probable that costs can be significantly improved over those listed in the text.

Edward L. Fuller, Project Manager
R. K. Winkleblack, Program Manager
Nuclear Power Division

ABSTRACT

A parameter study was conducted to determine the interrelated effects of: loosely or tightly coupled fuel regions separated by internal blanket assemblies, number of fuel regions, core height, number and arrangement of internal blanket subassemblies, number and size of fuel pins in a subassembly, etc. The effects of these parameters on sodium void reactivity, Doppler, "incoherence," breeding gain, and thermohydraulics were of prime interest. Trends were established and ground work laid for optimization of a large, radially-heterogeneous, LMFBR core that will have low energetics in an HCDA and will have good thermal and breeding performance.

Table of Contents

List of Figures

List of Tables

I. SUMMARY

In unprotected loss-of-flow transients in large homogeneous LMFBRs, high ramp rates from sodium voiding can result in energy releases that may challenge the integrity of the containment. Thus there is a strong incentive for designing large LMFBRs that have a low sodium void reactivity. Heterogeneous designs that consist of successive radial core and blanket zones are most promising. Based on the results of previous safety analyses of heterogeneous cores, a sodium void reactivity of $2.50 or less is considered sufficient to assure that the reactor will not become super-prompt critical. The sodium voided from the core is limited to that coming from the core fuel assembly and upper axial blanket regions. By properly arranging and sizing the core and blanket zones in such designs, a low value of sodium void reactivity can be obtained. The purpose of this research project was to determine what "properly arranged and sized core and blanket zones" meant in 1000 MWe LMFBRs and to develop optimum core configurations in regard to sodium void reactivity and compound system doubling time. During the course of this investigation the following questions had to be answered:

1. Should the different core regions be separated by blanket regions with a thickness of one or less row of blanket assemblies (tightly coupled) or more than one row (loosely coupled)?
2. Should the center of the reactor be a blanket or core fuel region? How thick should this region be?
3. Should the reactor have 2, 3, or more core regions?
4. Is the reduction in core height an effective means to lower the sodium void reactivity?
5. Is it more important to add blanket assemblies to the reactor core to lower sodium void reactivity or has a change in configuration a greater impact while maintaining the number of core fuel and blanket assemblies?
6. How important are the selection of the number of fuel pins per assembly and fuel pin diameter in regard to lowering sodium void reactivity?

Very early results showed that it was easy to construct reactors which had the same number of fuel and internal blanket assemblies but which differed as much as a factor of two in sodium void reactivity. This placed even greater emphasis on the optimization of the core layout.

The optimization of the core layout proceeded in three steps. Each step required more detailed analysis but yielded also more information.

The first step was a screening of the various means to lower sodium void reactivity. At the end of the screening phase, six basic configurations were selected for further design and performance analysis and optimization. The major criterion for the selection of those six configurations was the achievable sodium void reactivity. However, both doubling time and power shape sensitivity were also considered. The second step was a sub-optimization of those six configurations with respect to fuel pin diameter and doubling time. The figures of merit in this optimization were (a) sodium void reactivity, (b) doubling time, (c) breeding ratio, (d) specific inventory, and (e) maximum change in linear heat rating in fuel assemblies over one cycle. At the completion of the sub-optimization, two core layouts and specific design parameters were selected. These configurations were optimized in the third step, the optimization phase. Upon completion of this phase, two optimized configurations were selected for detailed design and performance analysis. After this design and performance analysis was completed one core design was recommended for conceptual design.

The screening phase (first step) dealt with a comparative study of tightly and loosely coupled heterogeneous center core and center blanket configurations. Earlier assembly designs for fuel and blankets were used; these had fuel, structure and coolant volume fractions of 0.3817/0.1689/0.3976 and 0.5664/0.1267/0.2438, respectively. The assembly size, however, was changed as the number of fuel pins per assembly changed.

Throughout this study the tightly and loosely coupled configurations were kept as separate as possible in order to identify more clearly the generic issues which must be taken into account when constructing a radially heterogeneous core. Although, as the final configurations of this study show, the optimum cores with respect to the design constraints are a hybrid of tightly and loosely coupled, the following conclusions were instrumental in arriving at these configurations.

1. With respect to achieving a low sodium void reactivity and a low doubling time neither center core nor center blanket configurations show a clear advantage.

2. It is very difficult to construct a "reasonable" tightly or loosely coupled, center blanket or center core configuration with a \$2.00 sodium void reactivity at the EOEC. On the other hand cores with a \$3.00 limit on the sodium void reactivity can be readily constructed.
3. Center blanket configurations are less sensitive with regard to power peaking than center core configurations. In addition, 2-core zone configurations show a better burnup vs. power peaking peformance than 3-core zone configurations. When a single enrichment is desirable a center core configuration leads to excessively high power peaking.
4. The sodium void reactivity contribution from the internal blanket assemblies on an assembly basis is significantly higher for tightly coupled cores than for loosely coupled cores.
5. Height reduction can be an effective means for reducing the sodium void reactivity for both tightly coupled and loosely coupled cores.
6. In general, primarily the configuration and not the number of internal blanket assemblies determines the sodium void reactivity.
7. In tightly coupled cores rearranging internal blankets to change the number of core zones does not significantly affect the sodium void reactivity.
8. Ranking configurations according to achievable sodium void reactivity favors loosely-coupled cores.
9. Ranking configurations according to breeding performance and power peaking sensitivity favors tightly-coupled cores.
10. Recommended for further analysis were the following basic configurations:

Coupling	Configuration	No. of Core Zones	No. of Pins/Fuel Assembly
LC	CB	2	271
LC	CB	3	271
LC	CC	3	271
TC	CB	3	331
TC	CB	4	331
TC	CC	4	331

TC - tightly coupled, LC - loosely coupled, CB - center blanket
CC - center core

During the sub-optimization phase (step 2) those six configurations were analyzed in more detail. Core height and fuel pin diameter were varied and for each configuration, detailed fuel assembly designs were developed which were all subject to the following basic design assumptions:

Reactor outlet temperature:	875°F
Reactor coolant temperature rise:	280°F
Fuel bundle pressure drop:	$\leq$ 75 psi
Fuel p/d ratio:	$\geq$ 1.18
Cladding thickness/fuel O.D.:	0.05
Peak linear heat rating:	13.4 kw/ft
Maximum allowable stress in duct wall:	18,000 psi

The performance analysis of a total of 36 cores which differed with respect to neutronic coupling, core height, and fuel pin diameter allowed the following conclusions:

1. To achieve sodium void reactivities of $2.50 or less, tightly coupled cores require core heights of 36 inches or less. For the loosely coupled cores, heights of less than 48 inches are required.
2. As fuel pin size increases, the sodium void reactivity decreases.
3. The tightly coupled cores have generally lower doubling times than the loosely coupled cores.
4. Among the tightly and loosely coupled cores, the fuel pin sizes of 0.24 inches and 0.26 inches, respectively, show the lowest doubling times.
5. For the cores analyzed, no clear advantage in regard to specific inventory and sodium void reactivity can be identified for either tightly or loosely coupled systems.
6. Because of the high power swing over an equilibrium cycle observed for the center core configurations, they were eliminated from further analysis. Earlier analyis had shown that those configurations showed also a higher sensitivity in power peaking for small enrichment split changes. They always performed equal to or worse than the center blanket configuration.
7. Loosely coupled systems show a greater power swing than tightly coupled systems.

8. A loosely coupled and a tightly coupled 3-core zone center blanket configuration with 271/331 fuel pins per assembly, core height of 40/36 inches and 0.26/0.24 in. fuel pins, respectively, were chosen for further optimization.

During the optimization phase (step 3) the core layouts of these two candidate cores were modified to see if any improvement could be made with regard to breeding performance, power peaking, power shape sensitivity, power swing, etc. The pin diameters for the respective cores remained unchanged during the optimization of the configurations. The modification for the 40 in. core concentrated on tightening the coupling and at the same time reducing the core region sizes to keep the sodium void reactivity below $2.50. The modifications for the 36 in. core emphasized the reduction of the center blanket size and the creation of a broken ring-arrangement of internal blanket assemblies to improve the power peaking performance and to simplify the reactivity control.

Upon completion of this task the following conclusions could be drawn:

1. The design constraints of
   a. ≤ $2.50 sodium void reactivity
   b. ≤ 15 year doubling time

   are very restrictive.
2. The selection of configuration is very important in regard to
   a. sodium void reactivity
   b. power shape sensitivity
   c. power swing
   d. burnup swing and control requirements
3. The following performance parameters are also affected by the configuration selection but to a lesser extent
   a. specific inventory
   b. breeding ratio
   c. doubling time
4. For a given core height, tightly coupled configurations generally perform better than loosely coupled configurations with respect to the performance parameters listed in 2 except for the sodium void reactivity.
5. The region size split among the three core regions is important for sodium void reactivity reductions.
6. The highest power swing over a burnup cycle exists in the outermost core region. This region has always a negative power swing.

7. The introduction of isolated internal blanket assemblies in the outermost core region
   a. lessens the need for loosely coupled systems to achieve a given sodium void reactivity
   b. reduces the power shape sensitivity
   c. leads to lower power and burnup swings
8. Broken ring arrangements are better than closed ring arrangements because
   a. there is better coupling between regions
   b. flux peaks are created which
      - determine the location of control rods
      - enhance control rod worth
9. Control rod positioning is very important
   a. burnup can be controlled very efficiently by control rods located in the outermost core region because
      - the outermost core region is the largest core region which makes a symmetrical arrangement less difficult
      - the withdrawal of control rods counteracts the drop in assembly power observed in cores burned without control
   b. control rods located next to an internal blanket region have a lower worth than control rods surrounded by fuel assemblies except for the outermost core region where for some configurations the worth of the control rod can be higher when placed next to an internal blanket assembly
10. While there is the potential for arranging the internal blanket assemblies such that only one core enrichment is needed, no extensive efforts were undertaken at this stage to develop such a core because of
    a. calculational uncertainties
    b. having different enrichment zones is a more conservative approach
11. The choice of calculational techniques is very important
    a. r-z models are good for
       - inventory calculation
       - breeding performance calculation
       - sodium void reactivity estimates
    b. hexagonal geometry models are needed for the calculation of
       - all power shape information
       - control rod worth

The two most promising core configurations chosen are both tightly coupled, although one evolved from a loosely coupled core. Both cores showed low power shape sensitivities to small enrichment split changes and low power and burnup swings and good power peaking characteristics.

A complete nuclear analysis of these two cores (derived from a loosely coupled configuration/derived from a tightly coupled configuration) determined the fissile inventories (4268.4/4213.4 kg at BOEC), burnup (83.90/100.7 MWd/t peak), reactivity swings (0.49/1.8 %Δk), control rod requirements (24/36 rods), total control rod worths (7.29/8.76 %Δk total), power and flux distributions for different control insertion patterns, the breeding peformance (15.7/15.3 yrs. CSDT), the safety parameters, such as sodium void reactivity ($2.38/$2.23 at EOEC), isothermal Doppler coefficients for both sodium-in (45.6/46.1 T dk/dT x 10^{-4} core at EOEC), and sodium-out conditions (28.6/28.2 dk/dT x 10^{-4} core at EOEC), and the transient behavior which shows very little space-dependence during a 60¢ reactivity step on a ramp insertion.

The thermal-hydraulic analysis dealt with the calculation of coolant flow distribution, temperature distributions for coolant, cladding and duct, orificing schemes, fission gas plenum pressures, and assembly pressure drop. Emphasis was placed on keeping peak clad temperatures low and producing a uniform assembly coolant exit temperature. The orificing strategy employed equalized the maximum 2σ cladding midwall temperature at the beginning-of-life for the core and the end-of-life for the blankets in all orificing zones. The resulting peak 2σ clad midwall temperatures consistent with an inlet temperature of 595°F and a mixed mean outlet temperature 875°F was (1200.4°F/1149.9°F).

Fuel assemblies for the two final cores were designed in detail taking into account duct rounding due to creep (0.140/0.133 in.), dilation due to swelling (0.0276/0.0707 in.), and peak stresses in duct corners (33,832/34,222 psi). Finally, the design and analysis cores concluded with fuel cycle cost calculations yielding (9.2/9.9 mils/kWh).

Recommended for conceptual design is the 40 in. high core with 0.26 fuel pins. The main reason for this selection is the low number of control rods needed.

1.0 INTRODUCTION

This report summarizes the work under EPRI contract No. RP620-25 on Task 1 of "Optimization of Safety and Breeding Characteristics of the PLBR Phase A Core Design" covering the period from May 1978 to December 1978.

1.1 DESIGN OBJECTIVE

The objective of the core design and analysis efforts is to develop practical design concepts of fuel assemblies, blanket assemblies, control assemblies and removable shield pieces as well as core, blanket, shield and restraint arrangements that are characterized by:

a. a doubling time of $\leq$ 15 years
b. a sodium void reactivity of $\leq$ \$2.50 for voiding the flowing sodium from all fuel zones
c. incoherence in boiling that contributes to ultimate safety
d. a negative prompt power coefficient during approach to power as well as at high powers
e. design conservatism in regard to maximum clad temperature, peak linear power, low power peak to average ratio, small outlet temperature gradients
f. economical fabrication cost

The design which has been developed and will be refined is a way to accomplish the objectives. It is expected to establish feasibility and a "yardstick" against which other designs can be measured.

The first task of this design and optimization effort was to develop a core configuration and determine specific core design parameters (core height, fuel pin and assembly design, environment for operation, etc.) which meet the design objectives. This preconceptual design phase will be followed by a conceptual design effort.

1.2 OUTLINE OF STUDY

The primary goal of the preconceptual design effort was to develop a core configuration and to determine core design parameters consistent with the overall design objectives. The study was very comprehensive, starting with an optimization procedure that led to selection of two designs for detailed analysis. This process led to many conclusions and recommendations, which are listed in Section 2. The methods used during the optimization and preconceptual design phases differred substantially, depending upon the goals for the various tasks. Section 3 describes the design approach, methodology, and optimization approach. The basis for the design was provided by design assumptions and constraints similar to those used in the Proliferation Resistant Core Design Study. Since there is a multitude of heterogeneous core arrangements, a procedure was designed in order to eliminate undesirable layouts, and identify the most promising layouts. A classification of different designs was made by dividing the possible arrangements into center core and center blanket configurations. The subdivison of these configurations into tightly and loosely coupled cores followed. This introduces an arbitrariness which is unavoidable since there is neither the tightly coupled core nor the loosely coupled core. There are differences in the degree of coupling and the assignment of "loosely" or "tightly" to measure coupling is by necessity arbitrary. In this study, cores with internal blankets of more than one row thickness are called loosely coupled. If the thickness of the internal blanket regions is one row or less, those cores are called tightly coupled.

At the beginning of the study an assessment was made of the various means of reducing sodium void reactivities in radially heterogeneous cores. Both tightly and loosely coupled systems with center blanket or center core zones were investigated. Variables in this study were the number and size of core regions, the number of internal blanket assemblies, core height, coupling, and the number of fuel pins per assembly. Upon completion of the study, six basic core configurations were selected, which were then optimized with respect to fuel pin diameter and core height. The two most promising tightly and loosely coupled cores were selected for further analysis.

The two most promising configurations were modified to see if it was possible to further improve the performance characteristics by changing the core layout slightly. The results of these analyses led to two cores which showed optimum performance. One core was derived from the loosely coupled systems and the other was derived from the tightly coupled systems. Both resultant cores are tightly coupled. The results of the performance analysis for those cores are shown in Section 4.0 of the main report.

The nuclear design effort covered the determination of core layout, fissile inventory, burnup and reactivity swing, control requirements, power and flux distribution, breeding performance, safety parameters, kinetics parameters and transient response. The details of this analysis are shown in Section 4.1.

The thermal-hydraulic analyses dealt with the calculation of coolant flow distribution, temperature distribution for coolant, cladding and duct, orificing schemes, fission gas plenum pressures, and assembly pressure drop. Emphasis was placed on keeping peak clad temperatures low and producing a uniform assembly coolant exit temperatures. Details of this analysis are shown in Section 4.2.

The results of the mechanical design analyses are detailed in Section 4.3. They encompass fuel pin design, assembly design and duct life analysis. Results of both bundle-duct and cumulative damage fraction analyses are reported.

The core design and analysis activities are concluded by fuel cycle cost calculations which are reported in Section 4.4.

An evaluation of center core vs. center blanket configuration, loosely vs. tightly coupled cores and tall vs. short cores is presented in Section 5.0.

The basis for this evaluation is presented in Appendices B, C, and D. A complete list of design assumptions and constraints is given in Appendix A. Details of the analysis leading to selection of the six basic core configurations are presented in Appendix B. Appendix C presents the results of the core height and pin diameter optimization of the six basic core configurations and the selection process leading to the choice of the two most promising tightly and loosely coupled cores. Details of the final step of configuration optimization of these most promising cores are presented in Appendix D.

The results of generic hardware design activities including design options for assembly keys, lower grid design option, mixing promoters in assemblies etc. are shown in Appendix E.

2.0 CONCLUSIONS AND RECOMMENDATIONS

2.1 CONCLUSIONS

Based on the analysis presented in this report, the following conclusions can be drawn:

1. Low sodium void reactivities can be achieved by
   a. decoupling
   b. core height reduction
   c. adding blanket assemblies to increase the parasitic absorptions
2. The design constraints of
   a. $\leq$ \$2.50 sodium void reactivity
   b. $\leq$ 15 year doubling time
   c. no significant power shape sensitivity

   are very restrictive
3. The arrangement of internal blanket assemblies is very important with regard to
   a. sodium void
   b. burnup swing
   c. doubling time
4. Tightly coupled cores perform better than loosely coupled cores regarding
   a. doubling time
   b. specific inventory
   c. power shape sensitivity
5. Center blanket configuration perform better than center core configuration because
   a. power peaking is less sensitive to
      - enrichment
      - burnup
   b. center core regions have very high power swings
   c. there is greater flexibility in core arrangement
   d. fewer discriminator zones are needed.
6. Three core regions are sufficient to meet design constraints
   a. four or more core regions increase complexity without improving performance

b. two core regions cannot meet all design constraints

7. Broken ring arrangements are better than closed ring arrangements because
   a. there is better coupling between regions
   b. flux peaks are created which
      - determine the location of control rods
      - enhance control rod worth

8. Control rod positioning is very important
   a. burnup can be controlled very efficiently by control rods located in the outermost core region because
      - the outermost core region is the largest core region, which makes a symmetrical arrangement less difficult
      - the withdrawal of control rods counteracts the drop in assembly power observed in cores burned without control
   b. control rods located next to an internal blanket region have a lower worth than control rods surrounded by fuel assemblies, except for the outermost core region, where for some configurations the worth of the control rod can be higher when placed next to an internal blanket assembly.

9. While there is the potential for arranging the internal blanket assemblies such that only one core enrichment is needed, no extensive efforts were undertaken at this stage to develop such a core because
   a. of calculational uncertainties
   b. having different enrichment zones is a more conservative approach

10. Meaningful figures of merit are
   a. sodium void reactivity
   b. doubling time
   c. breeding ratio
   d. specific inventory
   e. peak burnup
   f. damage fluence
   g. maximum assembly power change during life and over one cycle
   h. sensitivity of power shape
   i. burnup swing and control rod requirements

   Fuel cycle cost is not a meaningful figure of merit at present, although generic trends in fuel cycle cost should guide the design.

11. The choice of calculational techniques is very important
   a. r-z models are good for
      - screening

- inventory calculation
- breeding performance calculation
- sodium void reactivity estimates

b. hexagonal geometry models are needed for the calculation of
- enrichment split
- all power shape information
- control rod worth
- accurate sodium void reactivities

12. Between the two configurations which were analyzed in detail there were only small difference with respect to the different figures of merit except for the control requirements

2.2 RECOMMENDATIONS

Upon completion of the pre-conceptual activities presented in this report, the following recommendations are made:

1. The following core configuration is recommended for further design analysis
   a. tightly coupled
   b. center blanket
   c. 3-core region
   d. 40 inch core height
   e. 0.26 inch fuel o.d.
   f. 271 pins per fuel assembly
2. Proceed with conceptual design and analysis
   a. nuclear, thermal-hydraulic and mechanical design analyses
      - assembly and fuel pin design
      - core layouts
      - breeding performance
      - safety parameters
      - power distribution and sensitivities
      - temperature
      - orificing
      - cladding
      - duct
      - coolant
      - pin and assembly life
      - core restraint and seismic analyses
      - fuel management
      - fuel cycle cost assessment and optimization

b. trade-off and sensitivity analyses
   - number of enrichment zones versus power peaking versus fuel life
   - number of enrichment zones versus number of orificing zones for a fixed number of discriminating zones
   - axial and radial blanket thickness versus shield
   - performance vs. design parameter changes
   - performance vs. calculational methods

c. transient and safety analyses
   - operational transients
   - design-limiting transients
   - accident analysis

d. startup analysis
   - transition first core-equilibrium core
   - temperature

e. power shape and reactivity control

f. instrumentation needs

g. component designs
   - lower inlet plenum
   - assembly keys
   - assembly design (fuel, blanket, shield, control)
   - fuel pin
   - core restraint system
   - upper internals

3. Assess calculational methods and data

   a. nuclear analyses

   b. thermal-hydraulic analyses

   c. mechanical analyses

   d. results of critical experiments

3.0 DESIGN ENVIRONMENT

3.1 DESIGN GROUNDRULES

The reactor net electric power is in the 1000 MWe class. The reactor inlet temperature is 595°F and the reactor outlet temperature is 875°F. The resulting thermal efficiency is 0.316. The core layouts are those of heterogeneous reactors. Details of the design assumptions and constraints are listed in Appendix A. They cover:

1. Fuel assembly parameters
2. Blanket assembly parameters
3. Flow parameters
4. Limiting conditions
5. Material properties
6. Physics parameters
7. Fuel management
8. Economic parameters
9. Figures of merit

The hot channel factors used in this study are those developed for CRBRP. They are different for fuel and blanket assemblies. The structural material used in this study is an improved CW316SS similar to the N-lot stainless steel. In line with the design conservatism employed in this study the design was not pushed to every limit specified in the design assumptions and constraints. Examples for the conservatism in the selection of design parameters are bundle pressure drop (75 psi instead of 90 psi), linear heat rating of the reference design (less than 13.5 kW/ft instead of 15 kW/ft).

3.2 DESIGN APPROACH

The design analysis efforts consisted of a preliminary set of analyses and then a final analysis of two designs.

3.2.1. Preliminary Analyses

The purpose of all preliminary analyses was to narrow down the multitude of design options to two designs which then would be analyzed in detail. This process of narrowing down design options was very complex and extended over several steps. First the means to reduce sodium void reactivity in radially heterogeneous cores were investigated. This effort covered loosely and tightly coupled center core and center blanket configurations. The design modifications were developed by changing:

- number of core regions
- degree of coupling
- size of center blanket regions
- size of center core regions
- core height
- number of fuel pins per assembly
- number of fuel assemblies per core region

Details of this analyses are reported in Appendix B.

Upon completion of these analyses, six basic heterogeneous configurations were identified. They were three tightly coupled systems and three loosely coupled systems. Among both types of configurations were one center core configuration and two center blanket configurations. For the tightly coupled systems the center blanket configurations had either three or four core zones compared to two or three for the loosely coupled systems. The purpose of the analysis that followed was to determine optimum combination of fuel pin size, core height and core configuration. Since the power level was maintained at approximately 1000 MWe any change in core height required a change in core layout. For tightly coupled cores, the core heights selected were 32 inches and 36 inches. The fuel pin diameters selected were 0.24 inch, 0.26 inch and 0.28 inch. For the loosely coupled cores, the chosen core heights were 40 inches and 48 inches with fuel pin diameters of 0.26 inch, 0.28 inch, and 0.30 inch.

After completion of these analyses the two most promising cores, one tightly and the other loosely coupled, were selected. While the previous step in the preliminary analysis aimed mostly at an optimization of fuel pin diameter, core height, and an elimination of less promising core concepts (see Appendix C for details) the next step in the analysis attempted to optimize the core configuration. This was done by leaving the basic core configuration the same, i.e., a center blanket configuration with three core zones, but changing the detail of the assembly arrangements. After completion of the analysis, two core configurations with specific design parameters were selected for detailed performance analysis.

3.2.2 Final Design Analysis

After completion of the preliminary analyses two promising configurations were identified with core heights of 36 inches and 40 inches and fuel pin sizes of 0.24 inch and 0.26 inch, respectively. There were more than those two configurations which showed good performance. Three of the tightly coupled cores showed approximately the same performance. The core selected was the one which had the lowest sodium void reactivity ($2.23) and a low doubling time (15.3 years). Among the cores derived from the loosely coupled systems were several arrangements which showed low sodium void reactivity and also low doubling time. The core finally selected was synthesized from cores which had been analyzed during the preliminary analyses.

The final analysis encompassed nuclear, thermal-hydraulic and mechanical design analysis. This analysis was subject to the design assumptions and constraints outlined in Appendix A. Upon completion of this analysis, a reference design was recommended for conceptual design analysis.

3.3 OPTIMIZATION

3.3.1 Configuration

The optimization of the core configuration was constrained by the $2.50 sodium void reactivity limit. Only configurations which were able to meet this limit were analyzed in more detail. Among those configurations, the major criteria for the optimization were (1) the sensitivity of the power shape to slight changes in enrichment split and (2) the maximum power swing in a fuel assembly over a burnup cycle. Specific inventory, breeding ratio and doubling times were considered also in this optimization process but these figures of merit are less important than power shape sensitivity and power swing. The latter two performance characteristics relate to potential thermal hydraulic and subsequent safety problems. Since enrichment specifications have certain tolerances, these tolerances can be translated into a possible enrichment split uncertainty. If minor changes in enrichment split cause large changes in the peak power density, this leads to excessively high sodium and clad temperatures and possible pin failure. If this effect is taken into consideration in the design of the fuel assembly, it requires increased coolant flow through those assemblies which would be affected in case the enrichment split for the fuel as loaded was not at its nominal value. The possible undercooling on the other hand, raises peak clad temperature.

Another aspect of the sensitivity of the power shape to enrichment split changes relates to the enrichment split change due to burnup. Very delicate control rod insertion patterns would be required to control not only the reactivity change but also a highly sensitive power shape. Therefore, even though a quantitative description of the limiting power shape sensitivity is not possible at the time, the less sensitivity a configuration shows the better.

The same qualitative description applies to the power swing over a burnup cycle. The larger the power swing is over a cycle the higher is the required overcooling and the higher are the clad temperatures. Therefore, the smaller the power swing the better the configuration.

3.3.2 Design Parameters

The optimization of design parameters was subject to two constraints. For one, the core configuration had to meet the $2.50 sodium void reactivity criterion. Secondly, the configuration had to show low power shape sensitivity and a low power swing. The criteria for the optimization of design parameters were then in their order of importance:

- doubling time
- specific inventory
- control system simplicity

While the first two criteria are self-explanatory, the last criterion relates essentially to the control requirements. For example, a small pin design might yield a low specific inventory and also a low doubling time. However, the small fuel pin size might also lead to a very high burnup swing thus requiring a very large number of control assemblies. In this case, design trade-offs have to be considered. If doubling time and specific inventory are the same for several designs then the design with the least control requirements would be preferred if the reduced control requirements can also be translated into a reduction of the number of control assemblies. Because of the symmetry requirements this reduction might not always be possible. In this case that design is preferred which perturbs the power shape the least during a cycle.

Fuel cycle cost was used as another figure of merit. The significance was not the actual mills/kWh data but the trend in fuel cycle cost resulting from a design change. The current uncertainties in fuel cycle cost data do not render fuel cycle cost to be a meaningful figure of merit in absolute terms.

3.4 METHODOLOGY

Both detailed rigorous methods as well as approximate methods were employed in the design analyses presented in the report. Up to the selection of the reference design, approximate methods dominated the nuclear and thermal-hydraulic design analysis. For the final design analyses, the more detailed rigorous methods were used for both nuclear and thermal design. The nuclear analysis was based upon NSMH properties with minor modifications. The irradiation induced swelling correlation is derived from the NSMH Rev. 7 correlation by increasing the incubation period τ from 6.3 to 9.0. The steady-state swelling rate R is reduced to 0.7 R. The irradiation induced creep calculation is based upon the nominal proposed NSMH Rev. 4 correlation using only 70% of the steady-state swelling rate and $\tau = 9.0$. The stress rupture properties for steady-state analysis are the ones for nominal unirradiated N-lot steel.

3.4.1 Design Analysis Flow Sheet

The design analysis flow sheet is presented in Fig. 1. It shows schematically the various steps in the design evolution.

Performance Estimates: Estimates are required on clad and duct temperatures, fluence and power distribution.

Fuel Pin Design: Based on the design groundrules, the following fuel pin design parameters are fixed: cladding o.d., cladding thickness, fuel smear density, peak linear heat rating, plenum location and length. Active core length and axial blanket thicknesses are selected. CDF is estimated.

Fuel Assembly Design (NIFD Code): The following design parameters are calculated: duct diameter, duct wall thickness, creep and swelling dilation of the duct as a function of axial position, fuel pitch/diameter ratio, assembly pitch, pressure drop, spacer wire thickness. The code furthermore calculates bundle-duct-interaction (BDI), number of subassemblies required, flow requirements, as well as the following blanket assembly parameters: pin diameter, pitch-to-diameter ratio, wire thickness, assembly dimensions.

Preliminary Neutronics and T&H Design (SYNBURN and REBUS Codes): For r-z core models, the SYNBURN and REBUS codes calculate the following parameters: specific fuel inventory, burnup swing, burnup, fluence, breeding performance, power distribution, mass balances. Based on these results, improved estimates are derived for blanket overcooling, clad and duct temperatures.

Final Neutronics and T&H Design (REBUS, DIF2D, PARC1D, PARC2D, CORE-3D, FLORF, ENERGY): Determined are: detailed core layout and control system layout, control rod worth, breeding performance, inventories at beginning of life (BOL), beginning of equilibrium cycle (BOEC), end of equilibrium cycle (EOEC), power distribution, burnup swing, burnup, Doppler coefficient, sodium void coefficient. The T&H analyses cover the following subjects: orificing, maximum coolant velocity, maximum pressure drop, flow distribution, core-wide clad, duct and coolant temperatures.

Remaining Performance Analyses (FX2, COST, ORIGEN, CAFAIL): The remaining analyses cover transient analyses, fuel cycle cost calculations, fission product decay heat calculations and CDF calculations.

3.4.2 Computational Methods

In the following, the calculational methods used for design analysis will be described briefly.

The MC^2-2-SDX code system was used to determine heterogeneously and homogeneously self-shielded nuclear cross sections for core and blanket regions based on ENDF/B-IV cross section data.

For burnup analysis, 8-group cross sections and for sodium-void and Doppler calculations, 21 group cross sections were used. Separate cross section data sets were prepared for core and blanket regions as well as for four different temperatures and for cores with and without sodium.

The fuel assembly designs were carried out with the NIFD code. Input data for this code are coolant inlet and outlet temperature, bypass flow fraction, blanket temperature penalty, maximum coolant velocity, maximum linear heat rating, radial power peaking, core height and axial blanket thickness, fuel pin diameter, reactor power and power split, stress limits and fast fluence. Output data are fuel pitch-to-diameter ratio, duct wall thickness, duct stresses (corner, wall), duct inside flat-to-flat distance, required interassembly gap as a function of axial position (allowing for swelling, irradiation creep and handling), number of fuel assemblies needed, bundle pressure drop, and volume fractions. The code can handle both wire-wrapped as well as gridded assemblies. Based on the number of required fuel assemblies and the estimated number of control positions, the code also determines the actual number of fuel assemblies for a hexagonal core layout where the corners can be rounded off, if needed.

The approximate nuclear performance was obtained from the SYNBURN code. This code is a 2D synthesis burnup code which calculates beginning- and end-of-equilibrium cycle performance characteristics and mass balances. The buckling treatment which allows for some flexibility in this code was adjusted to bring good agreement with more rigorous methods. The SYNBURN code provided enrichment splits which were then used as first guesses in REBUS r-z geometry calculations.

The approximate thermal analysis was based on adjustments to results obtained from rigorous methods by correcting for differences in linear heat rating, coolant flow rates and heat fluxes. In case no detailed analysis for a similar design was available, orificing was based on concentric orificing zones and the local peak-to-average power ratios.

The rigorous nuclear analysis of the first cycle and the equilibrium cycle was carried out with the REBUS code package. The REBUS code package performs burnup calculations in 1 and 2D. The code system handles discrete burnup, equilibrium cycle analysis, homogenized fuel management, discrete fuel management, fuel shuffling as well as a large variety of fuel recycle options. DIF2D is the 2-dimensional diffusion code used in REBUS. Burnup analysis was carried out using both r-z and hexagonal geometry options. Control rod worth calculations were carried out in hexagonal geometry using bucklings obtained from r-z geometry calculations.

PARC1D and PARC2D are one- and two-dimensional perturbation codes which were used for worth calculations in general and sodium void and Doppler reactivity distribution in particular.

After completion of the nuclear analysis, core layout, fuel management, and power distribution feed into the thermal analysis. The codes CORE-3D and ENERGY were used together with the FLORF code for a rigorous thermal analysis.

The CORE-3D code determines steady-state core-wide temperature distributions. It is based on the ENERGY code and takes interassembly heat transfer into account without limiting the number of fuel assemblies of which the core consists. Fuel assemblies were orificed individually. Coolant temperatures were calculated inside all fuel assemblies as well as duct temperatures and cladding hot-spot temperatures.

The ENERGY code determines the temperature distribution inside a fuel subassembly. The various mixing modes are lumped into an equivalent turbulent cross flow which is described by an effective eddy diffusivity. The code was used for a detailed thermal analysis of the design limiting assemblies.

The FLORF code is used to assign orificing zone numbers to all assemblies in the core based solely on assembly power and regardless of the physical location of the assembly. Therefore, assemblies can be in the same orificing zone even though they are not positioned next to each other. The assignment of orificing zones is governed by maximum clad temperatures which should be equal in all zones. It is permissible to use different temperature limits in different regions of the reactor and/or to select power distributions at any time in life and any region which are considered the limiting distributions.

The steady state cumulative damage fraction (CDF) was calculated with the CAFAIL code which uses correlations for rupture life and cladding wastage as specified by the groundrules.

3.4.3 Calculational Approach

The methods employed in the various steps of the preliminary analysis and the final analysis differed greatly reflecting on the different purposes of each step.

During the preliminary analysis the first step was to investigate the means to reduce sodium void reactivity. Beginning-of-life (BOL) calculations were carried out in r-z geometry. The enrichment split for the multi-core region arrangements was obtained from 1-D calculations. BOL sodium void reactivity calculations were carried out with a 2D perturbation code. The justification for using BOL conditions rather than end-of-equilibrium cycle (EOEC) conditions was the finding that for a two year residence time, the difference in sodium void reactivity for BOL and EOEC conditions was always \$1.15 ± 5¢. Therefore, a sodium void reactivity target of \$2.50 at EOEC required a BOL value of \$1.35 or less. Using perturbation rather than direct eigenvalue calculations for the sodium void reactivity provided insight into the spatial distribution of the sodium void reactivity and helped in the development of core configuration. During the first step of the preliminary analyses, r-z burnup calculations were carried out for selected cores. No detailed fuel pin or assembly designs were developed. But instead those designs were derived from the original Phase A fuel pin and assembly design.

During the second step of the preliminary analyses, detailed burnup calculations were carried out in r-z geometry. Specific fuel pin and assembly designs were developed subject to the design groundrules. Since the emphasis was placed on determining fuel pin sizes and core heights, no hexagonal geometry calculations were carried out at this stage. The performance parameters calculated at this step of the preliminary analysis were EOEC sodium void reactivities, breeding ratios, doubling times, fissile inventories, fluences and changes in assembly power output.

The step in the elimination process which followed was an optimization of the configuration. This required both r-z and hexagonal geometry burnup analysis with explicit representation of control rods as well as their insertion and withdrawal.

The final analysis was carried out in r-z and hexagonal geometry and included nuclear, thermal-hydraulic and mechanical design calculation. These calculations were complemented by transient and fuel cycle cost calculations.

4.0 CORE DESIGN AND ANALYSIS

The analysis and optimization of the various types of tightly and loosely coupled configurations, as described in Appendices B, C, and D has resulted in the two configurations shown in Fig. 2. These represent preliminary optimum configurations with respect to a compound system doubling time of about 15 years and EOEC sodium void reactivity less than $2.50. We have two configurations because of the two distinct starting points in this study. Namely, the class of loosely coupled cores, which lead to configuration A, and the class of tightly coupled cores which lead to configuration B. The two configurations are similar in that they are both center blanket configurations and have three core zones. We note that neither of the final cores can be put into either the class of loosely or tightly coupled cores, and may be considered hybrids. A general feature of both configurations, with respect to the previous classification, is that the inner and middle core regions are more tightly coupled than the middle and outer core regions. Although the configurations have these common features, they also retain some features which reflect their evolutionary origin. For example, configuration B which derives from the tightly coupled cores is shorter (36 in.) than configuration A (40 in.) and the fuel assemblies have respectively 331 and 271 fuel pins. A more detailed description of the designs is given in section 4.3 of this report.

This section will present a detailed analysis of the nuclear, thermal-hydraulic, and mechanical performance characteristics of configurations A and B. Based on these data a final optimum core will then be chosen in a conceptual design study.

4.1 NUCLEAR DESIGN ANALYSIS

4.1.1 Core Layout

The core configurations for this analysis are given in Fig. 2. They are center-blanket cores with three core zones each. The number of assemblies per region are listed in Table I. The total number of core assemblies in configuration A is 330 and in configuration B it is 342. Configuration A has a total of 157 internal blanket assemblies divided into four region, while configuration B has 145 separated into three regions. The fourth internal blanket region in configuration A consist of clumps of three assemblies each and is not considered as a ring separating two core zones. It will be treated in the data tabulations as a part of internal blanket 3. The number of radial blanket and radial shield assemblies is the same for both configurations. The total number of assemblies in configuration A is 883 and in configuration B it is 889.

4.1.2 Fissile Inventory

The fissile inventories for the beginning of life (BOL), beginning of equilibrium cycle (BOEC), and the end of equilibrium cycle (EOEC), are listed for both configurations in Table II. The total reactor fissile inventory at BOL for configuration A is 3861.9 kg, at BOEC 4268.4 kg, and at the EOEC 4575.0 kg. For configuration B the respective values are 3790.9 kg, 4213.4 kg, and 4489.7 kg. In the inner and middle core zones the fissile inventories of configuration B are higher, while for the outer core zone, the fissile inventory of configuration A is higher. Overall, configuration A has a slightly higher fissile inventory. For BOEC conditions this difference of 1.3% is due mainly to the bigger pin size in configuration A.

The average fissile enrichment by region is given for the two configurations in Table III. The enrichment in the core zones varies from 17.7 to 19.4% H.M. at BOL, and reduces to from 16.3 to 17.5% H.M. at the EOEC as the power shifts from the core to the blankets.

4.1.3 Burnup and Reactivity Swing

The peak and average burnups for the two configurations under equilibrium cycle conditions are given in Table IV. Both peak and average core discharge burnups are higher for configuration B than for configuration A. The highest value for configuration B occurs in the outer core zone and is 100.7 MWD/Kg. This can be compared with the highest value of 83.90 MWD/kg for configuration A, which also occurs in the outer core zone. The higher core burnup is due to the smaller pin size in configuration B. The peak discharge burnup in the internal blankets are comparable; the highest values occur in internal blanket 3 and are 22.10 MWD/Kg and 20.96 MWD/Kg for configuration A and B, respectively.

The reactivity for both cores decreases over the equilibrium cycle. This reactivity swing is 0.49% Δk for configuration A and 1.8% Δk for configuration B.

This difference is due in part to the difference in the pin diameter between the two configurations, but mostly because of the enhanced internal breeding due to the addition of internal blanket four in configuration A. In addition, the larger reactivity swing in configuration B implies a greater control requirement. This has been taken into account in the construction of the configurations by allowing 30 control positions in configuration B as opposed to 24 in configuration A.

4.1.4 Control Requirements

The control assembly assignments for the two configurations are given in Table V. For configuration A there are 12 control assemblies in the primary system and 12 in the secondary system, and for configuration B there are 12 in the primary system and 18 in the secondary system, which were chosen arbitrarily. The primary system serves both a safety and an operational function. This system must have sufficient worth at any time in the reactor cycle to shut down the reactor from any operating conditions, and to maintain subcriticality over the full range of coolant temperatures expected during shutdown. In addition, the primary control system is designed to meet fuel burnup and load requirement for each cycle as well as to compensate for criticality and refueling uncertainties. The secondary control system must have sufficient worth at any time in the reactor cycle to shut down the reactor from any operating conditions to hot-standby conditions. Both primary and secondary control systems must be capable of performing the specified functions independently, even with the failure of any single active component (i.e., a stuck rod). Allowance must also be made for both control systems for the maximum reactivity fault associated with any anticipated occurence.

The control assembly compositions were assumed to be those of the CRBRP design with 92% enriched B_4C. The results of the control system worth calculations in hexagonal geometry are given in Table VI. The total worth of both the primary and the secondary system is somewhat greater for configuration B than for configuration A.

The item-by-item reactivity requirements for the primary and secondary control systems are listed in Table VII. The requirement for controlling the excess reactivity (for the primary control system only), which usually is the most important component for a homogeneous reactor, is about a third smaller for configuration A than for configuration B. This is because the burnup swing for the configuration A core (0.49% Δk) is also smaller when compared to that of configuration B (1.8% Δk). This difference in burnup swings also leads to the difference in the control requirements for the maximum reactivity fault, for the amount of excess reactivity (plus uncertainties) dictates the maximum reactivity insertion that can occur due to any single rod run-out. The control requirement for cold criticality prediction uncertainty for CRBRP is 0.3% Δk and is adopted here for both configurations. The control requirement for fissile refueling tolerance (0.3% Δk) is based on a 0.5% uncertainty in batch fissile enrichment. The hot-to-cold component (requirement for both control systems) is assigned large uncertainties because the reactivity insertion due to the radial and axial core contractions is not readily available. The maximum reactivity control requirements, including uncertainties, for the primary and secondary control systems of configuration A are 3.65 and 2.58% Δk respectively, while for configuration B they are 4.24 and 3.47% Δk, respectively.

In Table VII the control system worths including one stuck assembly are compared with the control requirements. For configuration A the primary system worth is 3.65% Δk and the secondary system worth 2.58% Δk. The values are substantially higher than the respective control requirements of 2.33% Δk and 1.31% Δk. On the other hand, for configuration B almost no margin exists between the primary system worth of 4.24% Δk and the requirement of 4.02% Δk. For the secondary system the control worth is twice that of the requirement. It is therefore more appropriate to reassign some secondary control rods of configuration B as defined in Table VI to the primary system.

In making the above comparisons, it must be kept in mind that the reactivity worth of each control rod depends strongly on the positions of other control rods. This is especially true for a parfait core in which the flux distribution is very sensitive to the control rod insertion pattern. Thus, the above results must only be viewed with respect to the preliminary control system assignments in Table V.

4.1.5 Power and Flux Distribution

The power fractions for the different regions of the two configurations at BOL, BOEC, and EOEC are given in Table VIII. For configuration A the power fraction in the core region decreases from 89.9% at BOL to 75.7% at EOEC, and in the internal blankets the power fraction increases from 6.5%

at BOL to 16.8% at EOEC. Similarly for configuration B, the change in core power is from 89.7% at BOL to 76.7% at the EOEC and in the internal blankets from 5.8% to 14.6% respectively.

The peak assembly powers at the mid-plane for BOL, BOEC, MOEC, and EOEC conditions for configuration A are given in Figs. 3 through 7. The peak power density of 809.1 watts/cc at BOL with no control rods inserted occurs in the outer core zone. Inserting the row 11 rods 15% to maintain reactor criticality decreases this peak to 643.4 watts/cc and shifts the peak power density to a value of 678.2 watts/cc in a subassembly in the middle core zone. In Fig. 5 the BOEC peak power densities are shown under the condition of the row 11 control rods inserted 15%. As the burn cycle proceeds and the row 11 rods are withdrawn to compensate for the reactivity loss the peak power density shifts to the outer core zone and is 623.4 watts/cc at the EOEC (see Figs. 5 through 7).

Similar results are given in Figs. 8 through 12 for configuration B. The BOL peak power density with the row 11 rods completely inserted is 772.9 watts/cc and occurs in the middle core zone. At the EOEC with the rods withdrawn the peak power density is 694.1 watts/cc and is in the outer core zone.

The peak-to-average power densities at BOL, BOEC, and EOEC for the various reactor regions of the two configurations are given in Table IX. The total core peaking factor for configuration A at BOL is 1.45 and increases to 1.54 at the EOEC. For configuration B the respective change is from 1.53 to 1.60. Overall, power peaking in configuration A is somewhat lower than in configuration B. Some further descriptions of the power distributions are given in Figs. 80 through 85.

The nominal peak nuclear linear heat ratings are listed for both BOL and EOL in Table X. Core configuration A has a higher peak linear heat rating both at BOL and EOL, 13.4 and 12.0 kW/ft as compared to 13.2 and 11.4 kW/ft respectively for configuration B. However, the EOL peak blanket linear heat ratings are higher for configuration B than for configuration A. For the internal blanket and the radial blanket of configuration A the values are 12.8 kW/ft and 8.7 kW/ft respectively, while 15.3 kW/ft and 10.7 kW/ft for configuration B.

The peak fast fluxes in the core and blanket regions are given in Table XI. In the core the peak fast flux for configuration A is 3.39×10^{15} n/cm^2-sec and 3.57×10^{15} n/cm^2-sec for configuration B. For a core residence time of 2 cycles at 255.5 days per cycle the peak fast fluence is 1.45×10^{23} nvt for configuration A and 1.50×10^{23} nvt for configuration B. For the internal blankets, whose residence time is also 2 cycles, the respective peak fluences are 1.28×10^{23} nvt and 1.32×10^{23} nvt.

In Figs. 13 through 21 contour flux maps are given for configuration A. The BOL reactor conditions are shown in Figs. 13 through 18 with different control rod insertions. The flux peaking at BOL about the row 11 primary rods is especially noteworthy, for this peak significantly enhances the worth of these control rods. The effect of inserting this rod can be seen in Figs. 13 and 14. The change in the flux distribution over the equilibrium cycle is shown in Figs. 19 through 21, where the reactivity swing is being controlled with the row 11 primary rods. As the burnup proceeds and these rods are withdrawn the buildup of the characteristic flux peak near this rod can be seen.

The analogous situations are shown in Figs. 22 through 29 for configuration B. We note (see Fig. 22 for example) that also in configuration B a flux peak exists at the row 11 primary control positions, and therefore enhances the worth of these control rods.

4.1.6 Breeding Performance

The breeding ratios for the different regions of the two reactors are listed in Table XII for BOL, BOEC, and the EOEC. The core breeding ratio of configuration A is 0.550 at BOL and reduces to 0.497 at the EOEC as the power shifts to the blankets. For configuration B the BOL core breeding ratio is 0.628 and reduces to the same value as that of configuration A, 0.497, at the EOEC. The total reactor breeding ratios for configuration A are 1.488 at BOL and 1.380 averaged over the equilibrium cycle. The respective values for configuration B are 1.530 and 1.354.

The compound system doubling times for the two configurations are listed in Table XIII. Under the assumptions of a two year residence time for core and internal blanket assemblies, a five year residence time for the radial blanket assemblies, a one year out-of-pile time, and 1% fuel cycle losses, the doubling time for configuration A is 15.7 years and for configuration B 15.3 years. This could be reduced somewhat, as is shown for configuration A, by using a one year residence time for the internal blankets. In this case configuration A has a 15.1 year compound system doubling time.

4.1.7 Safety Parameters

The sodium void reactivities for the two configurations are given in Table XIV and XV. The results are calculated in first order perturbation theory and thus the break down with respect to voiding the individual zones is given. The values are for the removal of the flowing sodium only. Both configurations have sodium void reactivities, for voiding the flowing sodium from the core plus the upper axial blanket, which are below $2.50 at the EOEC. The BOL value for configuration B is almost half of the BOL sodium void reactivity of configuration A. However, due to the greater burnup of configuration B its sodium void reactivity increases to within 15¢ of the sodium void reactivity of configuration A at the EOEC.

In Tables XVI and XVII the isothermal Doppler coefficients are given for both configurations with sodium-in and sodium-out conditions at BOL and at the EOEC. The total core Doppler coefficient at BOL for configuration A is 0.0053 for sodium-in and 0.0031 for sodium-out and decreases to 0.0046 and 0.0029 respectively at the EOEC. The total internal blanket Doppler coefficient, on the other hand, is 0.0039 and 0.0031 at BOL for sodium-in and sodium-out, and increases to 0.0048 and 0.0036 respectively at the EOEC. For configuration B the core Doppler coefficient is 0.0051 and 0.0031 at BOL for sodium-in and sodium-out, and at the EOEC 0.0046 and 0.0028 respectively. The internal blanket Doppler coefficients for configuration B are somewhat lower than for configuration A. At BOL these are 0.0026 and 0.0022 for sodium-in and sodium-out and 0.0038 and 0.0029 respectively at the EOEC.

4.1.9 Transient Response

4.1.9.1 Introduction

Investigation of transient response of both configuration A and B to reactivity insertions into the outer core region via control rod withdrawal was conducted. The aim here was primarily to assess the space dependent kinetics effect of these configurations. Comparison of results with the Phase A design was made.

4.1.9.2 Methodology

The two-dimensional space-time kinetics code FX2[2] was used to study the configuration A and B designs in one-sixth hexagonal symmetry. The Doppler feedback effect came from the temperature-dependent cross sections. An adiabatic heat transfer model (i.e., a constant heat transfer rate from fuel to coolant throughout the transient) was used in the transient analysis.

4.1.9.3 Reactivity Insertions

Two different reactivity insertion rates were studied: a 60¢ step and a 60¢/500 ms ramp, both coming from withdrawing the control rods from the outer core region.

4.1.9.4 Transient Results

4.1.9.4.1 Configuration A

When a 60¢ reactivity step was inserted into the outer core region, the peak power density normalized to its initial value for each of the three core zones (inner, middle and outer) rose rapidly in the first millisecond, and reached a peak value near 4 milliseconds. Furthermore, the outer core peak power density rise was only 2.3% and 3% higher than those of the middle core and inner core (2.507 vs. 2.511 and 2.501). These results were given in Table XVIII and Fig. 30.

For the 60¢/500 ms, again the normalized peak power density in all three core zones rose in unison, with that of the outer core zone slightly greater (2.3% and 2.7%) than those of the middle and inner core zones (2.113 vs. 2.064 and 2.056). These results were shown in Table XIX and Fig. 31.

4.1.9.4.2 Configuration B

The transient response of configuration B was similar to that of configuration A to both the 60¢ step and 60¢/500 ms ramp. With the 60¢ step insertion, the normalized peak power density in the outer core reached the peak value of 2.553, while those of the middle and inner cores respectively reached 2.503 and 2.490. The difference between the outer core normalized peak power density and those of the middle and inner cores were respectively 2.0% and 2.5%.

For the 60¢/500 ms ramp, the normalized peak power density in the outer core reached its maximum value of 2.131, relative to those of 2.083 and 2.071 for the middle and inner core. The difference here between the outer core normalized peak power density and those of the middle and inner cores were 2.3% and 2.9%. These results were shown in Tables XX-XXI and Figs. 32-33.

4.1.9.5 Conclusions

Based on the above analysis, the following conclusions can be made.

1. Both configuration A and B had very little space-dependence effects during a 60¢ step or ramp insertion transient. The normalized peak power density in the outer core zone where reactivity was inserted was never more than 3% greater than that of the middle or inner core for both configurations A and B for either the 60¢ step or ramp insertion.

2. In comparison, the Phase A design exhibited a maximum normalized peak power density of 3.3 in the inner core where reactivity was inserted, and about 2.5 in the middle and outer cores, when a 60¢ step reactivity was inserted in the inner core.

4.2 THERMAL-HYDRAULIC ANALYSES

4.2.1 Inlet and Outlet Temperature of Configuration A

Inlet and outlet temperatures for core, core plus internal and radial blankets, and the reactor are given in Table XXII. The core inlet temperature is 595°F, with a core ΔT of 313°F. The ΔT across the core and blankets is 295°F. The cold by-pass is 5% of the total reactor flow. Cold by-pass flow does not include flow through control channels. The γ heating in those channels was taken into account in calculating the coolant temperature rise.

4.2.2 Orificing Scheme of Configuration A

The orificing zones are shown in Fig. 34. There are three orificing zones in the core, four in the internal and radial blankets, and one for the control and radial reflector assemblies. BOL powers with control rods inserted were used for the core and EOL powers were used for the internal and radial blankets in determining the flow distribution. At these burnup stages, the peak cladding midwall temperatures (2σ values) were made equal for the hottest fuel or blanket pin in each orificing zone.

The coolant flow rates, coolant velocities, and the number of assemblies in each of the orificing zones are given in Table XXIV. The flow splits are 74.8%, 24.9%, and 0.5% for the core, internal and radial blankets, and control and shield assemblies. The maximum coolant velocity is 25.6 ft/sec.

The sensitivity of peak cladding temperatures to using EOEC powers for the core and blankets will be discussed in section 4.2.4.

4.2.3 Temperature Distributions of Configuration A

Temperature distributions for the duct and coolant on a core wide basis, orificed for minimum peak temperature, at various axial locations (core midplane, core and upper axial blanket interface, and the top of the upper axial blanket) are given in Figs. 35 to 46. The duct temperature calculations took into account the interassembly heat transfer. The averaged duct temperatures given in Figs. 41 to 46 were averaged over the six-flats of each assembly. The highest average duct temperature is 894°F, at the top of the upper axial blanket in an assembly in the twelfth row of the core at beginning of life.

The average coolant temperature is obtained from averaging the coolant subchannels interior to the assembly. The maximum coolant outlet temperature is 1013°F, and occurs in the same assembly which has the highest average duct temperature.

While the highest average outlet temperatures are achieved in the assembly in the twelfth row, the limiting (or hottest) fuel pin is in an assembly in row eight. For the assembly with the hottest fuel pin, the coolant as well as nominal and 2σ clad midwall temperatures are shown respectively in Figs. 47 to 55 for three axial locations. The peak coolant subchannel outlet temperature is 1003°F. With a hot channel factor of 1.232, the peak 2σ coolant subchannel outlet temperature is 1098°F. The peak nominal clad midwall temperature for the hottest pin in this assembly is 1026°F at the core and upper axial blanket interface. The peak 2σ clad midwall temperature for this pin is 1145°F at the same axial location. These temperatures occur at beginning-of-life conditions. How they vary from beginning-of-life to end-of-life conditions is shown in Tables XXVI and XXVII. At EOL, the peak nominal and 2σ clad midwall temperatures are 973 and 1077°F, which is a reduction of 53 and 68°F, respectively. from their BOL values. Tables XXVI and XXVII also give the nominal and 2σ temperature at the clad outer diameter. The temperature drop across half of the clad thickness is 23°F at the core and axial blanket interface where the clad midwall temperature reaches its maximum.

A summary of nominal and 2σ peak temperatures for the cladding, coolant, and duct is given in Table XXVIII. The 2σ peak cladding temperatures are 1122, 1145 and 1178°F at the outer diameter, midwall and inner diameter, respectively. These temperatures occur for the hottest pin at BOL. As mentioned before, at EOL, a reduction of 68°F is observed. The 2σ peak duct and coolant temperatures are 926 and 1024°F, respectively.

4.2.4 Sensitivity of Cladding Temperature to Orificing Criteria of Configuration A

The orificing strategy employed equalized the maximum 2σ cladding temperature at beginning-of-life for the core and end-of-life for the blankets in all orificing zones. This means that the blanket pins and some of the driver fuel pins are overcooled for most of their life.

The flow split between core and blanket assemblies was changed to equalize the peak clad temperature at end-of-equilibrium cycle conditions. This led to the orificing scheme shown in Fig. 56. The coolant flow rates, velocities and number of assemblies in each zone are shown in Table XXV. While this orificing strategy lowered the peak clad temperatures at EOEC for the core from 1145°F to 1134°F, some fuel assemblies had much higher temperatures at beginning-of-life conditions than obtained with the reference orificing. This is due to the fact that control rod insertion and the power shift to the blanket assemblies over an equilibrium cycle cause a large decrease in rating in driver fuel assemblies located far from the inserted rods. Consequently, determining the flow for these assemblies at EOEC conditions causes them to be undercooled at beginning-of-life. The fuel assemblies on the flats of rows thirteen and fourteen are very sensitive to control rod insertion. Orificing these assemblies for EOEC when control rods are withdrawn leads to clad midwall temperatures of more than 1200°F at BOL when the row twelve rods are inserted.

It needs to be assessed which orificing strategy improves performance. The latter strategy leads to higher clad temperatures at BOL when cladding hoop stresses are very small and lower temperatures at EOL when hoop stresses are high thus possibly improving fuel life.

4.2.5 Inlet and Outlet Temperature of Configuration B

Inlet and outlet temperatures for core, core plus internal and radial blankets, and the reactor are given in Table XXIX. The core inlet temperature is 595°F, with a core ΔT of 312°F. The ΔT across the core and blankets is 295°F. The reactor ΔT is 280°F. The cold by-pass flow is 5% of the total reactor flow. Cold by-pass flow does not include control channels since γ heating is taken into account in calculating the temperature rise through them.

4.2.6 Orificing Scheme of Configuration B

The orificing zones are shown in Fig. 57. There are three orificing zones in the core, four in the internal and radial blankets and one zone for the control and radial reflector assemblies. BOL powers with control rods inserted were used for the core and EOL powers were used for the radial and internal blankets in determining the coolant flow distribution. At these burnup stages the 2σ peak cladding midwall temperatures were made equal for the hottest fuel or blanket pin in each of the orificing zones.

The number of assemblies in each zone, the coolant flow rates and the coolant velocities are shown in Table XXXI. The flow splits are 78.1%, 21.6% and 0.3% for the core, internal and radial blankets, and control and shield assemblies. The maximum coolant velocity is 25.6 ft/sec.

The sensitivity of cladding temperatures to using EOEC powers for the core and blanket assemblies will be discussed in section 4.2.8.

4.2.7 Temperature Distributions of Configuration B

Temperature distributions for the duct and coolant on a core wide basis at three axial locations (core midplane, core and upper axial blanket interface, and top of the upper axial blanket) are shown in Figs. 58 to 69. The calculations of duct temperatures took into account interassembly heat transfer. The average duct temperatures given in Figs. 64 to 69 were averaged over the six flats of each assembly. The highest average duct temperature is 817°F, at the top of the upper axial blanket in an assembly in the thirteenth row of the core at beginning of life.

The average coolant temperature is obtained from averaging the coolant temperatures of the subchannels interior to the assembly. The maximum coolant outlet temperature is 1009°F, and occurs in the same assembly which has the high average duct temperature.

While the highest average coolant temperatures are achieved in row 13, the limiting (or hottest) fuel pin is in an assembly in the ninth row. For the assembly with the limiting fuel pin, the coolant as well as nominal and 2σ clad midwall temperatures are shown in Figs. 70 and 78 for three axial locations. The peak coolant subchannel outlet temperature is 1016°F. Applying a hot channel factor of 1.232 for the coolant ΔT gives a 2σ peak outlet temperature of 1114°F. The peak nominal clad midwall temperature for this assembly is 1041°F at the core and upper axial blanket interface. The peak 2σ clad midwall temperature for the hottest pin in this assembly is 1164°F at the same axial location. These temperatures occur at beginning of life conditions. Tables XXXIII and XXXIV show how the temperatures vary from beginning-of-life to end-of-life conditions. At EOL, the peak nominal and 2σ clad temperatures are 990 and 1100°F, which is a reduction of 51 and 64°F, respectively, from BOC values. Tables XXXIII and XXXIV also give the nominal and 2σ temperature at the clad outer diameter. The temperature drop across half of the clad thickness is 24°F at the core and upper axial blanket interface where the clad temperature reaches its maximum.

A summary of nominal 2σ peak temperatures for the cladding, coolant, and duct is given in Table XXXV. The 2σ peak cladding temperatures are 1140, 1164, and 1188°F at the outer diameter, midwall and inner diameter, respectively. These temperatures occur for the hottest pin at BOL. As mentioned before, at EOL, a reduction of 64°F is observed. The 2σ peak duct and coolant temperatures are 936 and 962°F, respectively.

4.2.8 Sensitivity of Cladding Temperature of Orificing Criteria of Configuration B

The orificing strategy employed equalized the maximum 2σ cladding temperature at beginning-of-life for the core and end-of-life for the blankets in all orificing zones. This means that the blanket pins are overcooled for most of their life and the driver fuel pins are overcooled after the initial core loading.

The flow split between core and blanket assemblies was changed to equalize the peak clad temperature at end-of-equilibrium cycle conditions. This resulted in the orificing scheme show in Fig. 79. The coolant flow rates, velocities and number of assemblies in each zone are shown in Table XXXII. This orificing strategy lowered the peak clad temperatures in the core at BOL from 1164 to 1125°F. However, some fuel assemblies had much higher temperatures at beginning-of-life conditions than obtained with the reference orificing. This is due to the fact that control rod insertion and the power shift to the blanket assemblies over an equilibrium cycle cause a large decrease in rating in driver fuel assemblies located far from the inserted rod. Consequently, determining the flow for these assemblies at EOEC conditions causes them to be undercooled at beginning-of-life. Orificing for EOEC caused the fuel assemblies on the flats of rows five and six to be placed in flow zone three while the reference orificing placed them in zone two. The resulting decrease in flow raised the peak 2σ clad midwall temperature from 1164 to 1204°F at BOL. This emphasizes the importance of using a detailed hexagonal power distribution including control rod insertion when orificing heterogeneous cores.

4.3 MECHANICAL DESIGN ANALYSES

The structural material used for claddings and ducts is 20% CW316SS. In the following, the designs of fuel pin, fuel assembly, blanket pin, blanket assembly, control assembly, as well as duct life will be discussed for both configurations A and B.

4.3.1 Fuel Pin Design

The fuel pin design parameters are summarized in Table XXXVI. The optimization studies gave optimum fuel pin diameters of 0.26 in. and 0.24 in. The cladding thickness to diameter ratio (t/d) selected is 0.050 which gives cladding thicknesses of 0.013 in. and 0.012 in. for configurations A and B, respectively. At this stage of analysis, the fuel inside the cladding tube was characterized only by a fuel smear density of 88% T.D. The core fuel sections are 40 in. and 36 in. long. The fuel pins are wire-wrapped with a helical pitch of 12 in. and wire thicknesses of 0.051 in. and 0.048 in.

The top fission gas plenum is 40 in. long for Core A and 36 in. long for Core B. The top and bottom axial blanket sections are 15 in. and 16 in. long and have a fuel smear density of 90% T.D.

It is expected that the plenum length for both cores can be reduced after detailed fuel lifetime analyses are carried out.

4.3.2 Fuel Assembly Design

The fuel assembly design parameters are summarized in Table XXXVI.

For Core A, the fuel assembly contains 271 fuel pins with a p/d ratio of 1.197. The fuel bundle pressure drop is 71.5 psi. For this design, the peak stress in the duct corner is 33,832 psi. This stress level is well below the maximum allowable stress for 20% CW316SS. The duct wall thickness was determined such that the combined primary membrane plus bending stress intensity is 18,000 psi. Further reduction in duct wall thickness are, therefore, possible.

For Core B, the fuel assembly contains 331 fuel pin with a p/d ratio of 1.200. The fuel bundle pressure drop is 73.3 psi. The peak stress in the duct corner is 34,222 psi. As for Core A, the duct wall thickness for Core B can be further reduced.

4.3.3 Blanket Fuel Pin

The blanket fuel pin design parameters are summarized in Table XXXVII. The pin diameters are 0.425 in. and 0.484 in. and the cladding thicknesses are 0.013 in. and 0.012 in. for Core A and Core B, respectively. The fuel smear density is 90%. The wire wrapped around the fuel pin is 0.030 in. thick and has a helical pitch of four in. At this stage of the analysis, no attempt was made to optimize the length of the fuel column to minimize fuel cycle cost. Blanket fuel pin analysis will also lead to a significant reduction in the plenum length.

4.3.4 Blanket Assembly

The assembly dimensions are identical to those of the fuel assemblies. The assembly contains 127 blanket pins with a p/d of 1.07.

4.3.5 Control Assembly

No specific design for a control assembly was developed. For the control system design it was assumed that the control assembly for this reactor has the same volume fractions of steel, sodium, and poison as for the CRBRP control assembly shown in Table XXXVIII.

4.3.6 Duct Life

Three sets of constraints govern the duct life analysis carried out for this study:

a. maximum duct wall stress
b. duct-duct interaction
c. bundle-duct interaction

The maximum wall stress defined for this study was 0.55 maximum allowable stress. With an ultimate tensile strength for 20% CW316SS of 78 ksi, the calculated nominal maximum primary membrane plus bending stress intensities for driver ducts are 18,000 psi which are well below the allowable limit.

To avoid duct-duct interaction, the distance between ducts was selected such that at end-of-life conditions none of the assemblies exceeds the pitch line. In calculating the duct dilation, both the swelling and creep effects were taken into consideration. The duct wall pressure differential profiles for the design limiting duct is shown in Table XXXIX. The maximum duct dilations for the hottest fuel assembly subject to the maximum fluence in the core occurs six in. above the core midplane. These dilations are 0.215 in. and 0.200 in. for Core A and Core B, respectively. They were chosen as the gap distances between assemblies.

A simplified seismic analysis showed that the thickness of a 4 in. wide load pad has to be approximately 0.200 in. to withstand the stresses in a seismic event. The load pad thickness was calculated according to the following formula:

$$t = 0.0013\ (L_F)^{\frac{1}{2}}\ (\sum_i w_i + B)^{\frac{1}{2}}$$

with

t = load pad thickness for a four-in. wide pad (in.)

L_F = duct inside flat-to-flat distance (in.)

$\sum_i w_i$ = sum of the weights of heavy metal of a radial row of assemblies from the core center to the shield section

B = correction term to account for bridging and even load distribution = 400

The actual ACLP thicknesses for Core A and Core B are 0.328 in. and 0.317 in. which are well above the required thickness of 0.200 in. Using the correlations for bundle-duct interaction developed by GE and modified by CE for the Proliferation Resistant Large Core Design Study (PRLCDS) showed bundle-duct interferences of less than one spacer wire which is well below the allowable interference of 2-3 wires.

4.4 FUEL CYCLE COST

Fuel cycle cost were determined for Core A and Core B. The economic assumptions for this analysis are shown in Appendix A. The fabrication cost were determined using the N-factor formula HEDL developed for the Proliferation Resistant Large Core Design Study. The results of the fabrication cost calculation are shown in Table XL. On an assembly basis, the fabrication cost are about the same for Core A and Core B. The total fuel cycle cost shown in Tables XLI and XLII show a 0.8 mill/kWh (or 9%) advantage of Core A over Core B. Since neither of those cores is cost-optimized this difference is insignificant. By cutting down the length of the radial blanket pins the reprocessing charges can be reduced. This together with a slight increase in fuel residence time can bring the fuel cycle cost well below 8 mill/kWh.

Nomenclature:

Zone 1-3	Core Zones
Zone 4-6	Axial Blanket Zones
Zone 7	Internal Blanket Zones
Zone 8	Radial Blanket Zones

5.0 DESIGN EVALUATION

The basis for this evaluation is established in Appendices B, C, and D, which outline the steps of the elimination/optimization process. Thus, the following conclusions can be drawn regarding the choices between center core vs. center blanket configurations, loosely-coupled vs. tightly-coupled cores, and continuous ring vs. broken ring configurations.

5.1 CENTER CORE VS. CENTER BLANKET CONFIGURATION

Both types of configurations can lead to feasible designs. For center core configurations, the relation between core region size and power plant output is of special significance. The center core region has to be small to permit a low overall sodium void reactivity. Typically it has not more than 4-5 rows of fuel, i.e. 37 to 61 fuel assemblies. The power output for this region is only approximately 300-450 MW which represents 10-15% of the total reactor power output of a 3000 MW plant. Therefore, for such a power level the reactor has to have at least three core regions. In case of a tightly coupled system, at least four core regions seem to be necessary to achieve a low sodium void reactivity core.

Center blanket configuration, on the other hand, can be constructed with as little as two core zones in a loosely coupled configuration and three in a tightly coupled configuration.

The different requirements on the number of core regions affects directly the number of different enrichments needed to flatten the power. Even though it might be possible to arrange the internal blanket assemblies such that they flatten the power sufficiently even for only one or perhaps two different core fuel enrichments, the uncertainties in the prediction of power shapes in heterogeneous cores are currently too great to rely solely on calculation for such arrangements. Therefore, center blanket configuration allows for core designs with fewer discriminator zones than center core configurations.

Because of the small size of the center core region required to yield low sodium void reactivities, a greater sensitivity especially in power peaking is observed in the center core configuration compared to center blanket configurations. Changing the enrichment in the inner-most core zone by 0.5%

leads to substantially greater changes in peak power density in the inner-most core zone in center core than in center blanket configuration. Because any enrichment specification will have certain tolerances a center core configuration would require more corrective action by the control system to flatten the power than a center blanket configuration.

Center core configurations showed significantly higher assembly power swings over a burnup cycle than center blanket configurations. The result of these greater changes in assembly power is a higher peak clad temperature because the enhanced overcooling in one part of the core has to be compensated by higher coolant temperature rises in other parts of the core.

Center core configurations had in some instances slightly smaller specific inventories than center blanket configurations but whenever this occurred the differences were small. In regard to doubling time, sodium void reactivity and control requirements, no advantage could be identified for either configuration.

Therefore, center blanket configurations were chosen over center core configurations since the latter perform at best as well as the former but in addition have serious flaws in regard to power shape sensitivity.

5.2 LOOSELY VS. TIGHTLY COUPLED CORES

The neutronic coupling concept was introduced to distinguish between different core configurations. "Loosely" and "tightly coupled" cores were configurations which differed in the degree of neutronic coupling. Both terms are used to qualitatively describe different core configurations. The degree of neutronic coupling depends on the thicknesses of the internal blanket regions separating the core regions from each other. For a reactor with two core regions, Avery's coupling coefficients can be determined easily and related to power peaking. When going to more than two core zones and a broken ring rather than a continuous ring configuration is used, it is very difficult if not impossible to determine meaningful coupling coefficients and relate them to power peaking. Therefore, no efforts were made to determine coupling coefficients for the various cores which have been analyzed. The terms "loosely" and "tightly coupled" cores were applied to cores with more than one or less than one row of blanket assemblies separating core zones, respectively.

Loosely coupled cores achieved low sodium void reactivities at core heights of 40 in. or more. However, they showed high specific inventories, large doubling times and very strong sensitivities in power peaking.

Tightly coupled cores on the other hand required core heights of less than 40 in. to achieve sodium void reactivities of less than $2.50. They generally showed lower specific inventories, lower doubling times and lower sensitivities in power peaking, than loosely coupled cores. For optimized cores, the reactor diameters for loosely and tightly coupled cores were quite similar since the lower core height required smaller fuel pins for optimum conditions thus offsetting the otherwise unavoidable increase in reactor size coming from the increase in the number of fuel pins necessary to maintain the reactor power level.

While the tightly coupled cores showed generally a better performance than the loosely coupled cores, neither the strictly tightly coupled cores nor the strictly loosely coupled cores were considered optimal. However, the optimum core configuration is closer to the tightly coupled system rather than a loosely coupled system. The disadvantages of the strictly tightly coupled cores were the low core height which either led to an increase in the number of fuel assemblies which had to be fabricated or an increase in the number of fuel pins per assembly which leads to increased fuel bundle-duct interaction. The lower core height and the resulting smaller fuel pin size led to higher fuel burnups. The major disadvantage of the loosely coupled core is the strong sensitivities of the power shape to either uncertainties in enrichment or fuel burnup. Furthermore, the transient response of the core is very dependent on the specific location of the reactivity perturbation.

The core configuration finally selected is a "hybrid" in that it is more tightly coupled in the center of the reactor were the core regions are small in size and more loosely coupled in the outer core regions. With this arrangement, the advantages of both the loosely and tightly coupled cores were combined at only minor penalties in sodium void reactivity and doubling time.

5.3 CONTINUOUS RING VS. BROKEN RING CONFIGURATIONS

The broken-ring arrangements showed definitive improvements over continuous ring configurations with regard to power peaking, power swing, and control rod worth. The broken ring arrangements create flux peaks where control rods can be located. These flux peaks enhance the worth of control rods.

But by placing the control rods in the outermost core region additional benefits can be derived. For all core configurations, the outermost core region always has a substantial power reduction over an operating cycle if the burnup analysis is carried out with the control rods in their fully withdrawn position. By creating a flux peak in the outermost core region the insertion of a control rod would level out the fluxes at beginning-of-cycle condition. As burnup progresses the control rods are withdrawn thus counteracting the otherwise decreasing flux level.

In analyzing both configurations, it is important to realize the limitations of the calculational methods employed. r-z models are not suitable for optimization of core configurations since the discrete control rod location have to be modelled as a control ring. This model will not give any valid information at all as to the required enrichment split, power peaking and control rod worth. To obtain these information, hexagonal geometry models have to be analyzed.

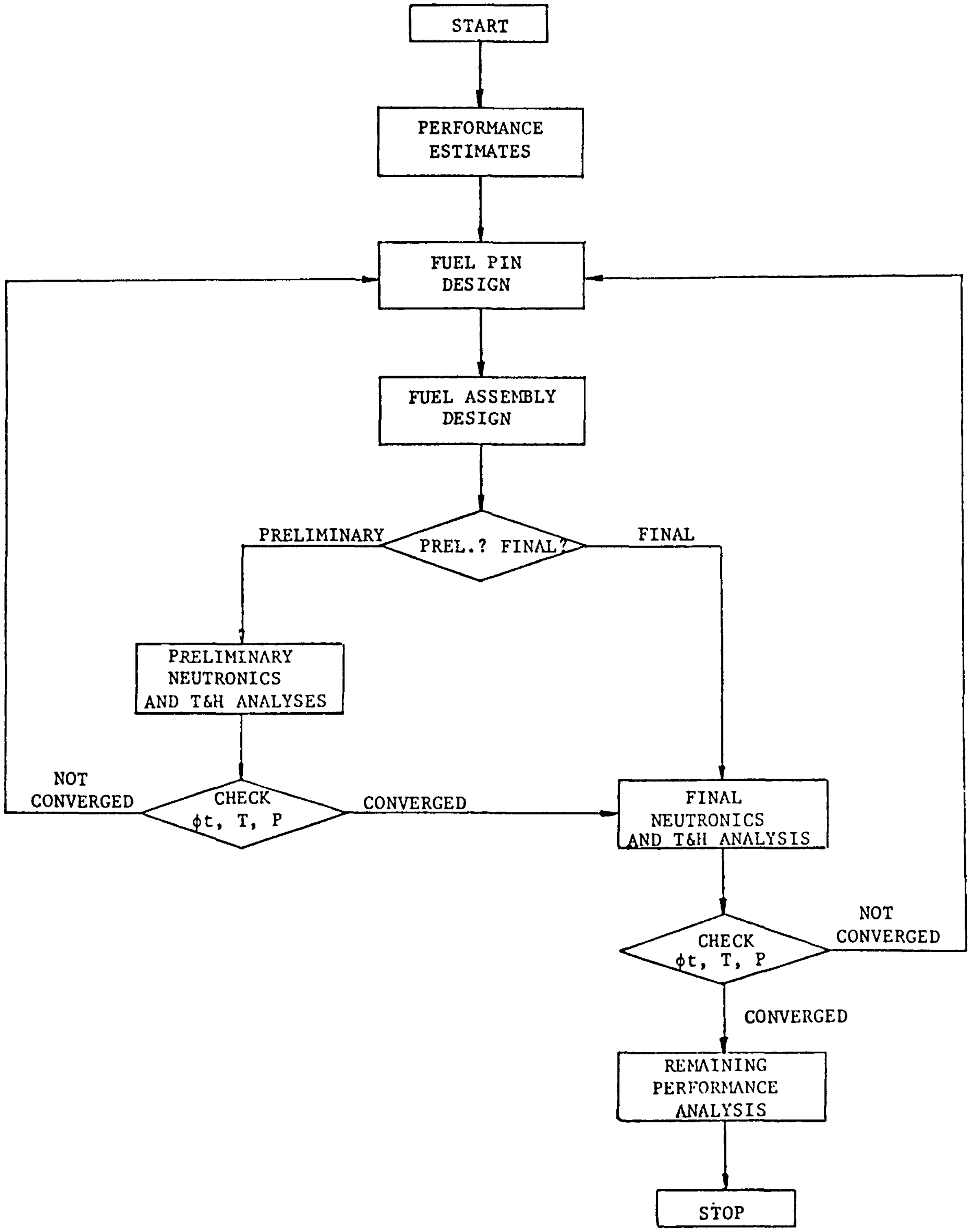

Fig. 1. Design Analysis Flow Sheet

Configuration A

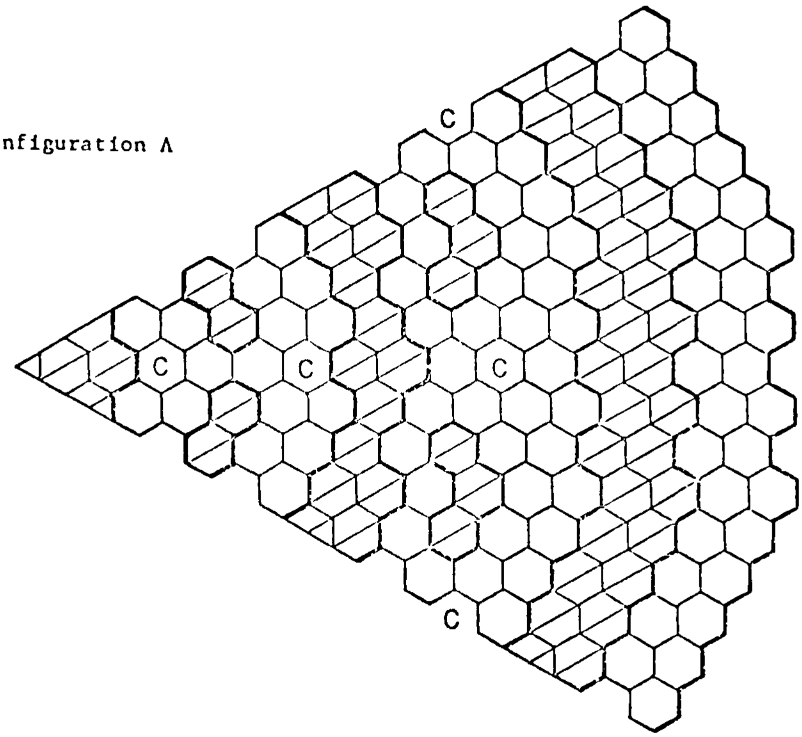

Configuration B

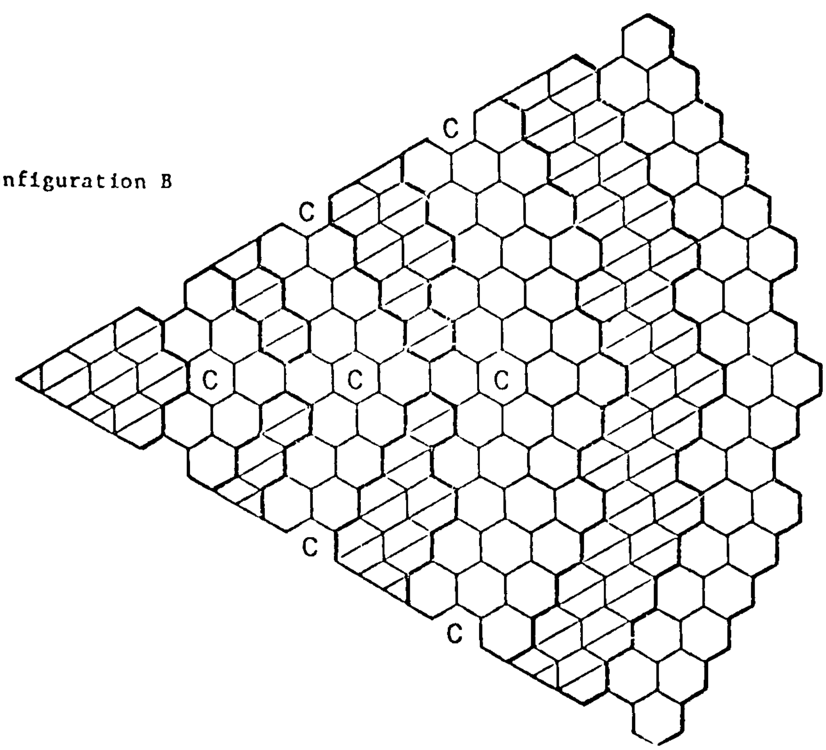

Fig. 2. Preliminary Optimum Configurations

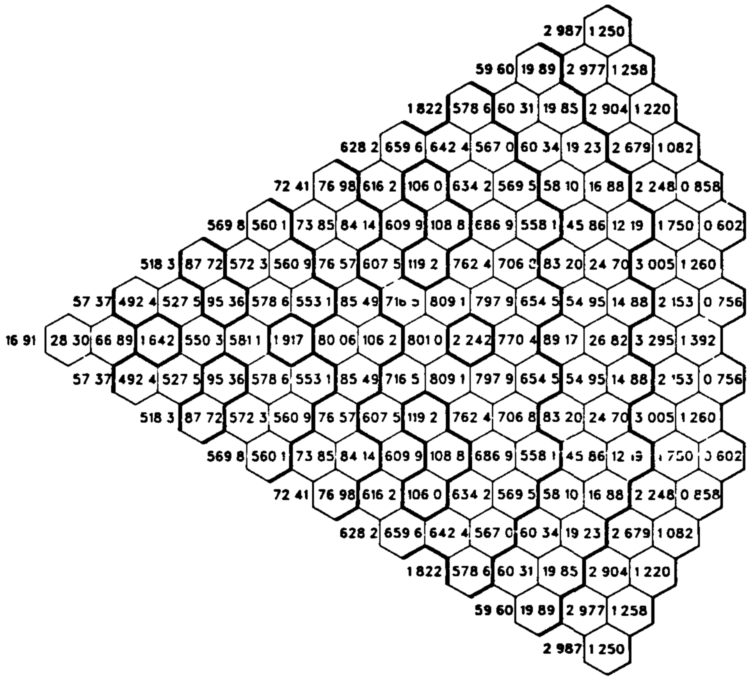

Fig. 3. Configuration A, Peak Power Density at BOL, No Rods Inserted

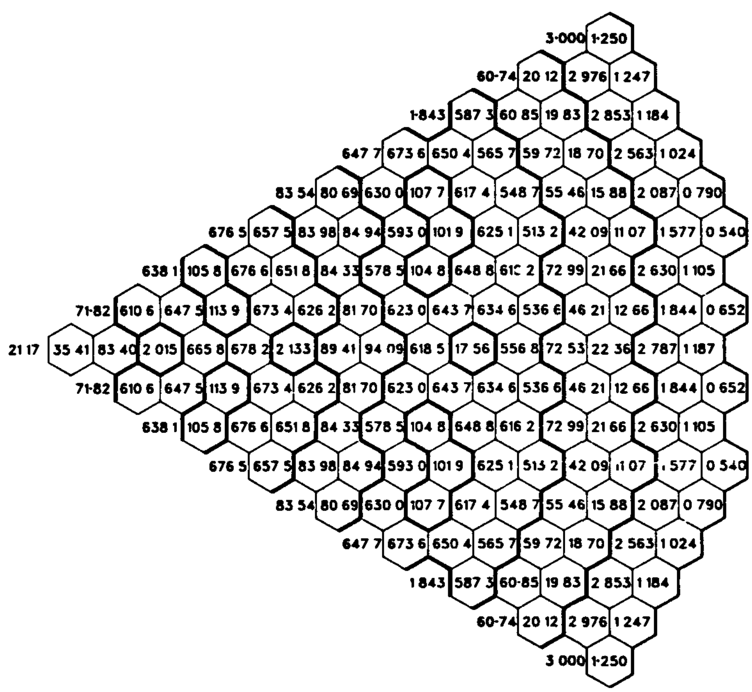

Fig. 4. Configuration A, Peak Power Density at BOL, Row 11 Rods 15% Inserted

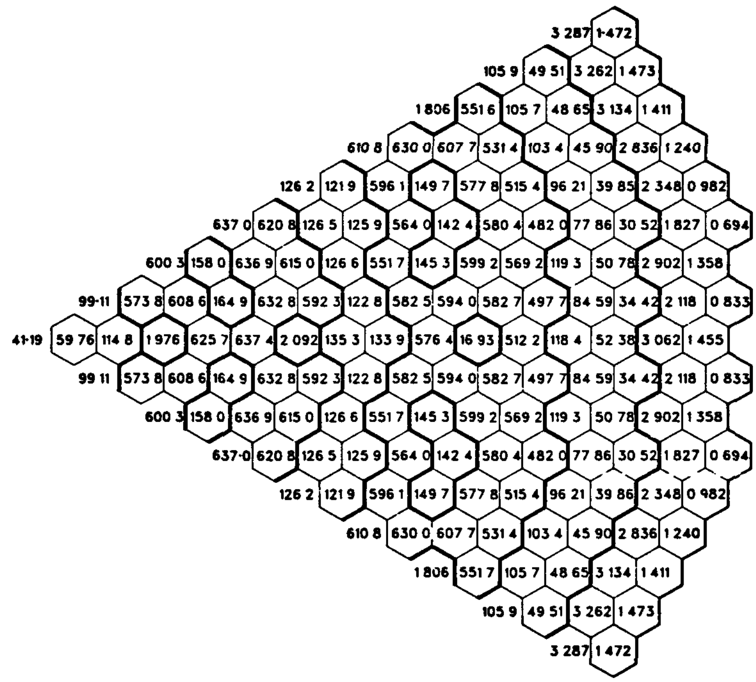

Fig. 5. Configuration A, Peak Power Density at BOEC Conditions

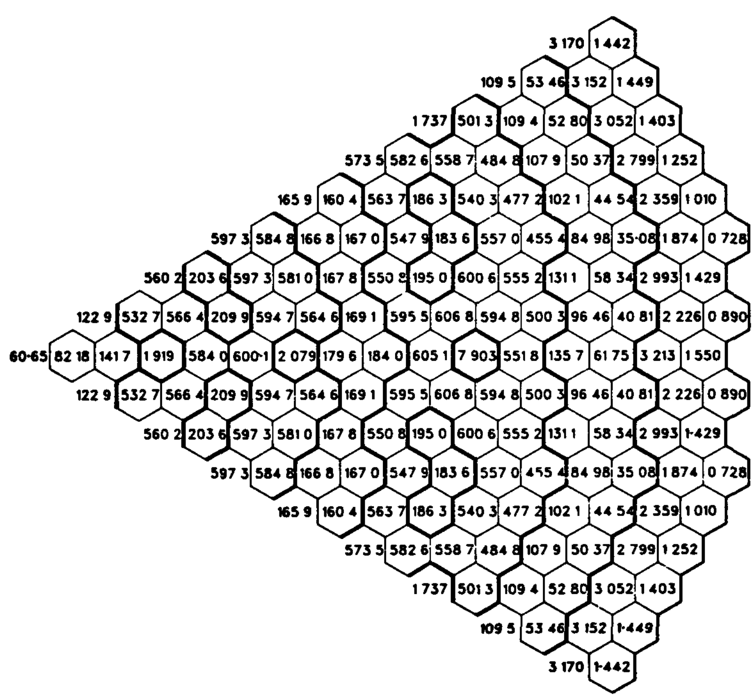

Fig. 6. Configuration A, Peak Power Density at MOEC Conditions

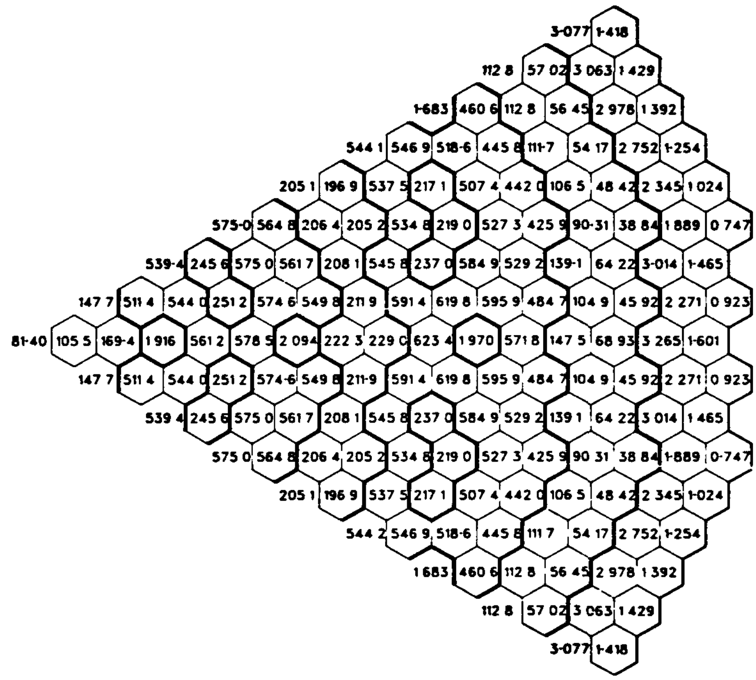

Fig. 7. Configuration A, Peak Power Density at EOEC Conditions

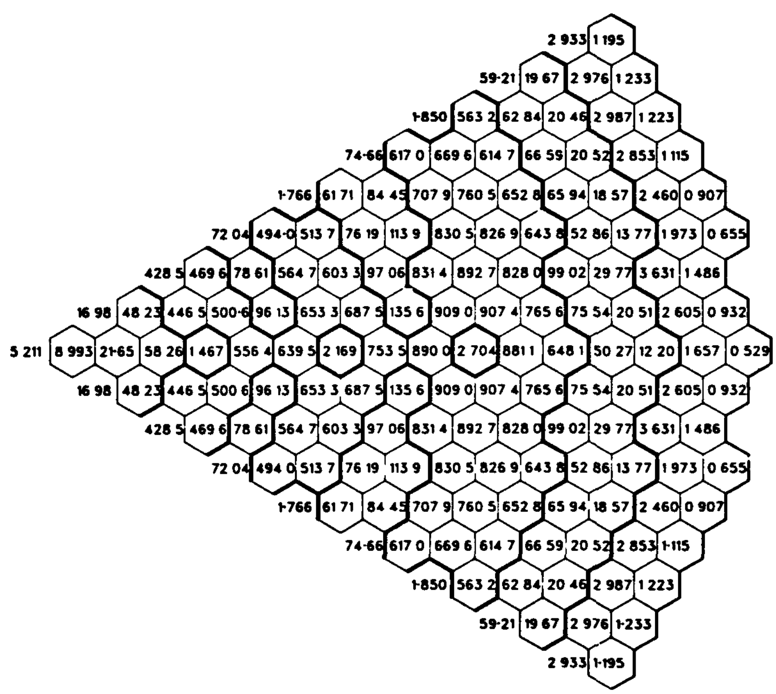

Fig. 8. Configuration B, Peak Power Density at BOL, No Rods Inserted

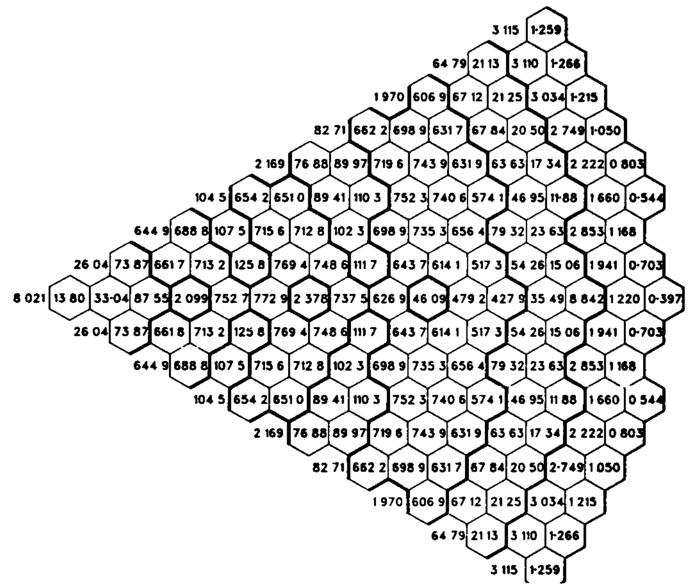

Fig. 9. Configuration B, Peak Power Density at BOL, Row 11 Rods Inserted

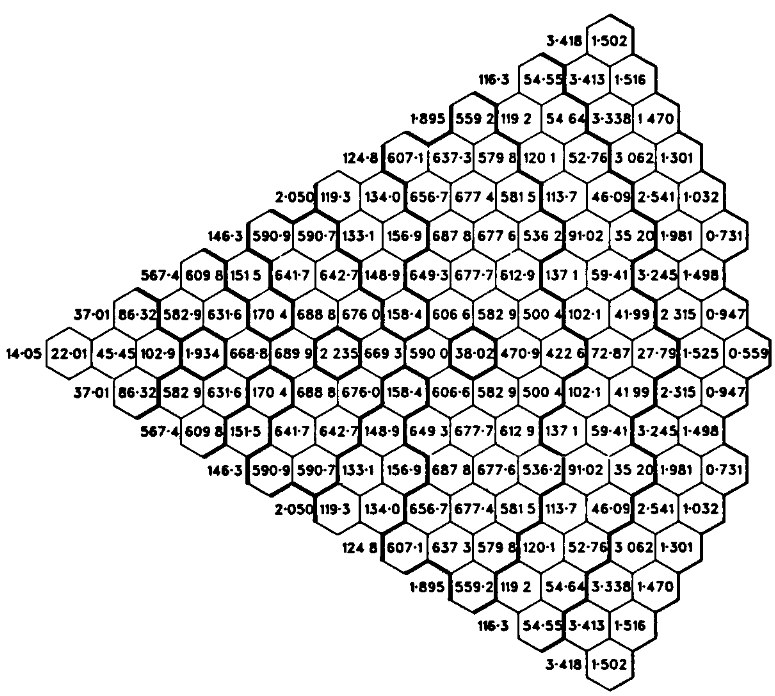

Fig. 10. Configuration B, Peak Power Density at BOEC

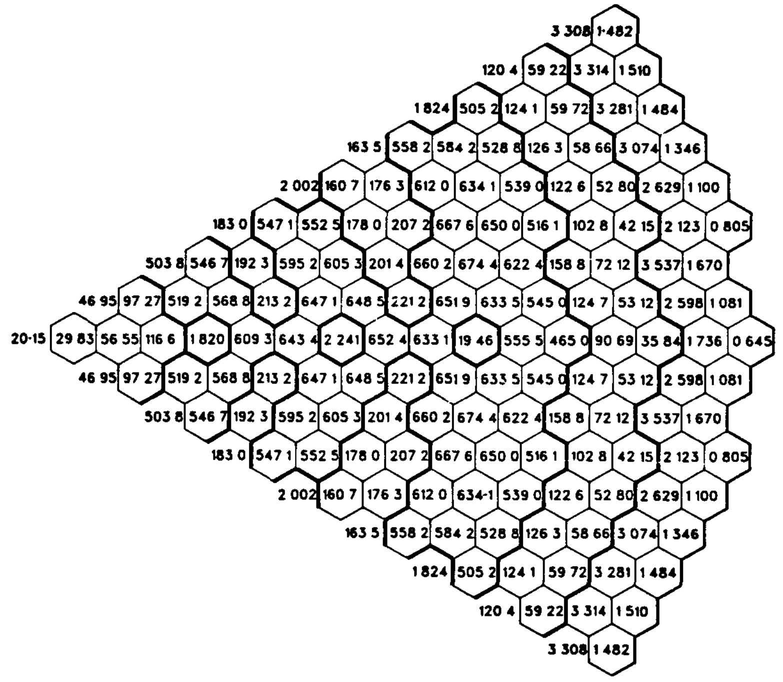

Fig. 11. Configuration B, Peak Power Density at MOEC

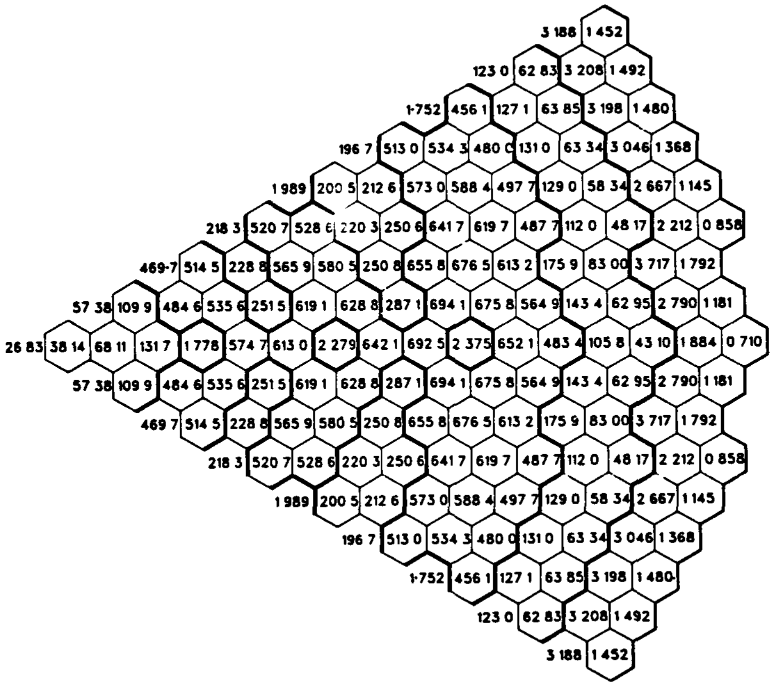

Fig. 12. Configuration B, Peak Power Density at EOEC

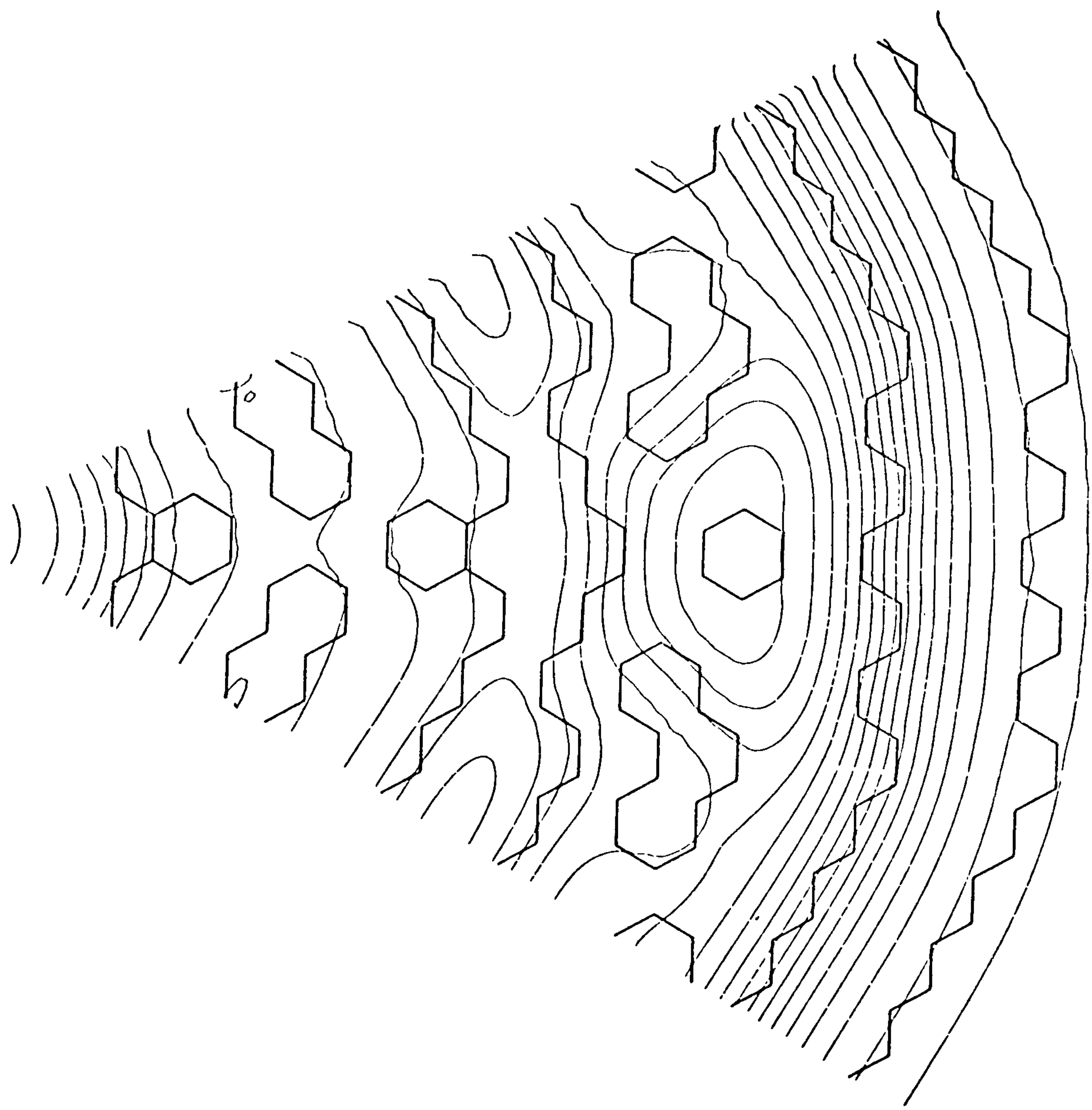

Fig. 13. Configuration A, Total Flux Distribution at BOL, No Control Inserted

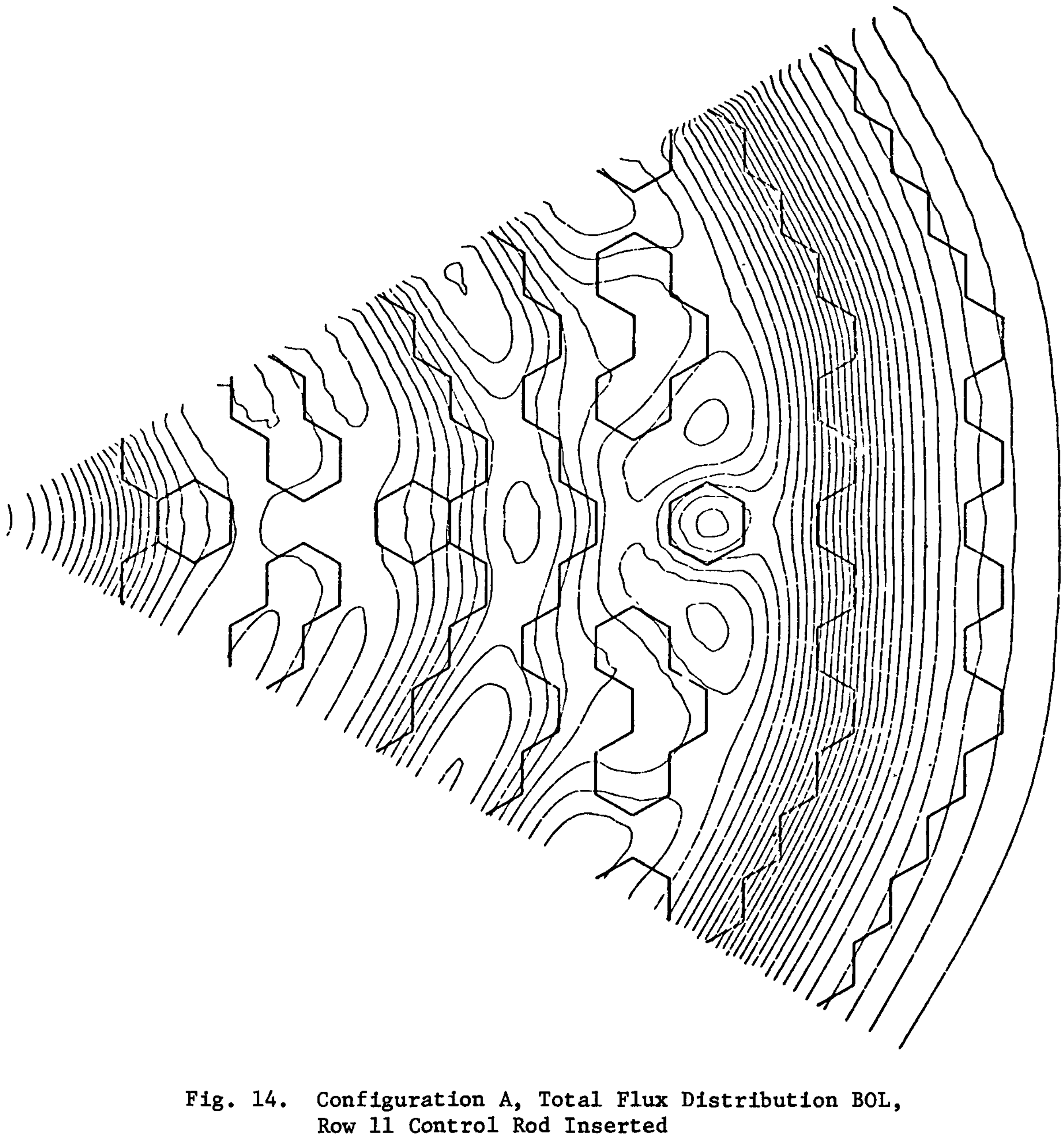

Fig. 14. Configuration A, Total Flux Distribution BOL, Row 11 Control Rod Inserted

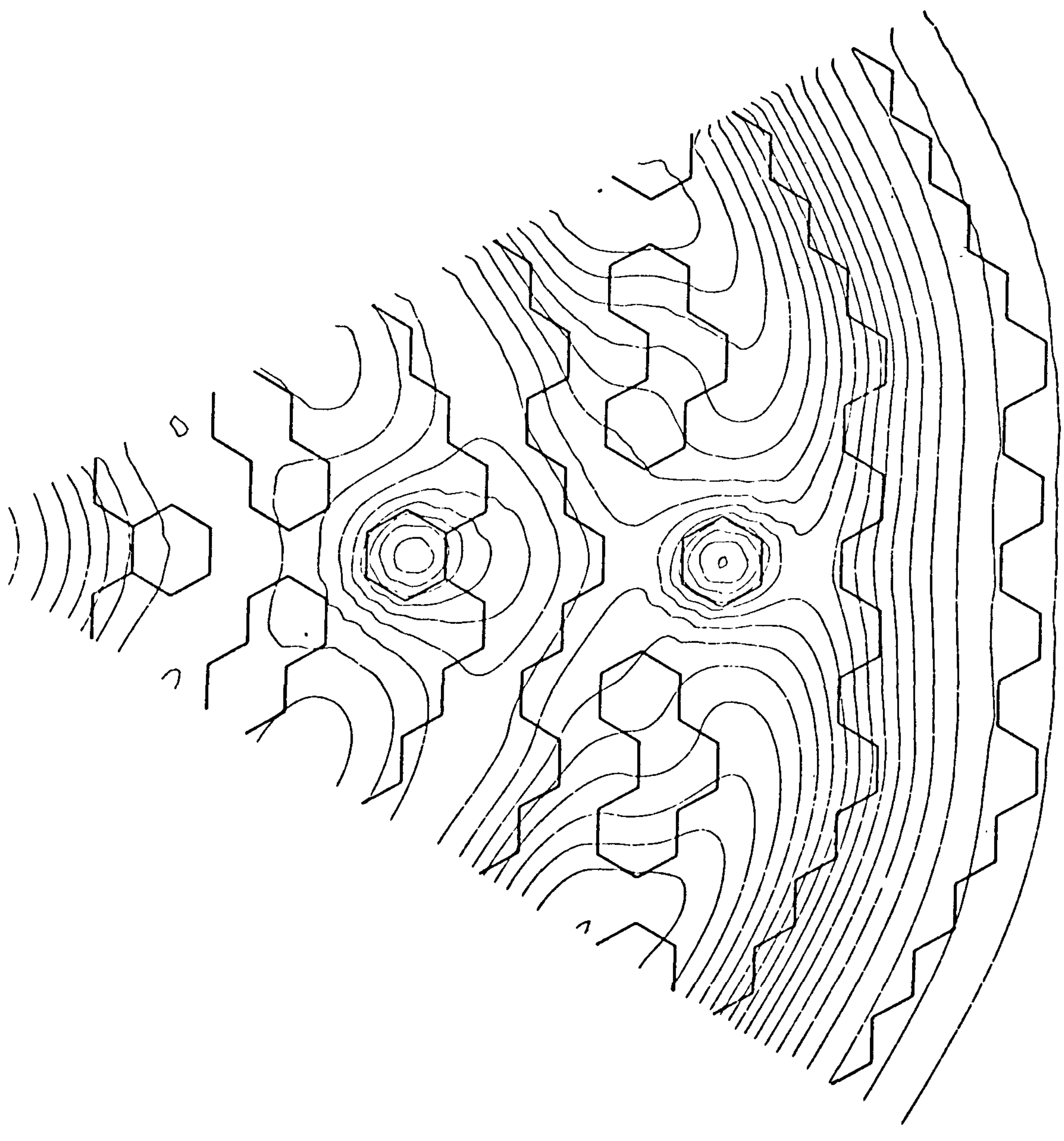

Fig. 15. Configuration A, Total Flux Distribution at BOL, Primary Control Rods Inserted

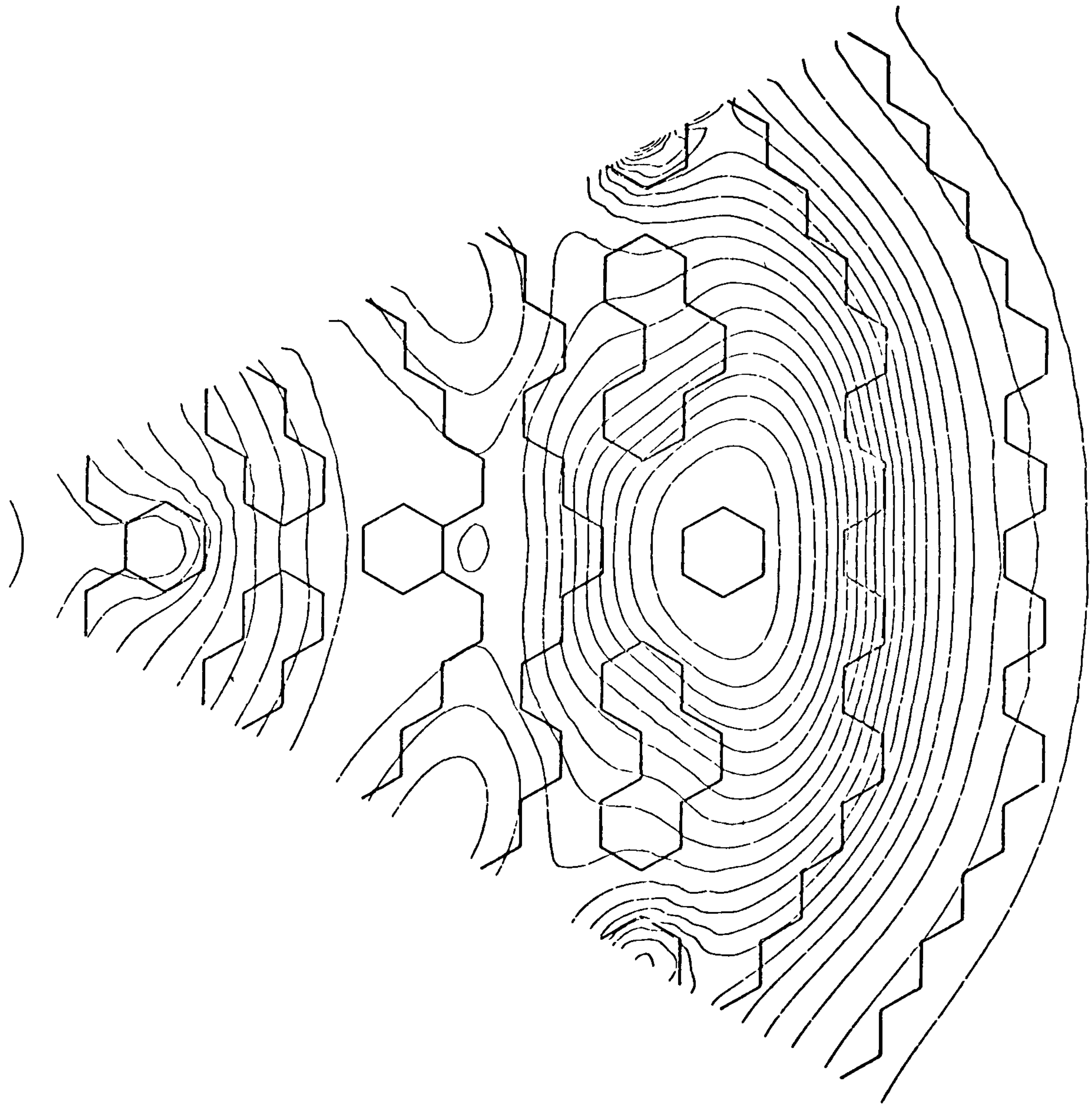

Fig. 16. Configuration A, Total Flux Distribution at BOL, Secondary Control Rods Inserted

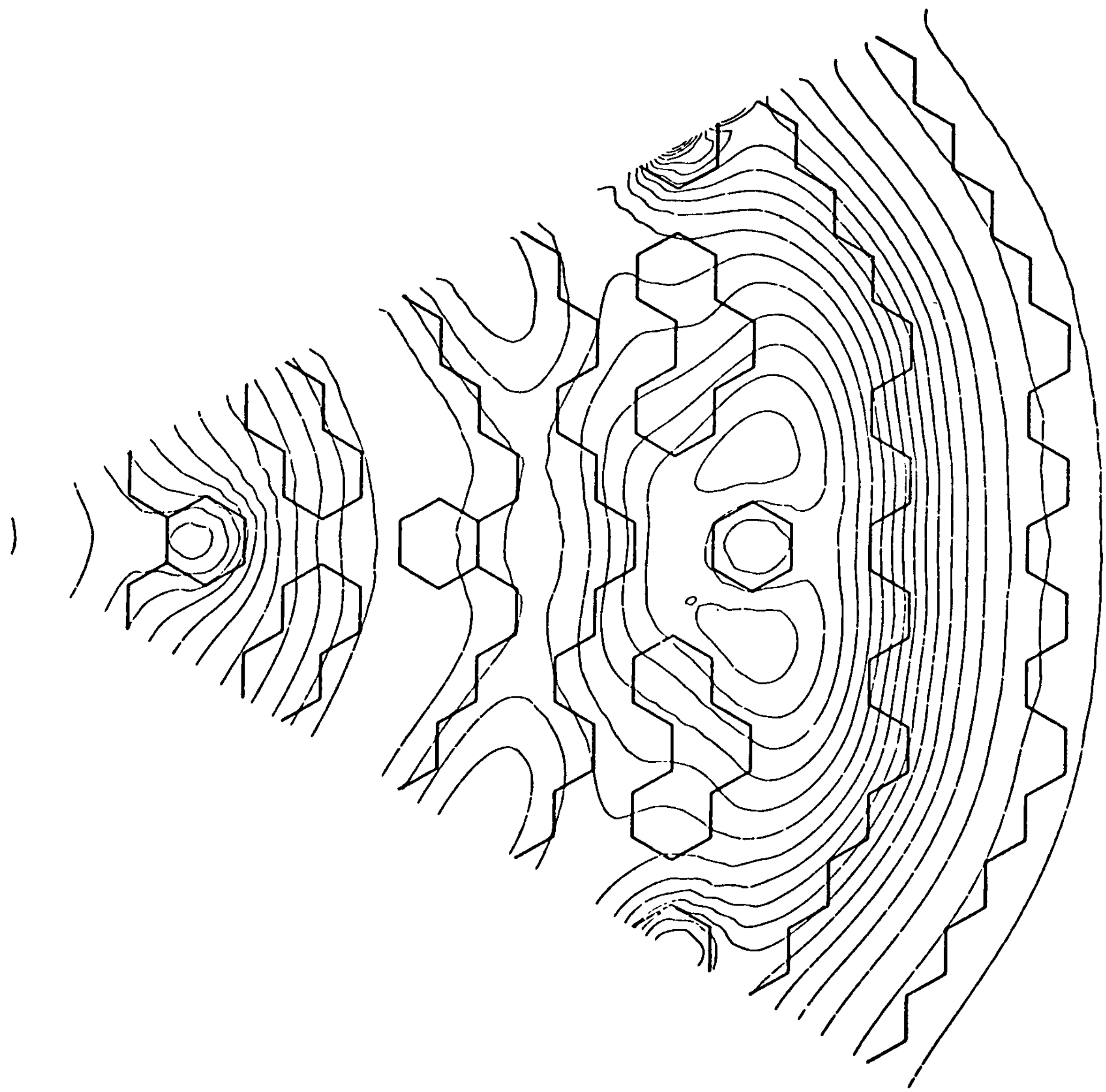

Fig. 17. Configuration A, Total Flux Distribution at BOL, Row 11 and Secondary Control Rods Inserted

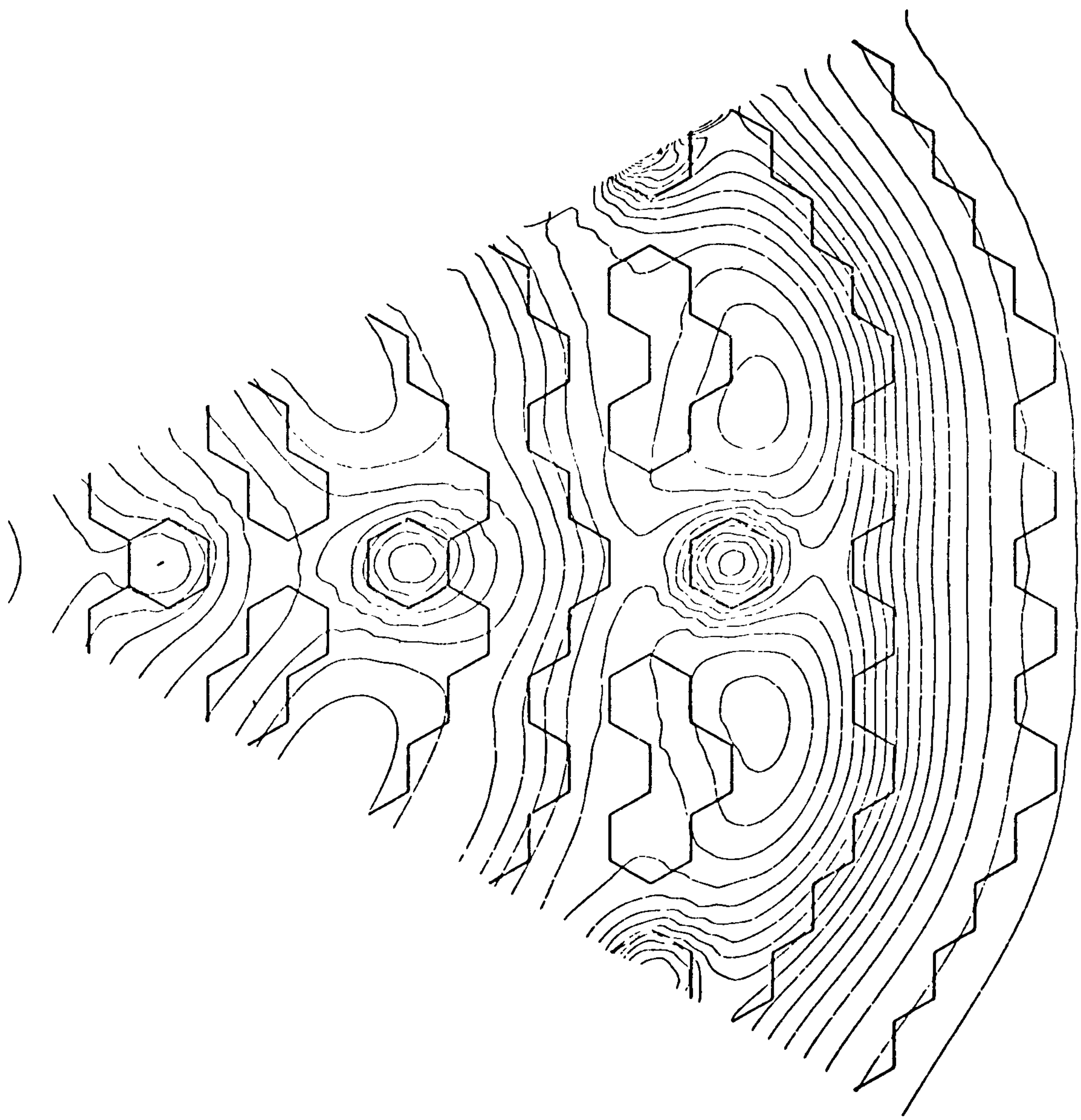

Fig. 18. Configuration A, Total Flux Distribution at BOL, All Rods Inserted

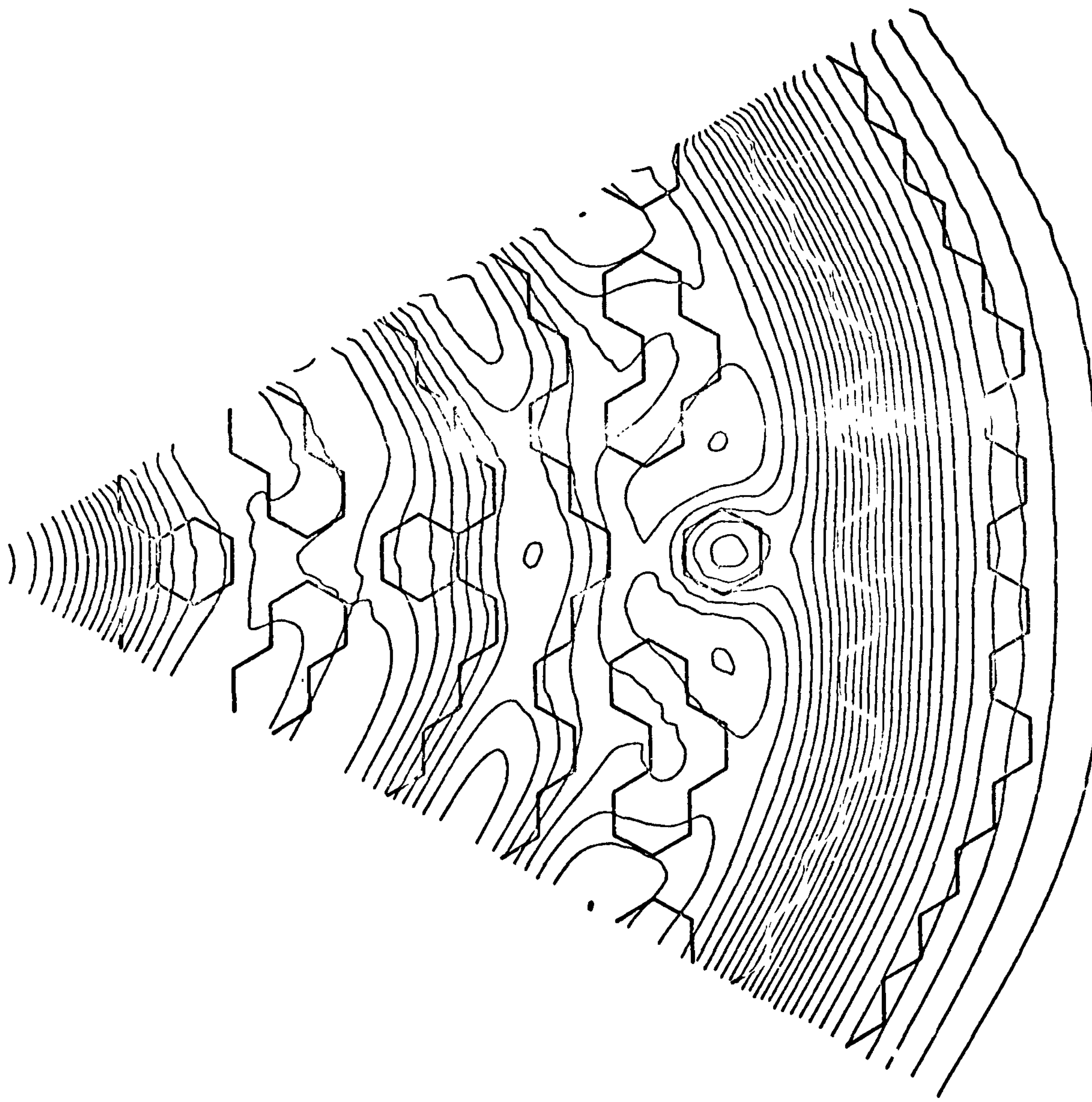

Fig. 19. Configuration A, Total Flux Distribution at BOEC

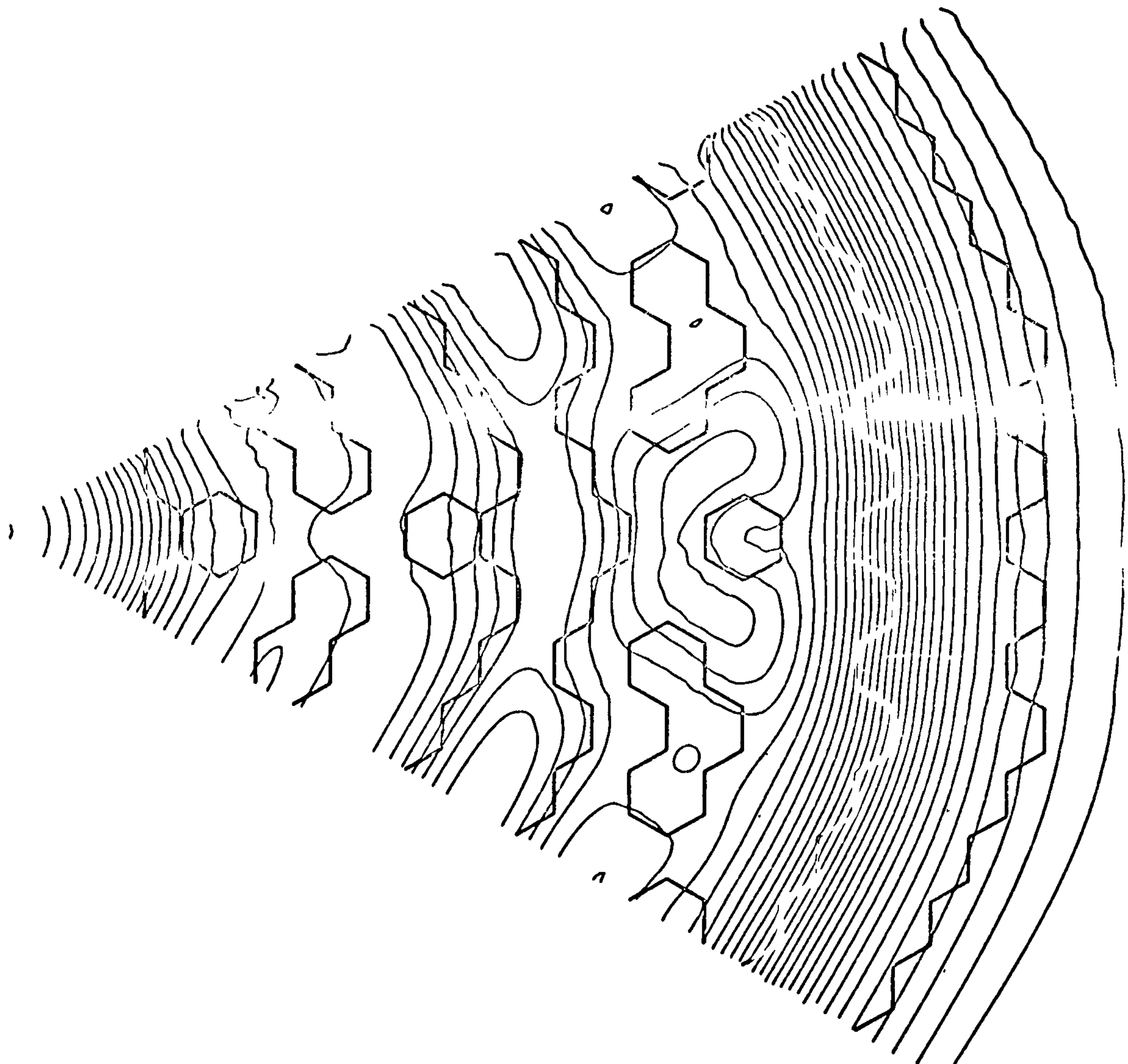

Fig. 20. Configuration A, Total Flux Distribution at MOEC

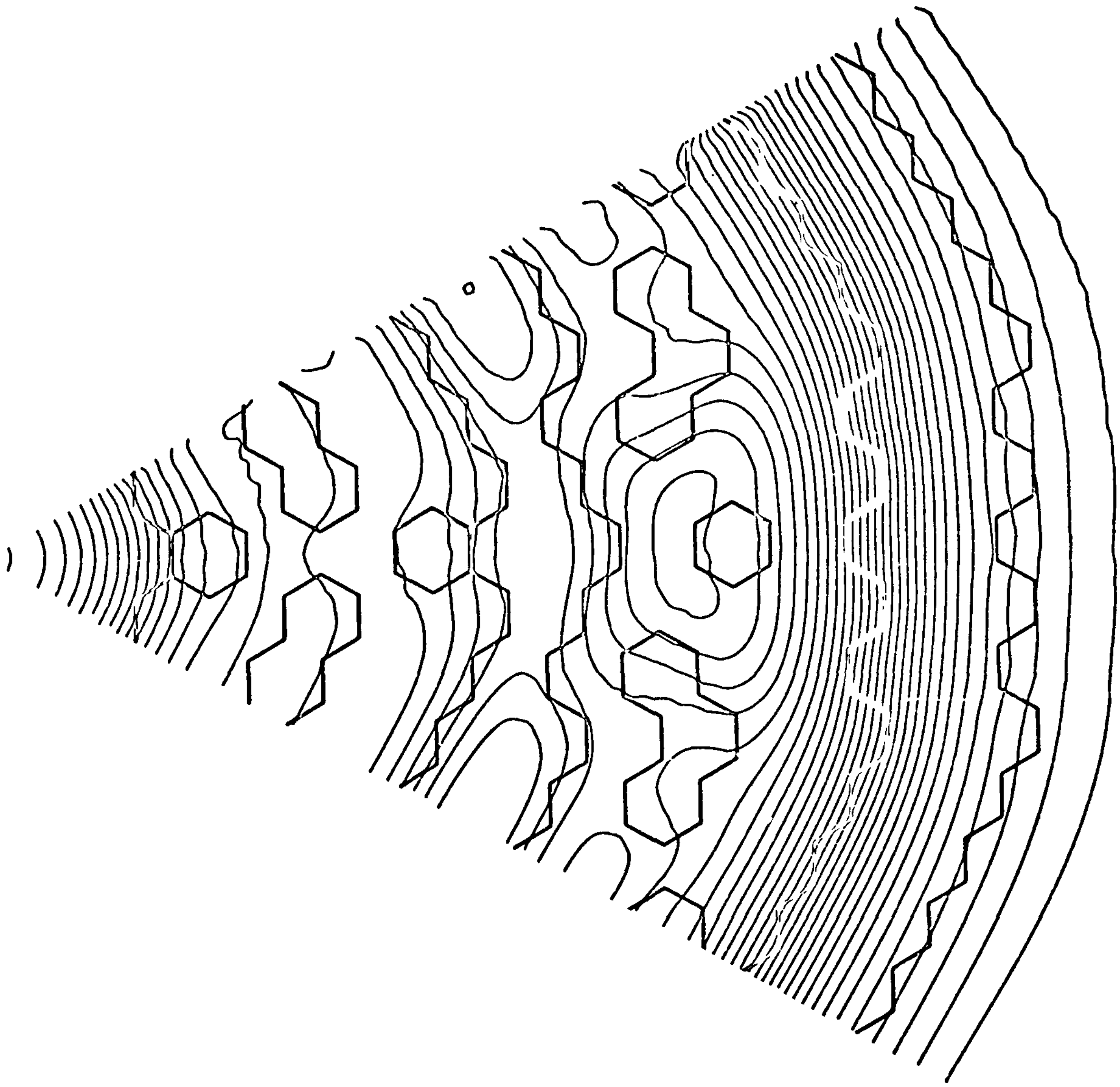

Fig. 21. Configuration A, Total Flux Distribution at EOEC

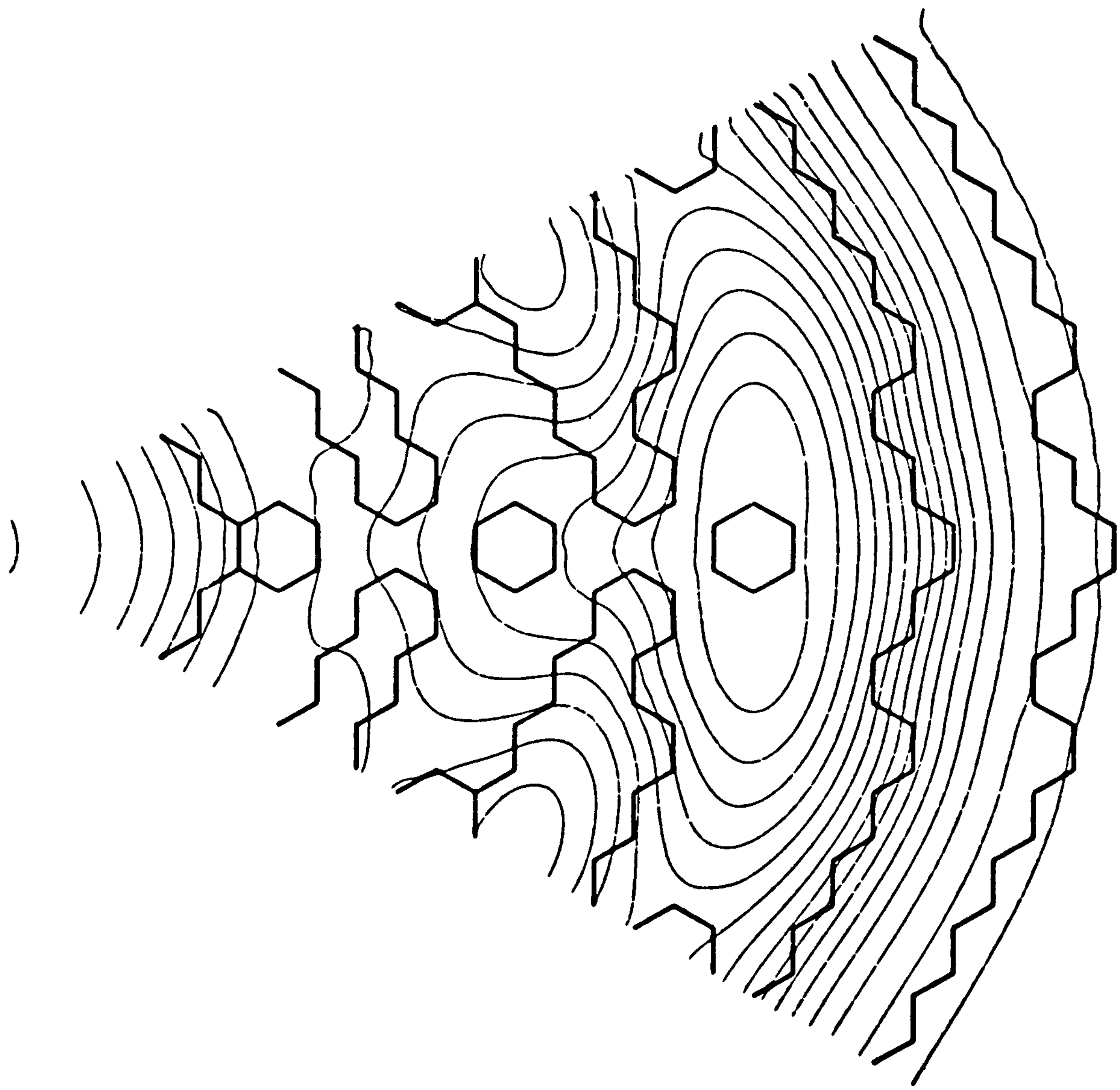

Fig. 22. Configuration B, Total Flux Distribution BOL, No Control Rods Inserted

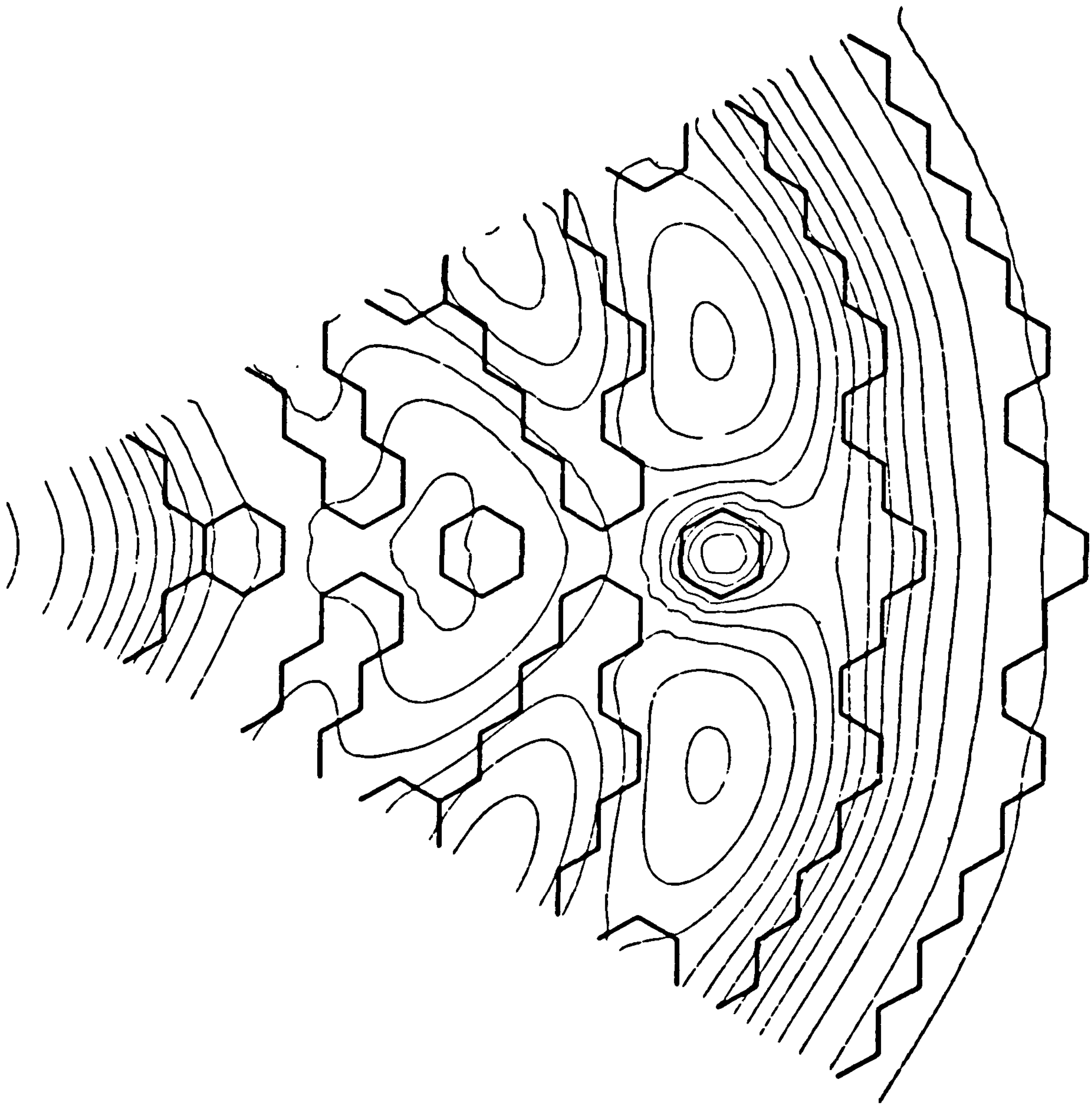

Fig. 23. Configuration B, Total Flux Distribution at BOL, Row 11 Control Rods Inserted

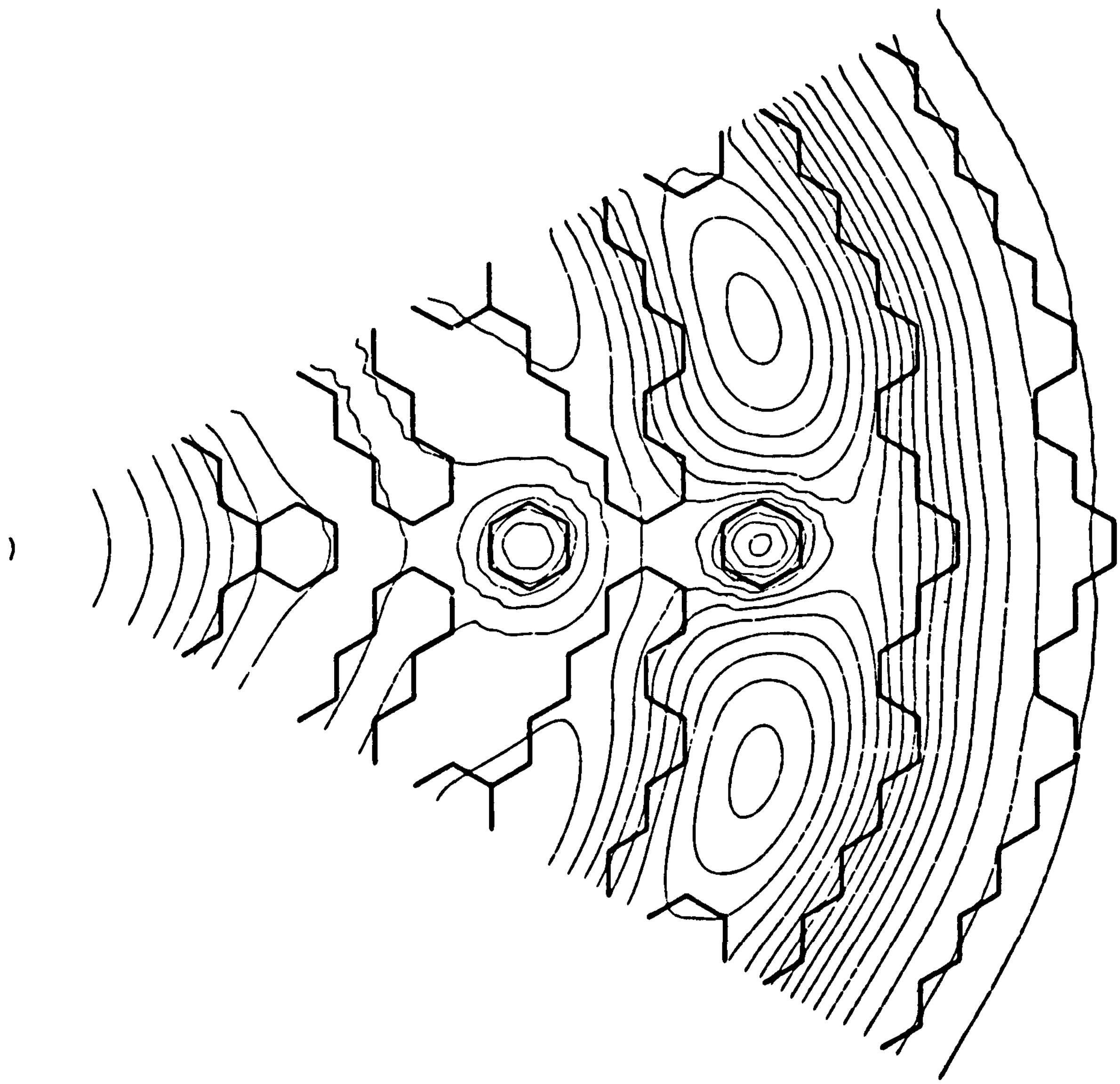

Fig. 24. Configuration B, Total Flux Distribution at BOL, Primary Control Rods Inserted

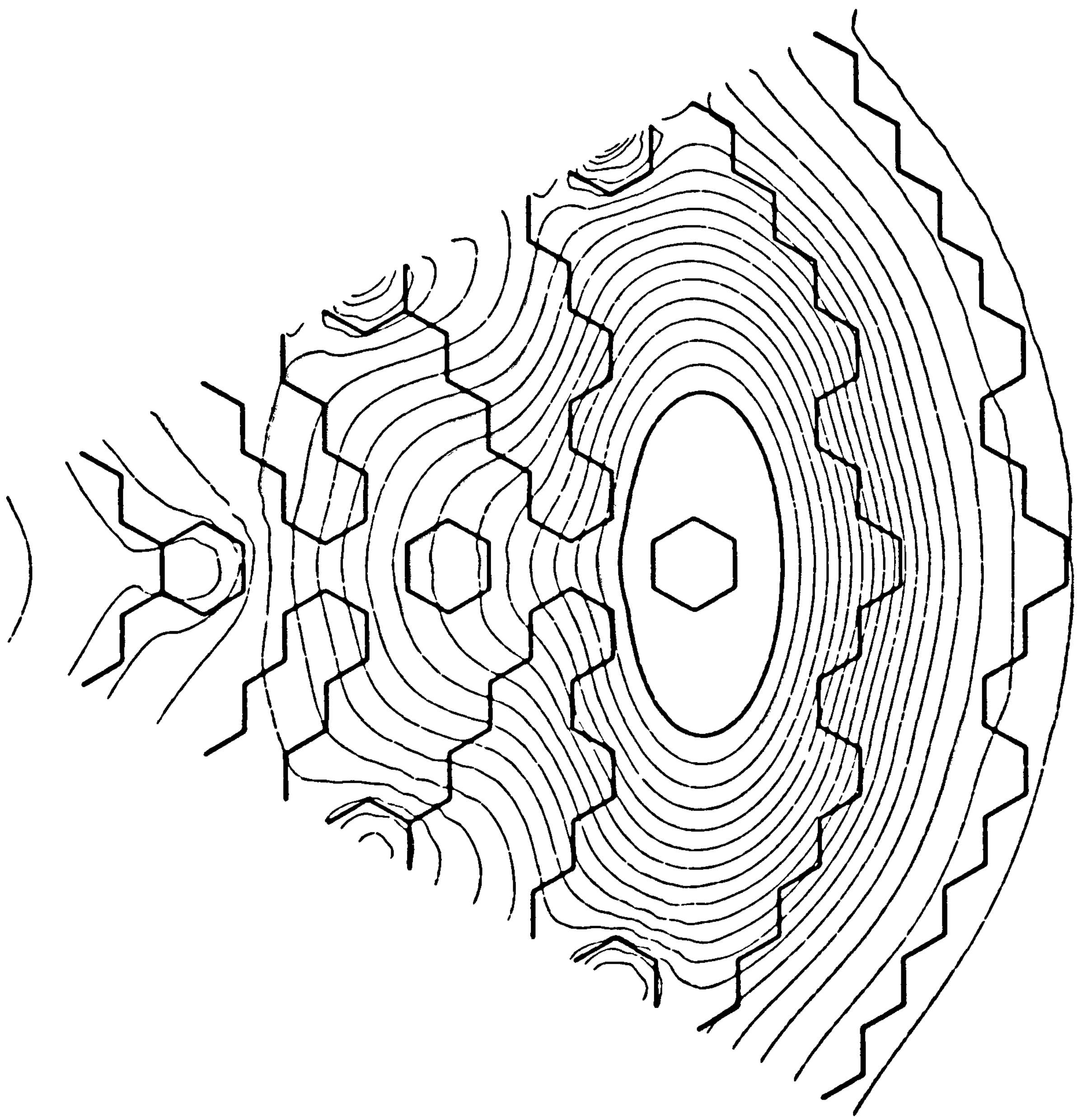

Fig. 25. Configuration B, Total Flux Distribution at BOL, Secondary Control Rods Inserted

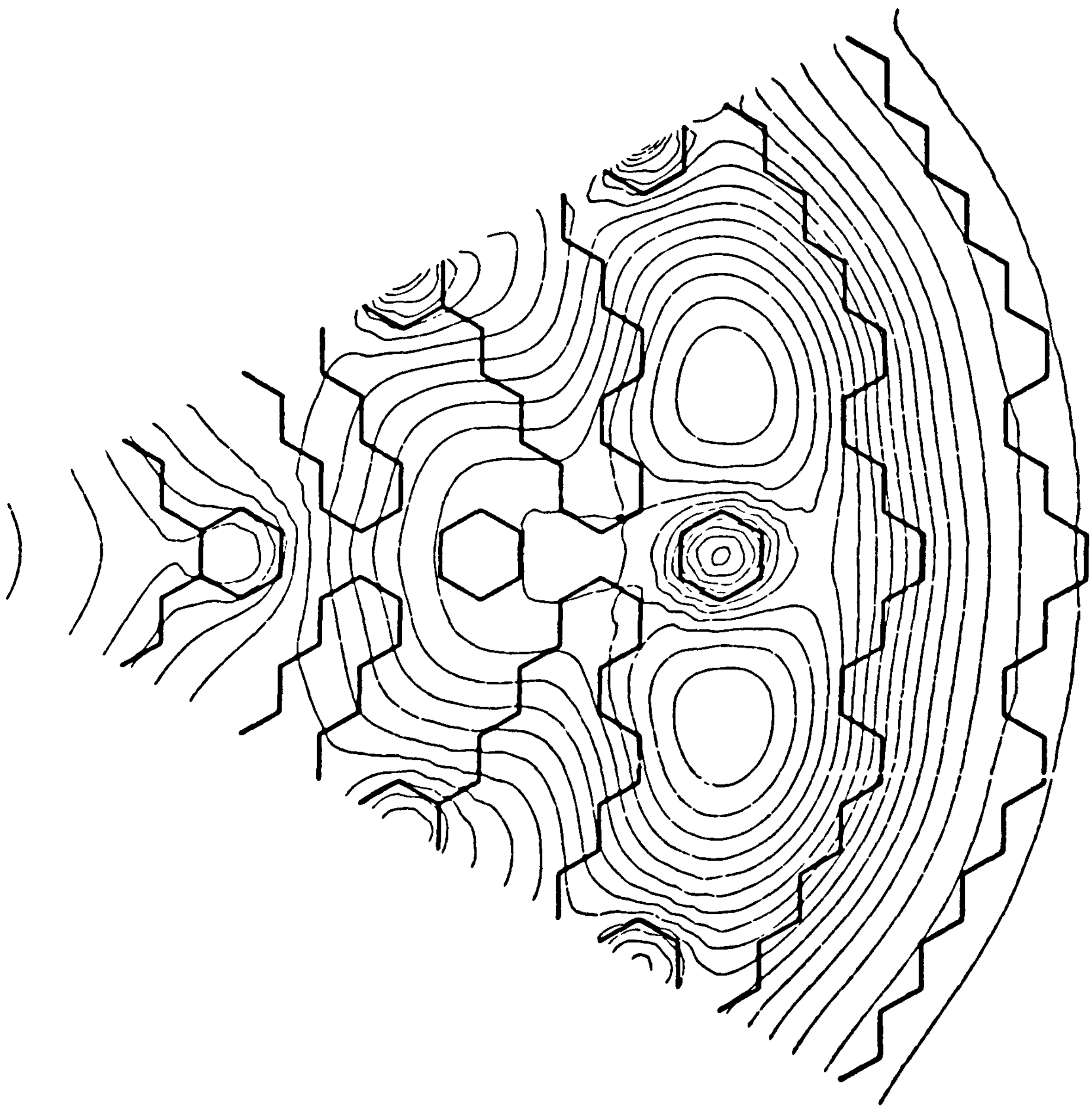

Fig. 26. Configuration B, Total Flux Distribution at BOL, Row 11 and Secondary Control Rods Inserted

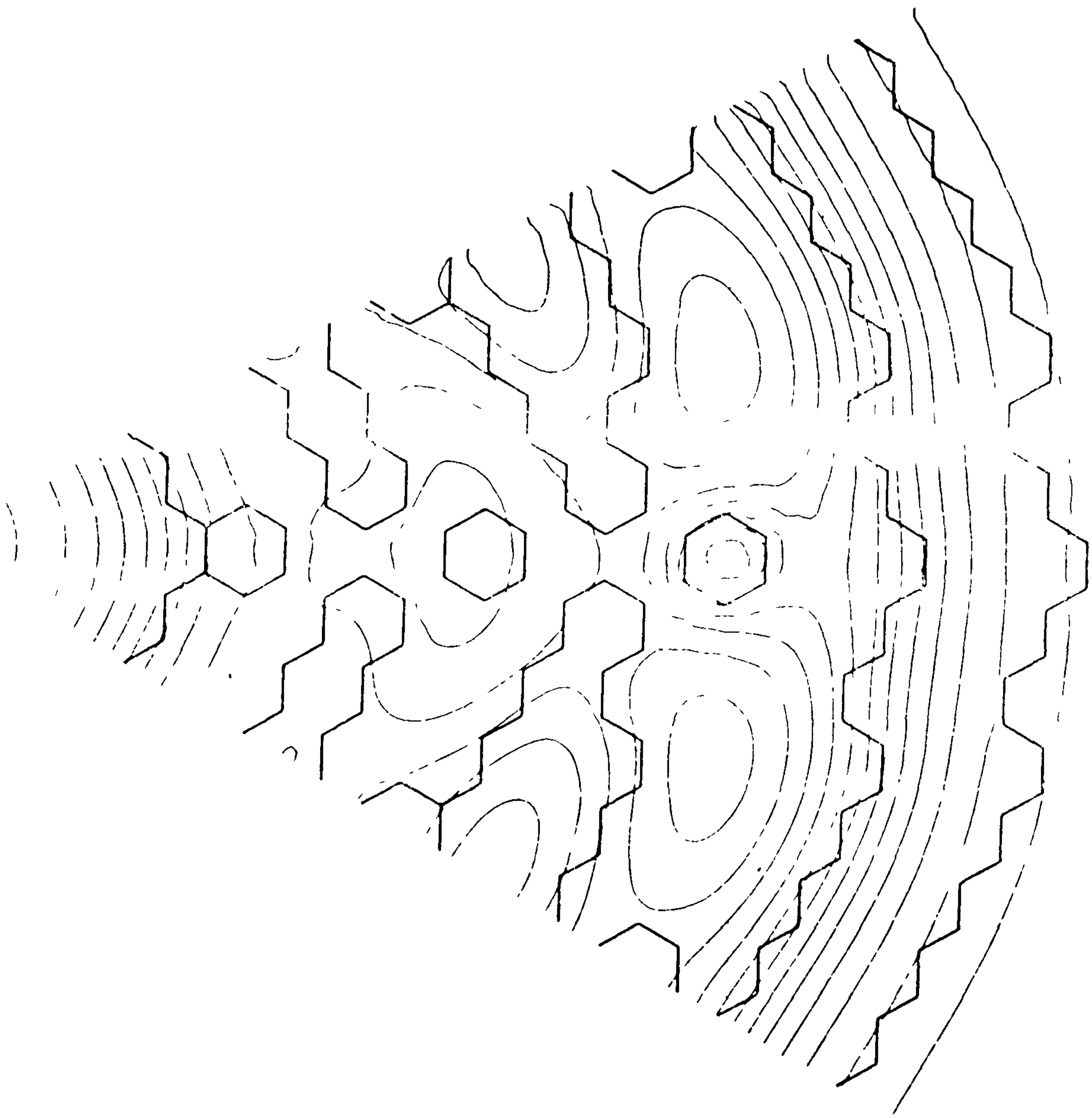

Fig. 27. Configuration B, Total Flux Distribution at BOEC

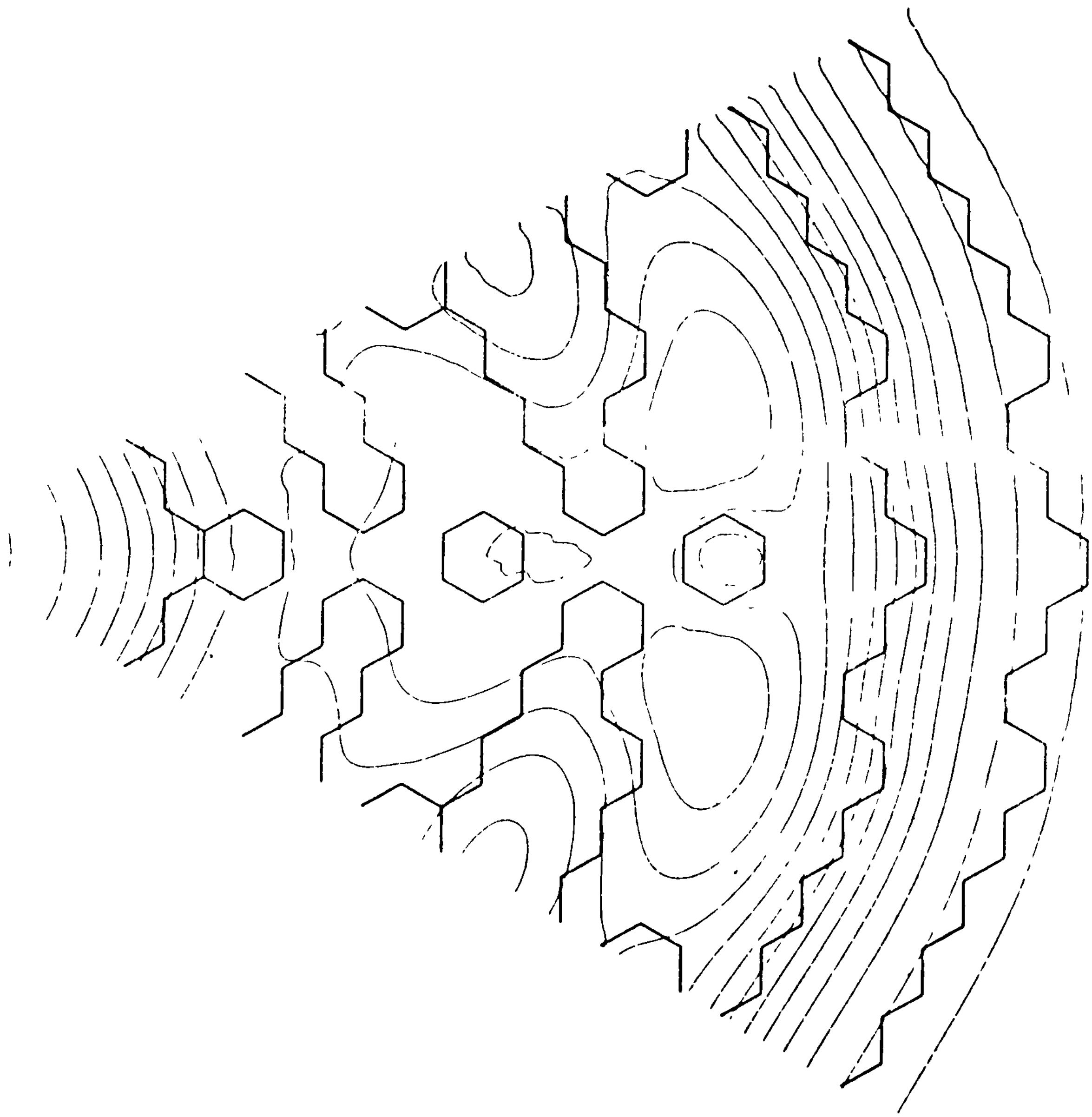

Fig. 28. Configuration B, Total Flux Distribution at MOEC

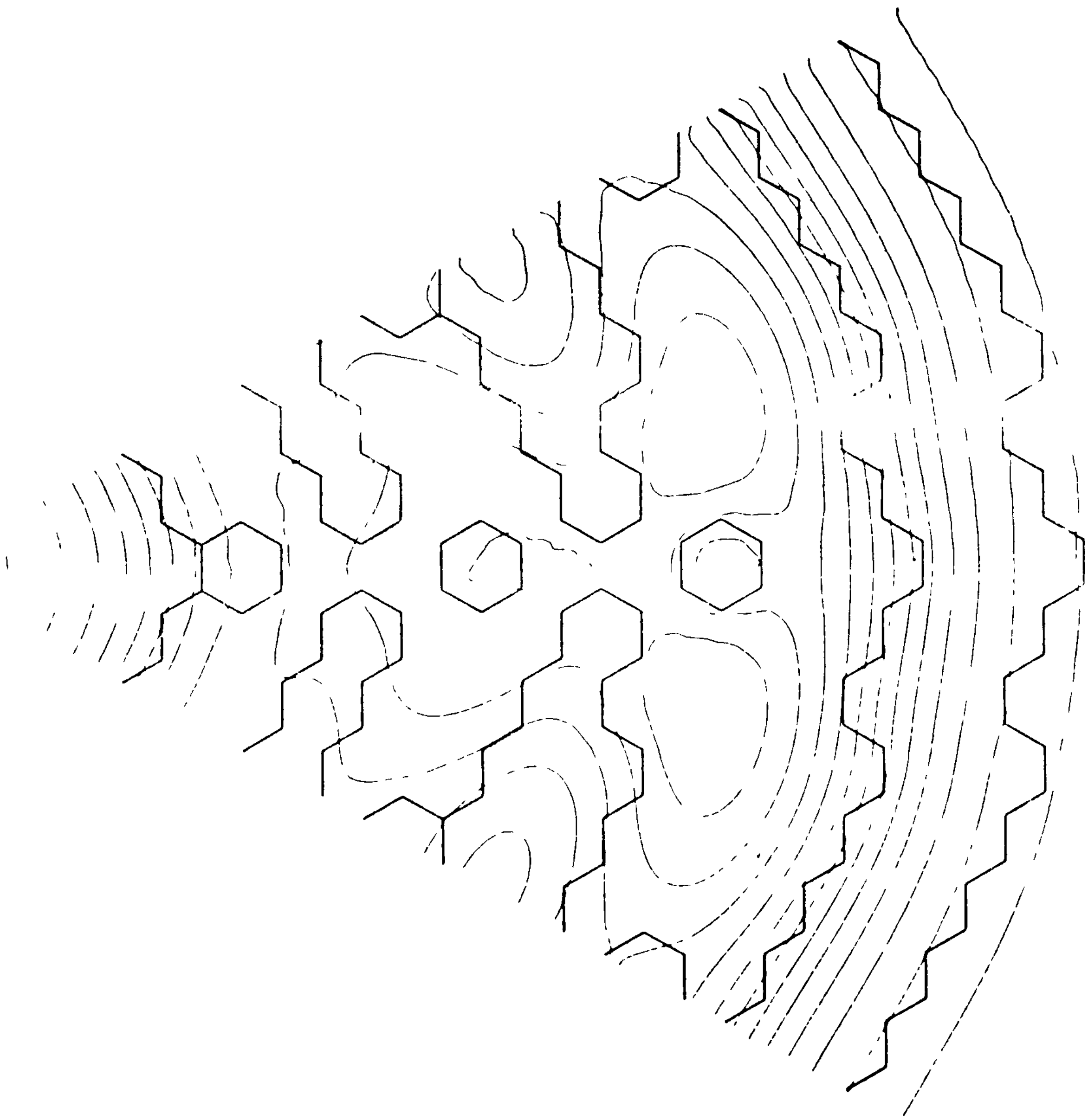

Fig. 29. Configuration B, Total Flux Distribution at EOEC

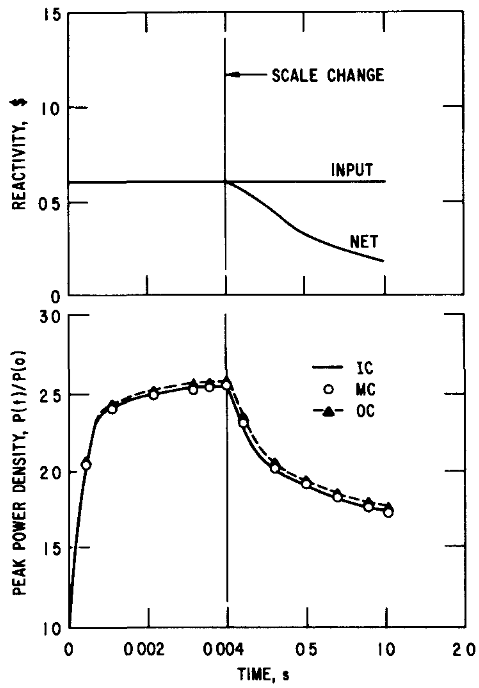

Fig. 30. 60¢ Reactivity Step Insertion, Configuration A

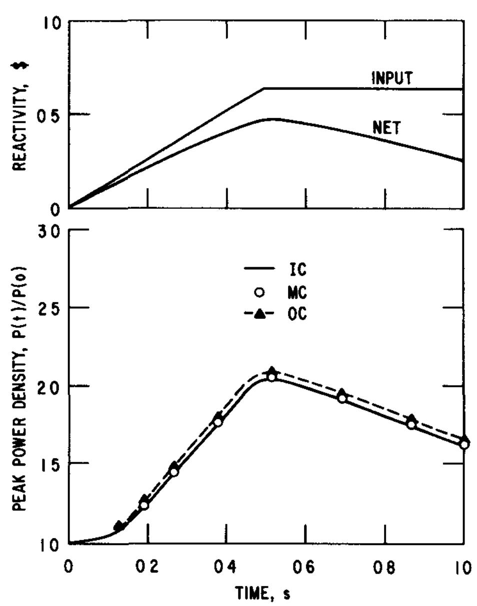

Fig. 31. 60¢/500 ms Reactivity Ramp, Configuration A

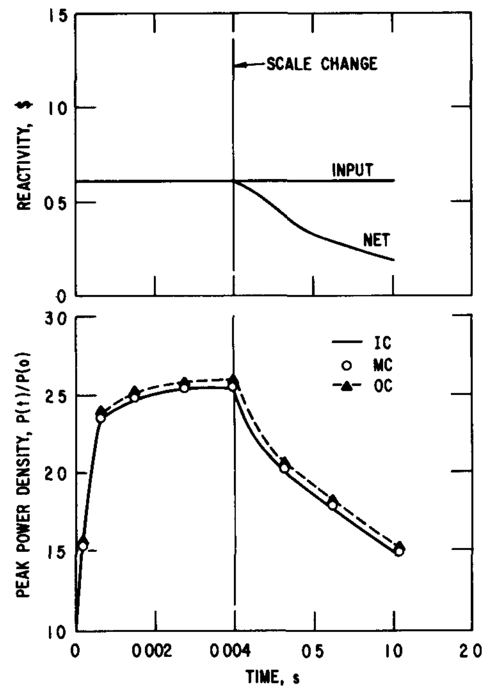

Fig. 32. 60¢ Reactivity Step Insertion, Configuration B

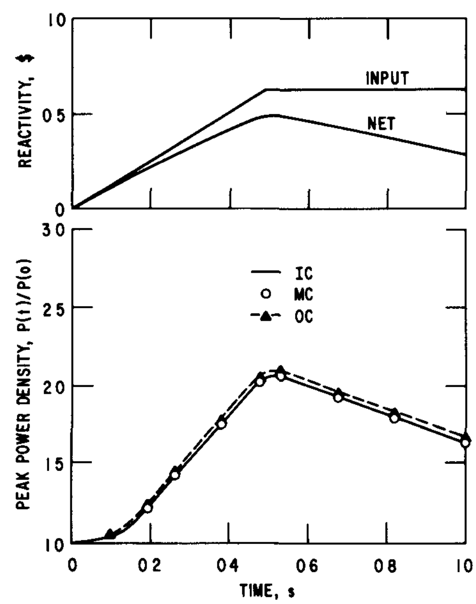

Fig. 33. 60¢/500 ms Reactivity Ramp, Configuration B

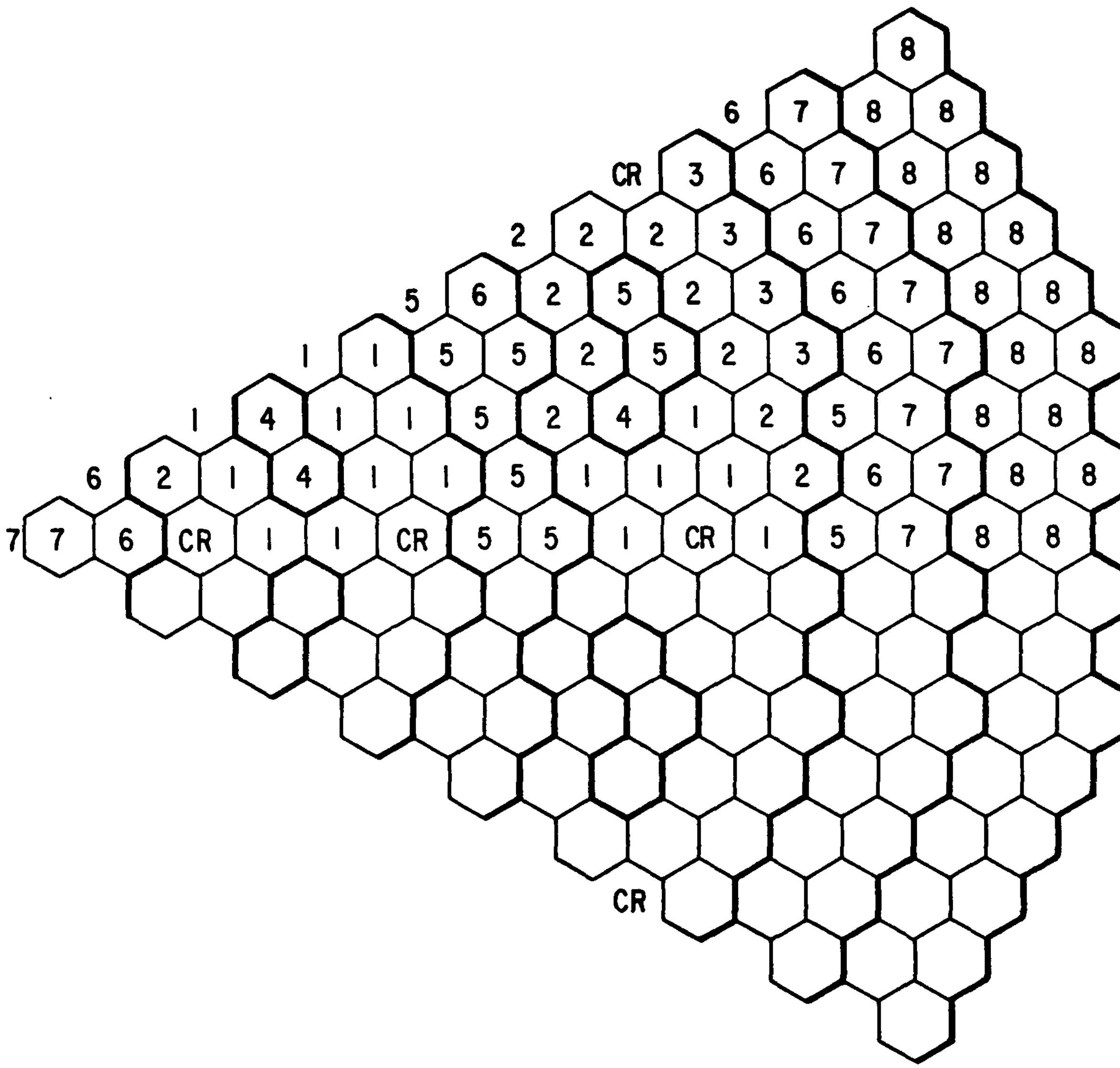

Fig. 34. Orificing Scheme of Configuration A with Equal Peak Clad Temperature at BOL in Core and at EOL in the Internal Blankets

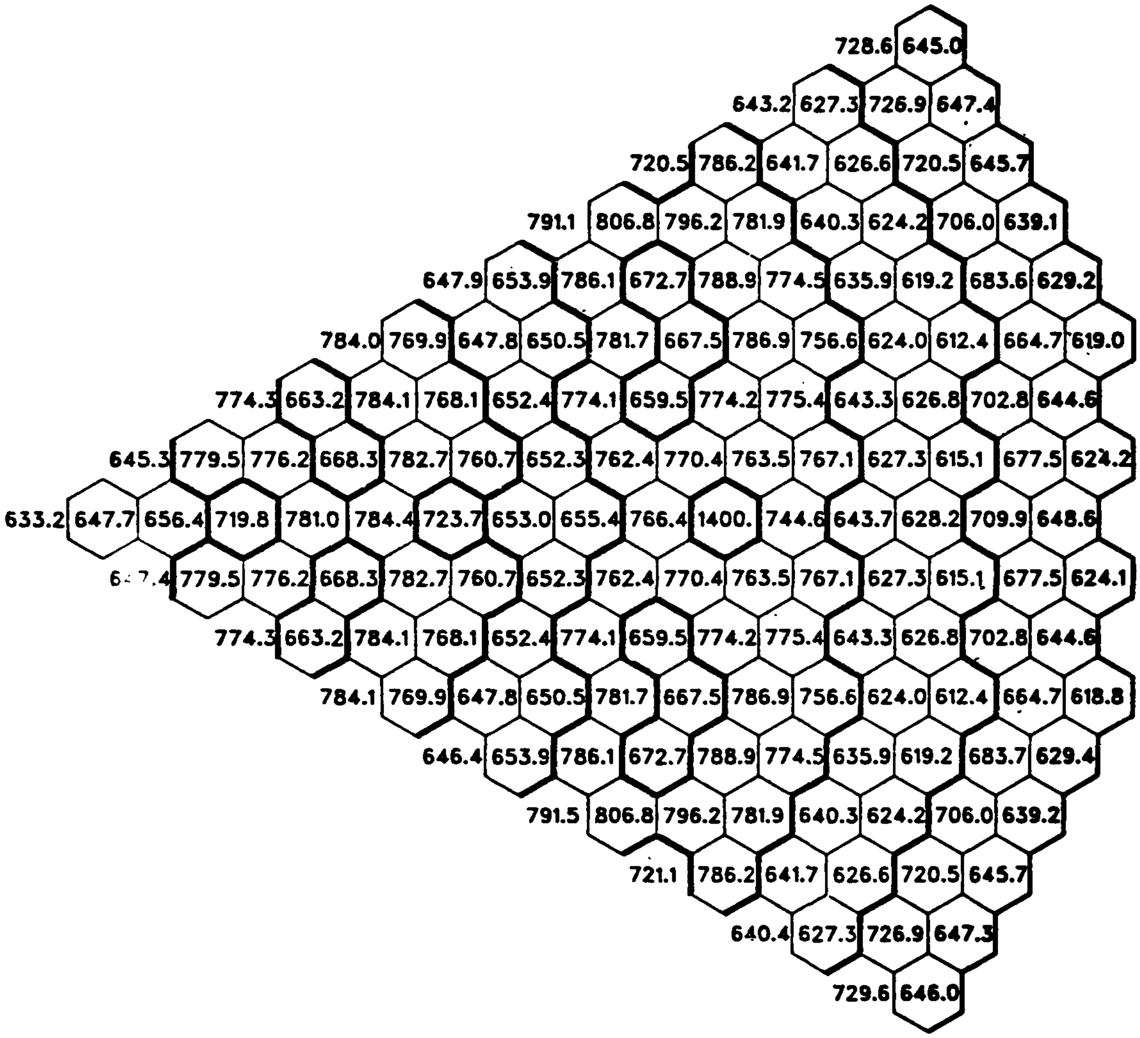

Fig. 35. Configuration A BOL Average Coolant Temperature at Core Mid-Plane (Orificed for Minimum Peak Temperature)

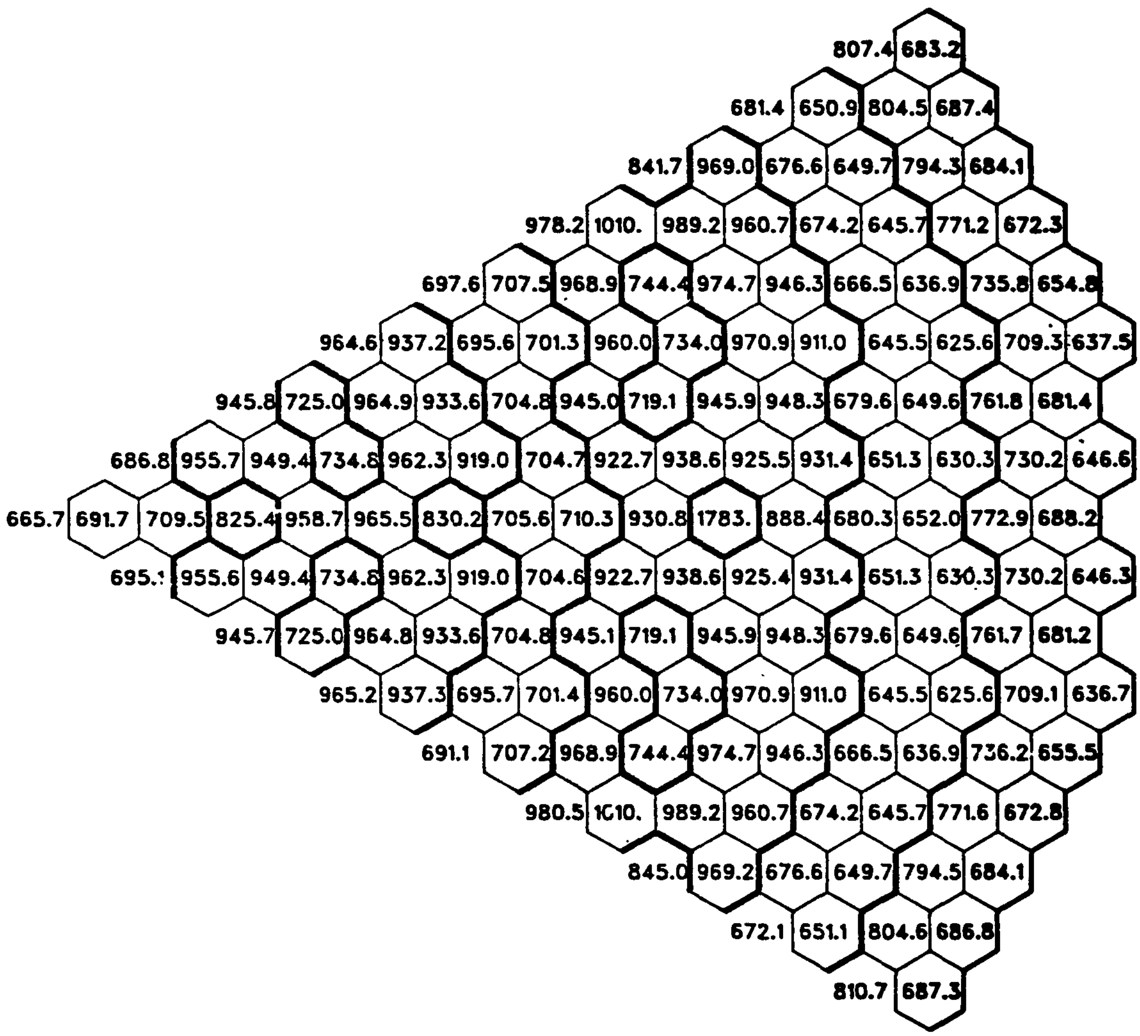

Fig. 36. Configuration A BOL Average Coolant Temperature at Top of Core (Orificed for Minimum Peak Temperature)

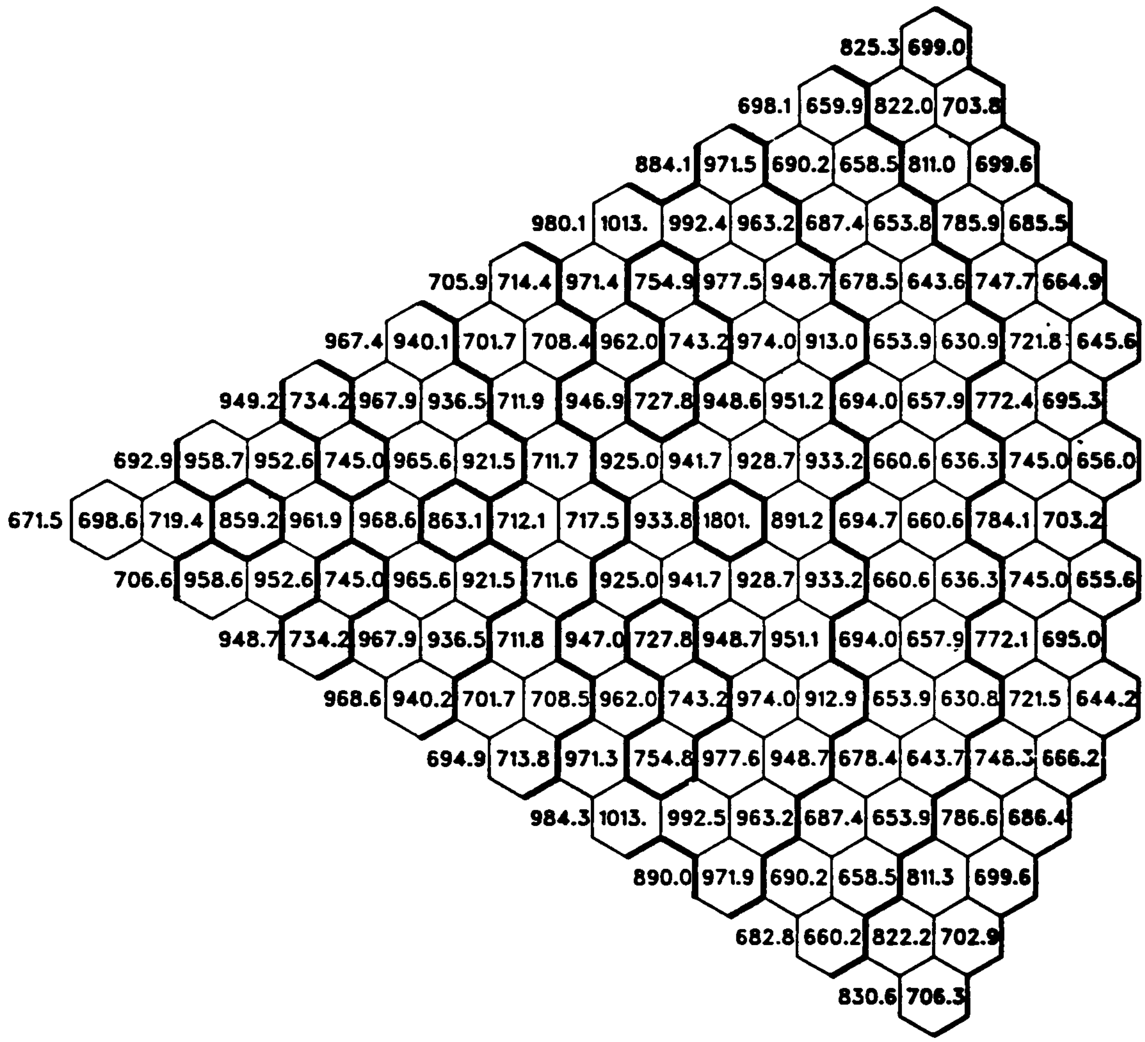

Fig. 37. Configuration A BOL Average Coolant Temperature at Outlet (Orificed for Minimum Peak Temperature)

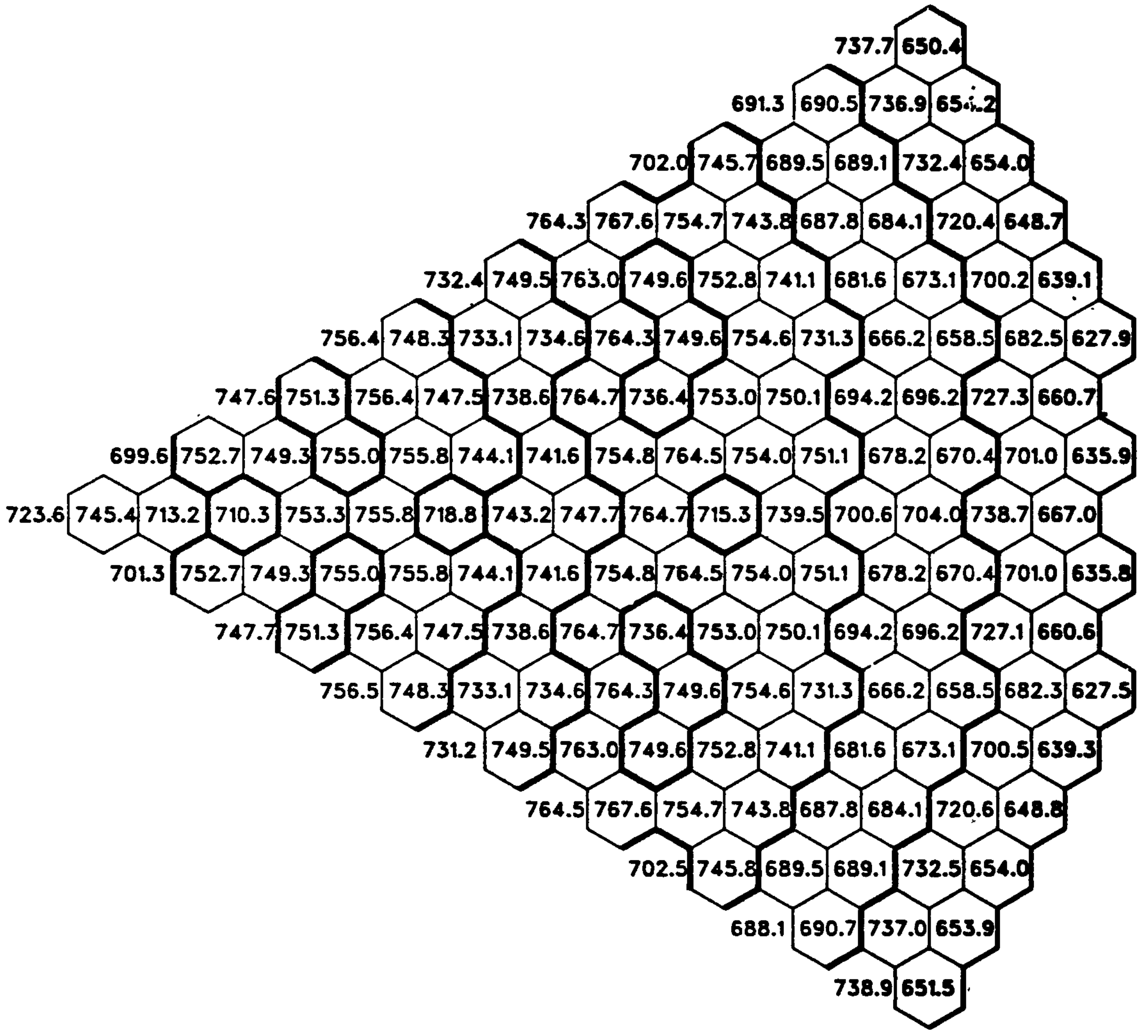

Fig. 38. Configuration A EOEC Average Coolant Temperature at Core Mid-Plane (Orificed for Minimum Peak Temperature)

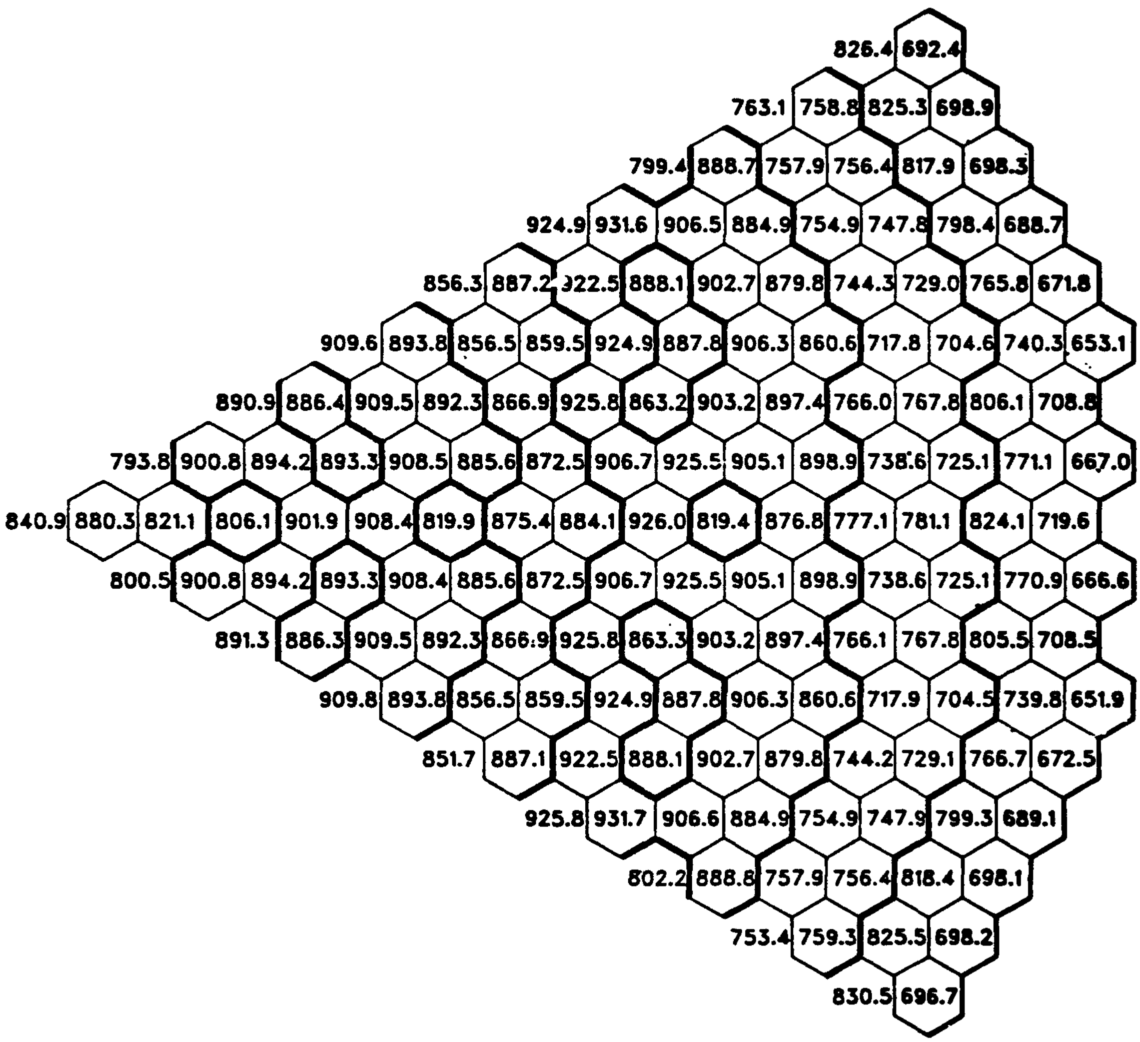

Fig. 39. Configuration A EOEC Average Coolant Temperature at Top of Core (Orificed for Minimum Peak Temperature)

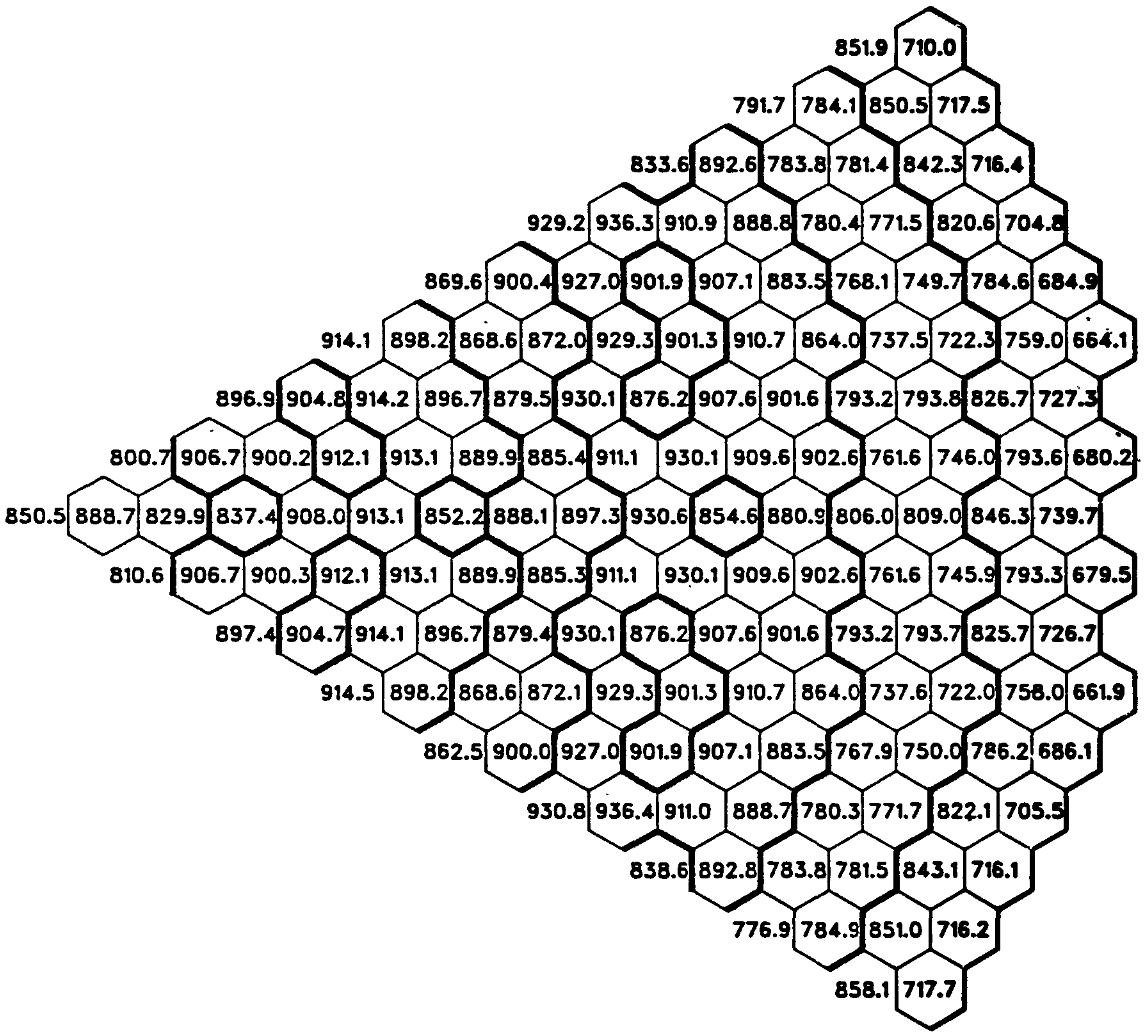

Fig. 40. Configuration A EOEC Average Coolant Temperature at Outlet (Orificed for Minimum Peak Temperature)

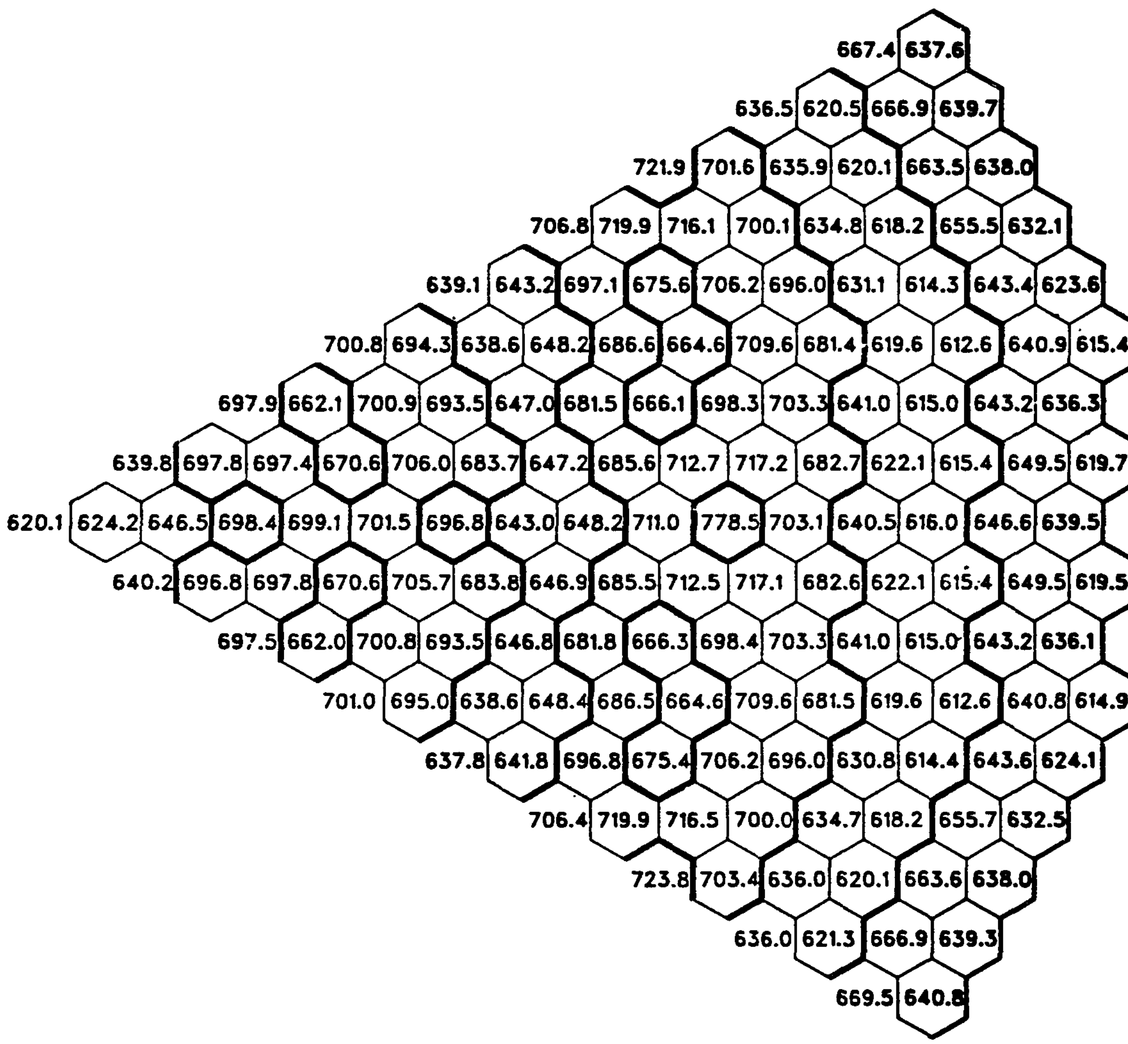

Fig. 41. Configuration A BOL Average Duct Wall Temperature at Core Mid-Plane (Orificed for Minimum Peak Temperature)

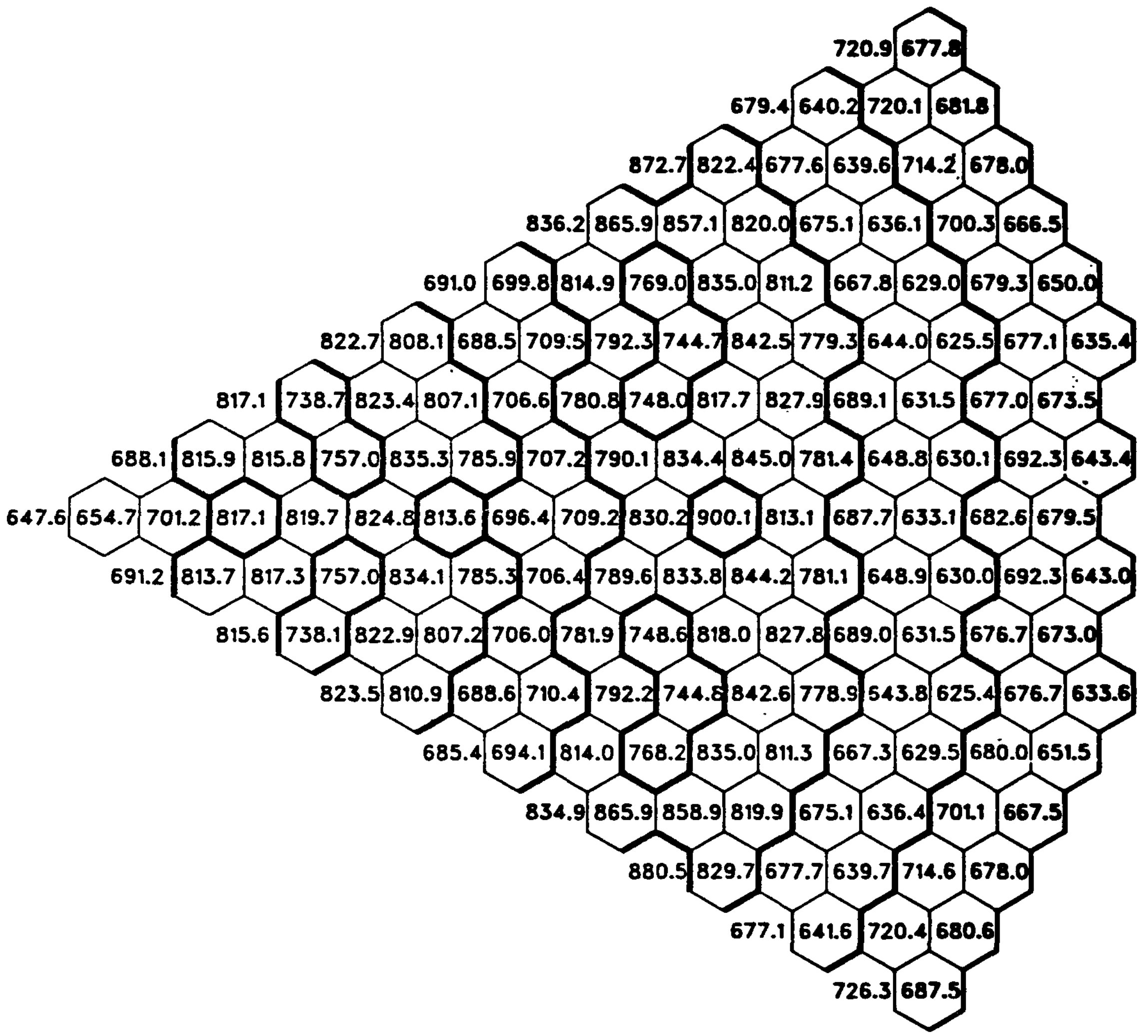

Fig. 42. Configuration A BOL Average Duct Wall Temperature at Top of Core (Orificed for Minimum Peak Temperature)

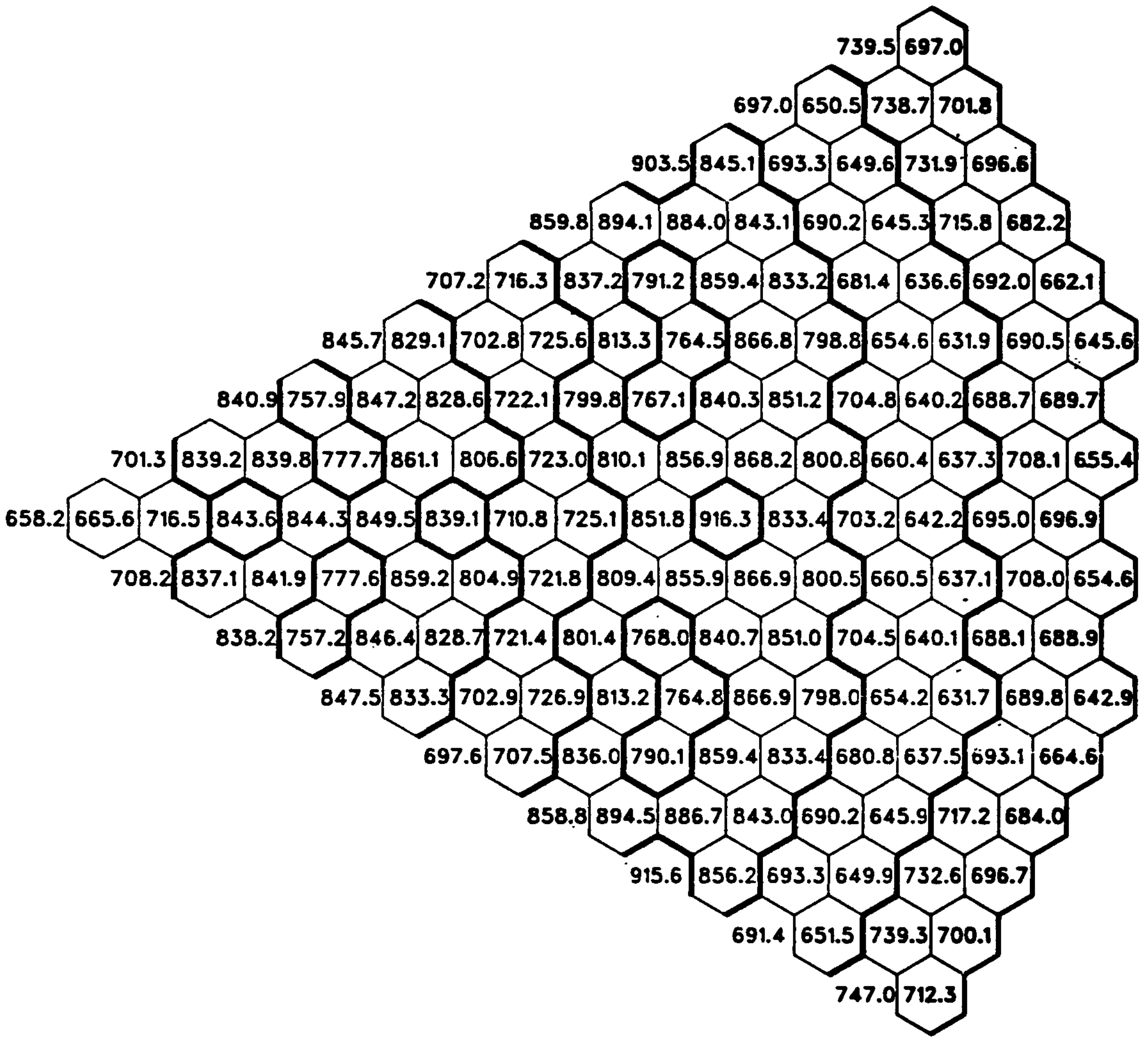

Fig. 43. Configuration A BOL Average Duct Wall Temperature at Outlet (Orificed for Minimum Peak Temperature)

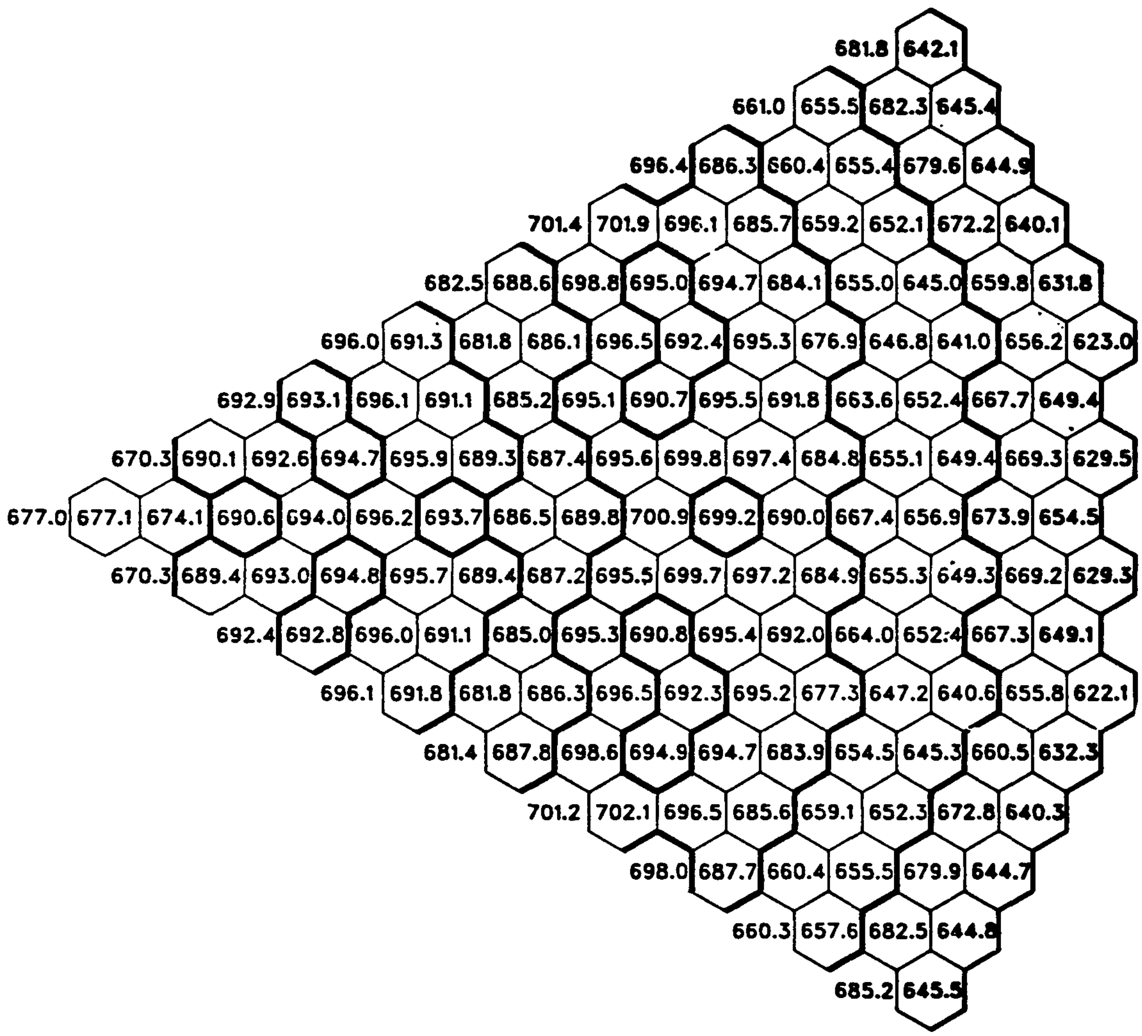

Fig. 44. Configuration A EOEC Average Duct Wall Temperature at Core Mid-Plane (Orificed for Minimum Peak Temperature)

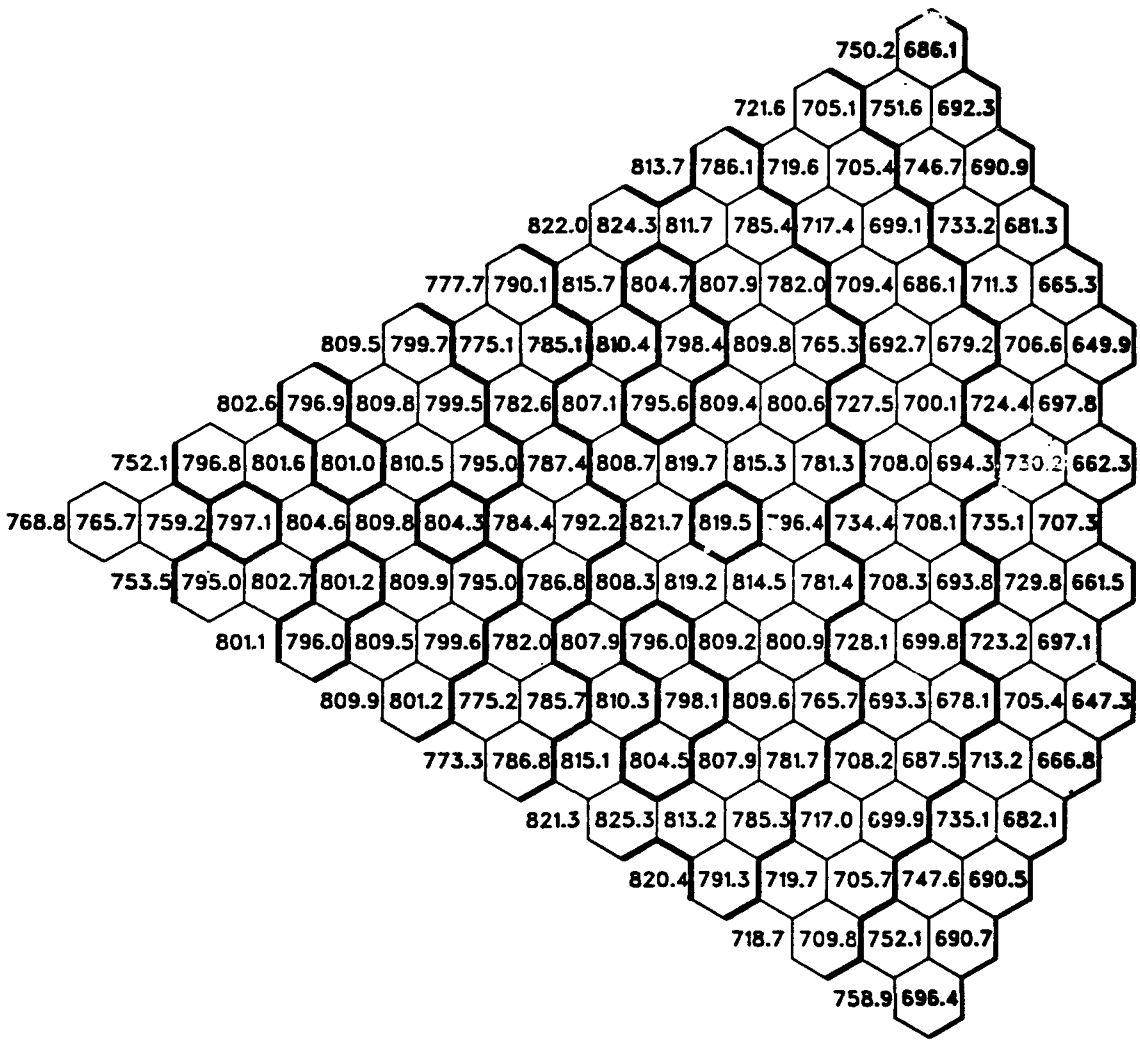

Fig. 45. Configuration A EOEC Average Duct Wall Temperature at Top of Core (Orificed for Minimum Peak Temperature)

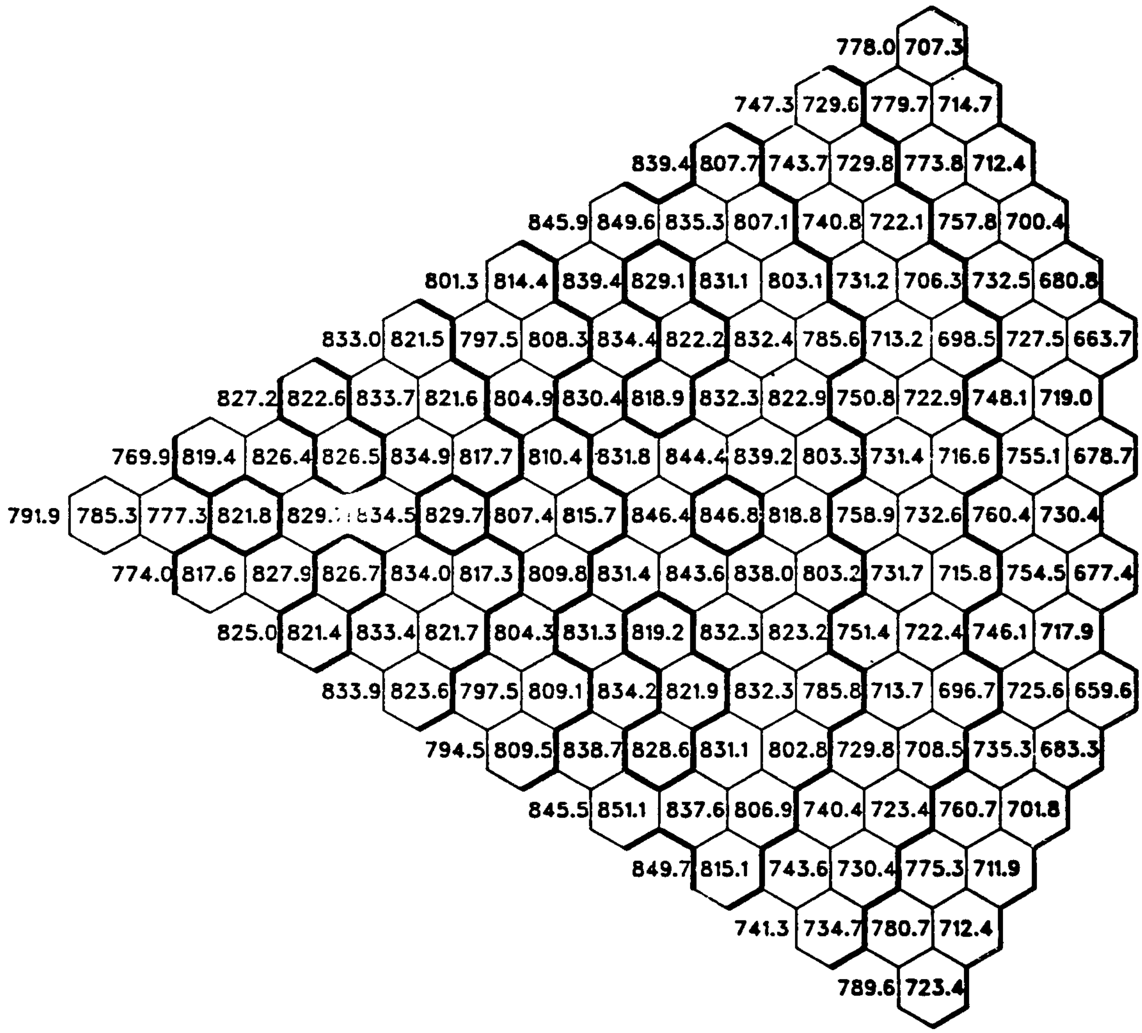

Fig. 46. Configuration A EOEC Average Duct Wall Temperature at Outlet (Orificed for Minimum Peak Temperature)

AXIAL DIST (IN)	ZSTAR	ALPSTA	AVERAGE TEMP	AVERAGE WALL TEMP
35.00	1.3461E 02	1.2556E-03	767.9	706.6

COOLANT TEMPERATURE BY SUBCHANNEL

```
                        708   710   709   708   706   705   703   702   700   698   697

                        710   767   769   767   765   763   761   759   756   751   699
                           768   783   782   779   777   775   773   770   767   750

                     712   785   791   790   787   785   782   780   778   775   765   699
                        773   793   792   790   787   785   783   780   778   774   753

                  713   787   794   793   790   788   786   783   781   778   775   765   698
                     775   794   794   792   789   787   784   782   780   777   773   752

               714   788   796   794   792   789   787   785   782   780   777   774   764   697
                  776   796   795   793   791   788   786   783   781   779   776   772   751

            715   790   797   795   793   791   788   786   783   781   779   776   773   763   697
               777   797   796   794   792   789   787   785   782   780   777   775   771   750

         716   791   798   797   794   792   789   787   785   782   780   777   775   772   761   696
            778   798   798   795   793   791   788   786   783   781   779   776   774   770   749

      717   792   799   798   795   793   791   788   786   783   781   779   776   774   771   760   695
         779   799   799   797   794   792   789   787   785   782   780   777   775   773   768   748

   718   793   801   799   797   794   792   789   787   785   782   780   777   775   773   770   759   694
      780   800   800   798   795   793   791   788   786   783   781   779   776   774   771   767   747

718   793   802   800   798   795   793   791   788   786   783   781   779   776   774   771   768   757   694
   777   801   801   799   797   794   792   789   787   785   782   780   777   775   773   770   766   742
716                                                                                                       694
   777   801   801   799   797   794   792   789   787   785   782   780   777   775   773   770   766   743
717   793   802   800   798   795   793   791   788   786   783   781   779   776   774   771   768   758   696

      780   800   800   798   796   793   791   788   786   784   781   779   776   774   771   767   747
   717   793   801   799   797   794   792   790   787   785   782   780   778   775   773   770   759   697

         779   799   799   797   794   792   790   787   785   782   780   778   775   773   769   748
      718   792   800   798   796   793   791   788   786   784   781   779   776   774   771   761   698

            779   798   798   796   793   791   788   786   784   781   779   776   774   770   749
         718   791   798   797   794   792   790   787   785   782   780   778   775   772   762   698

               778   797   797   794   792   790   787   785   782   780   778   775   771   751
            717   790   797   796   793   791   788   786   784   781   779   776   773   763   699

                  777   796   795   793   791   788   786   784   781   779   776   772   752
               717   789   796   794   792   790   787   785   782   780   778   775   764   700

                     776   795   794   792   790   787   785   782   780   777   773   753
                  716   788   795   793   791   788   786   784   781   779   776   765   700

                        774   793   792   790   788   785   783   781   778   774   753
                     716   786   792   790   788   785   783   780   778   775   766   700

                           769   784   782   780   778   776   773   771   768   751
                        715   768   770   768   766   764   762   760   758   752   700

                        712   712   711   710   709   708   707   705   704   700   701
```

Fig. 47. Coolant Temperatures at Mid-Plane

AXIAL DIST (IN)	ZSTAR	ALPSTA	AVERAGE TEMP	AVERAGE WALL TEMP
55.00	2.1153E 02	1.1925E-03	938.5	839.0

COOLANT TEMPERATURE BY SUBCHANNEL

```
                    840  842  841  838  834  831  828  825  822  819  818

                    842  913  922  919  915  911  906  902  897  883  821
                      914  946  946  943  938  934  929  925  917  883

                  845  950  973  973  968  964  959  954  949  941  913  821
                    928  975  981  977  972  968  963  958  952  939  892

                849  957  985  986  982  977  972  968  963  958  948  915  819
                  932  982  989  985  981  976  971  966  961  955  941  891

              852  960  989  990  986  981  977  972  967  962  957  947  914  818
                935  984  992  989  984  979  974  969  965  960  953  939  889

            855  962  991  993  989  984  979  974  970  965  960  954  944  911  816
              937  987  994  991  986  982  977  972  967  962  957  951  936  887

          857  964  994  995  991  986  982  977  972  967  962  958  952  942  909  815
            940  989  997  994  989  984  979  974  970  965  960  955  949  934  885

        859  967  996  998  994  989  984  979  975  970  965  960  955  950  940  907  814
          942  992  995  996  991  987  982  977  972  967  962  958  953  946  932  883

      861  969  999 1000  996  991  987  982  977  972  967  963  958  953  947  937  905  813
        943  994 1001  998  994  989  984  979  975  970  965  960  955  950  944  929  880

    861  966 1000 1002  999  994  989  984  979  975  970  965  960  955  950  945  934  899  813
      932  992 1003 1001  996  991  987  982  977  972  967  963  958  953  948  941  924  870
  858                                                                                          815
      932  992 1003 1001  996  992  987  982  977  972  967  963  958  953  948  941  924  871
    859  966 1000 1003  999  994  989  984  979  975  970  965  960  955  951  945  934  901  818

        943  994 1002  999  994  989  984  980  975  970  965  960  955  950  944  930  883
      861  969  999 1000  996  992  987  982  977  972  968  963  958  953  948  938  906  821

          943  992  995  996  992  987  982  977  972  968  963  958  953  947  932  886
        862  968  997  998  994  989  984  980  975  970  965  960  955  950  940  909  822

            942  990  997  994  989  984  980  975  970  965  960  955  949  935  888
          863  966  994  996  992  987  982  977  972  968  963  958  952  943  911  824

              940  988  995  992  987  982  977  972  968  963  958  952  937  890
            863  964  992  993  989  984  980  975  970  965  960  955  945  913  825

                939  986  992  989  984  980  975  970  965  960  954  939  892
              863  962  990  991  987  982  977  972  968  963  957  947  915  826

                  937  983  989  986  981  977  972  967  962  956  942  894
                862  960  986  987  983  978  973  968  964  958  949  917  827

                    934  977  982  978  973  969  964  959  954  941  895
                  861  953  975  974  970  965  960  956  951  943  916  829

                      921  949  949  946  942  937  933  929  920  887
                    858  918  926  924  920  917  913  909  904  890  830

                    855  852  851  850  848  846  844  841  837  830  833
```

Fig. 48. Coolant Temperatures at Top of Core

```
AXIAL DIST (IN)      ZSTAR          ALPSTA       AVERAGE TEMP      AVERAGE WALL TEMP
     70.00        2.6922E 02      1.1906E-03        943.0               864.2

COOLANT TEMPERATURE BY SUBCHANNEL
                   862   863   861   858   855   852   848   846   843   841   841

                   863   901   912   910   906   902   898   894   889   875   843
                      902   931   934   930   926   922   918   913   903   874

                866   934   962   965   962   957   953   948   943   932   901   843
                   917   964   976   974   969   965   960   955   948   930   885

             870   943   980   986   983   979   974   969   964   958   944   905   842
                923   974   989   988   984   979   974   969   964   956   935   885

          873   947   985   993   990   986   981   976   971   966   959   944   904   841
             926   977   993   993   989   984   979   974   969   964   955   933   884

       876   949   988   996   993   989   984   979   974   969   964   957   942   902   840
          928   980   996   996   991   987   982   977   972   967   962   953   931   882

    879   952   990   998   996   992   987   982   977   972   967   962   955   940   900   839
       931   983   998   998   994   989   984   979   975   970   965   959   950   929   880

 882   954   993  1001   999   994   989   984   979   975   970   965   960   953   937   898   839
    933   985  1001  1001   996   992   987   982   977   972   967   962   957   948   927   879

885   956   995  1003  1001   997   992   987   982   977   972   967   962   957   950   935   896   839
   933   986  1003  1003   999   994   989   984   980   975   970   965   960   954   946   924   876

885   950   995  1005  1003   999   994   989   984   980   975   970   965   960   955   947   930   889   840
   921   981  1004  1005  1001   997   992   987   982   977   972   967   962   958   952   942   916   865
883                                                                                                        842
   921   981  1004  1005  1001   997   992   987   982   977   972   967   963   958   952   942   917   867
884   950   995  1005  1004   999   994   989   985   980   975   970   965   960   955   948   931   891   845

   933   987  1003  1003   999   994   989   985   980   975   970   965   960   955   946   925   880
885   956   995  1004  1001   997   992   987   982   977   972   967   963   957   950   936   899   848

   935   986  1001  1001   997   992   987   982   977   972   968   963   957   948   928   884
887   956   994  1001   999   994   989   985   980   975   970   965   960   953   938   901   850

   935   984   999   998   994   990   985   980   975   970   965   960   951   930   886
889   955   991   999   996   992   987   982   977   972   968   962   955   941   904   851

   934   982   996   996   992   987   982   977   972   967   962   953   933   888
889   953   989   996   994   989   985   980   975   970   965   958   943   906   853

   933   980   994   993   989   984   980   975   970   964   956   935   889
890   952   987   994   991   986   982   977   972   967   960   945   908   854

   932   976   990   989   985   980   975   970   965   957   936   891
890   949   982   987   984   980   975   970   965   959   945   909   856

   928   967   977   975   971   966   962   957   950   933   891
889   940   965   968   964   960   956   951   946   935   906   858

   914   936   939   937   933   929   925   921   911   884
887   912   920   920   917   914   910   907   901   887   861

885   881   880   879   878   876   874   871   867   861   864
```

Fig. 49. Coolant Temperatures at Outlet

```
AXIAL DIST (IN)      NOMINAL BUNDLE AVG H.W.      NOMINAL PEAK H.W.
   35.00                     820.8                      858.3

CLAD TEMPERATURE BY SUBCHANNEL

                    762   770   768   766   764   762   759   757   755   752   746

                    770   822   824   821   818   815   813   810   807   801   753
                       823   837   835   832   830   827   824   821   817   800

                 772   840   846   843   840   837   834   831   828   825   815   752
                    829   847   846   843   840   837   834   831   828   823   802

              774   843   849   847   844   841   838   835   832   829   825   814   751
                 830   849   848   845   842   839   836   833   830   827   822   801

           775   844   851   848   845   842   839   836   833   830   827   824   812   750
              832   851   850   847   844   841   838   835   832   829   826   821   800

        777   846   852   850   847   844   841   838   835   832   829   826   822   811   749
           833   852   851   848   845   842   839   836   833   830   827   824   819   798

     778   847   854   851   848   845   842   839   836   833   830   827   824   821   810   748
        835   854   853   850   847   844   841   838   835   832   829   826   823   818   797

  779   849   855   853   850   847   844   841   838   835   832   829   826   823   819   808   747
     836   855   854   851   848   845   842   839   836   833   830   827   824   821   816   795

780   850   857   855   852   849   845   842   839   836   833   830   827   824   821   818   807   746
   837   857   856   853   850   847   844   841   838   835   832   829   826   823   820   815   794

781   851   858   856   853   850   847   844   841   838   835   832   829   826   823   820   816   805   744
   835   858   857   855   852   849   846   843   839   836   833   830   827   824   821   818   813   790
772                                                                                                        739
   835   858   857   855   852   849   846   843   840   836   833   830   827   824   821   818   813   790
779   851   858   856   853   850   847   844   841   838   835   832   829   826   823   820   816   805   747

   837   857   856   853   850   847   844   841   838   835   832   829   826   823   820   815   795
780   850   857   855   852   849   846   843   840   837   834   830   827   924   821   818   807   748

     837   855   855   852   849   846   843   840   837   834   831   827   824   821   817   796
  780   849   855   853   850   847   844   841   838   835   832   829   826   823   819   809   749

        835   854   853   850   847   844   841   838   835   832   829   826   823   818   797
     780   847   854   852   849   846   843   840   837   834   831   828   824   821   810   750

           834   853   852   849   846   843   840   837   834   831   828   824   820   799
        779   846   852   850   847   844   841   838   835   832   829   826   822   811   751

              833   851   850   847   844   841   838   835   832   829   826   821   800
           778   845   851   849   846   843   840   837   834   831   828   824   813   752

                 831   850   849   846   843   840   837   934   831   827   823   802
              777   843   849   847   844   841   838   835   832   829   925   814   753

                    830   848   846   844   841   838   835   832   828   [illegible]   [illegible]
                 776   841   846   844   841   838   835   832   829   825   815   753

                       825   838   836   833   830   828   825   822   818   801
                    775   823   825   822   820   817   814   811   808   802   754

                    766   771   769   768   766   764   762   760   758   754   749
```

Fig. 50. Nominal Clad Temperatures at Mid-Plane

```
AXIAL DIST (IN)     NOMINAL BUNDLE AVG M.W.     NOMINAL PEAK M.W.
     55.00                   960.3                    1026.3

CLAD TEMPERATURE BY SUBCHANNEL

                              862   867   865   862   858   855   851   848   845   842   838

                              867   936   944   941   937   932   928   923   918   904   843
                                 937   969   969   964   960   955   950   945   937   903

                           870   972   996   995   990   985   980   975   970   962   934   843
                              951   998  1003   999   994   989   984   979   973   960   912

                        874   979  1008  1008  1004   999   994   989   984   978   968   936   841
                           955  1004  1011  1007  1002   997   992   987   982   976   961   911

                     877   982  1011  1012  1008  1003   998   993   988   983   977   967   934   840
                        958  1007  1014  1011  1006  1001   996   991   985   980   974   959   909

                  880   985  1014  1015  1011  1006  1001   996   991   986   980   975   964   931   838
                     960  1010  1017  1013  1008  1003   998   993   988   983   978   971   956   907

               883   988  1016  1018  1013  1008  1003   998   993   988   983   978   972   962   929   837
                  963  1012  1019  1016  1011  1006  1001   996   991   986   981   975   969   954   905

            885   990  1019  1020  1016  1011  1006  1001   996   991   986   981   976   970   960   927   835
               965  1015  1022  1018  1014  1009  1003   998   993   988   983   978   973   966   952   903

         887   992  1022  1023  1019  1014  1009  1003   998   993   988   983   978   973   967   957   924   835
            966  1017  1024  1021  1016  1011  1006  1001   996   991   986   981   976   970   964   949   900

      887   990  1023  1025  1021  1016  1011  1006  1001   996   991   986   981   976   971   965   954   919   834
         956  1015  1026  1024  1019  1014  1009  1004   998   993   988   983   978   973   968   961   944   890
   882                                                                                                            834
         955  1015  1026  1024  1019  1014  1009  1004   999   993   988   983   978   973   968   961   944   891
      885   990  1023  1025  1021  1016  1011  1006  1001   996   991   986   981   976   971   965   954   920   839

            966  1017  1024  1021  1016  1011  1006  1001   996   991   986   981   976   971   964   949   903
         887   992  1022  1023  1019  1014  1009  1004   999   994   988   983   978   973   968   957   926   842

               966  1015  1022  1019  1014  1009  1004   999   994   989   983   978   973   967   952   906
            888   991  1019  1021  1016  1011  1006  1001   996   991   986   981   976   970   960   929   844

                  965  1013  1020  1016  1011  1006  1001   996   991   986   981   976   969   955   908
               888   989  1017  1018  1014  1009  1004   999   994   989   984   978   973   963   931   845

                     964  1011  1017  1014  1009  1004   999   994   989   984   978   972   957   910
                  888   987  1015  1016  1011  1006  1001   996   991   986   981   975   965   933   847

                        962  1008  1015  1011  1006  1001   996   991   986   981   974   960   912
                     888   985  1012  1013  1009  1004   999   994   989   983   978   968   935   848

                           960  1005  1012  1008  1003   998   993   988   983   976   962   914
                        887   982  1009  1009  1005  1000   995   990   984   979   969   937   849

                              957   999  1004  1000   995   990   985   980   974   961   915
                           886   976   997   996   991   987   982   977   972   964   936   851

                                 943   971   971   968   963   959   954   949   941   908
                              883   941   948   946   942   938   934   930   925   911   852

                              877   877   875   874   872   869   867   864   859   852   853
```

Fig. 51. Nominal Clad Temperatures at Top of Core

```
AXIAL DIST (IN)      NOMINAL BUNDLE AVG M.W.      NOMINAL PEAK M.W.
     70.00                    943.5                       1005.8

CLAD TEMPERATURE BY SUBCHANNEL

                        862   863   862   859   855   852   849   846   844   842   842

                        864   902   912   911   907   903   899   895   889   875   843
                           903   931   934   931   927   922   918   913   903   875

                     867   934   963   966   962   958   953   948   943   932   901   843
                        918   965   976   974   970   965   960   955   948   931   885

                  870   943   980   987   984   979   975   970   965   958   944   906   842
                     923   974   989   989   984   979   975   970   964   956   935   886

               874   947   986   993   991   986   981   977   972   966   960   944   904   841
                  926   978   994   993   989   984   979   975   970   964   955   934   884

            877   950   988   996   994   989   985   980   975   970   965   958   942   903   840
               929   981   996   996   992   987   982   977   972   968   962   953   932   882

         880   952   991   999   997   992   987   982   977   973   968   962   955   940   901   840
            932   983   999   999   994   990   985   980   975   970   965   960   951   929   881

      883   955   993  1001   999   995   990   985   980   975   970   965   960   953   938   899   839
         934   985  1001  1001   997   992   987   982   978   973   968   963   957   949   927   879

   885   956   995  1004  1002   997   992   987   982   978   973   968   963   958   951   935   896   840
      934   987  1003  1004   999   995   990   985   980   975   970   965   960   955   946   924   876

885   951   995  1006  1004  1000   995   990   985   980   975   970   965   960   955   948   931   889   840
   922   982  1004  1006  1002   997   992   987   983   978   973   968   963   958   952   942   917   866
884                                                                                                          843
   921   982  1004  1006  1002   997   992   987   983   978   973   968   963   958   952   942   917   868
884   951   995  1006  1004  1000   995   990   985   980   975   970   965   961   955   948   931   891   845

      934   987  1004  1004  1000   995   990   985   980   975   970   965   961   955   946   925   880
   886   957   996  1004  1002   997   992   987   983   978   973   968   963   958   951   936   899   848

         936   986  1002  1001   997   992   988   983   978   973   968   963   958   949   928   884
      888   957   994  1002   999   995   990   985   980   975   970   966   960   953   939   902   850

            936   984   999   999   995   990   985   980   975   970   966   960   951   931   886
         889   955   992   999   997   992   988   983   978   973   968   963   956   941   904   852

               935   982   997   997   992   988   983   978   973   968   962   954   933   888
            890   954   990   997   994   990   985   980   975   970   965   958   943   906   853

                  934   980   994   994   990   985   980   975   970   965   956   935   890
               891   952   987   994   991   987   982   977   972   967   960   945   908   855

                     932   977   990   989   985   980   975   971   965   957   937   892
                  891   949   982   988   985   980   976   971   966   959   946   909   857

                        928   968   978   976   971   967   962   957   950   933   892
                     890   941   966   968   965   961   956   952   946   936   906   859

                           914   937   940   937   934   930   926   921   911   884
                        888   912   921   920   917   914   911   907   902   887   861

                        885   882   881   880   878   876   874   872   867   861   865
```

Fig. 52. Nominal Clad Temperatures at Outlet

```
AXIAL DIST (IN)     2-SIGMA BUNDLE AVG M.W.     2-SIGMA PEAK M.W.
     35.00                  917.3                      966.1

CLAD TEMPERATURE BY SUBCHANNEL

                        846   860   857   854   851   848   845   841   838   834   821

                        861   921   922   918   914   910   906   902   898   890   834
                           922   939   936   932   928   924   919   915   910   889

                     864   943   949   945   941   937   933   929   924   920   907   833
                        929   951   949   945   941   936   932   928   924   918   891

                  866   946   953   950   946   941   937   933   929   925   920   905   832
                     931   954   952   948   944   939   935   931   927   922   916   889

               868   948   955   952   948   944   939   935   931   927   923   919   904   830
                  933   956   954   950   946   942   937   933   929   925   920   914   888

            870   950   958   954   950   946   942   937   933   929   925   921   916   902   828
               935   958   956   952   948   944   940   935   931   927   923   919   912   886

         872   952   960   956   952   948   944   940   935   931   927   923   919   913   900   827
            937   960   958   954   950   946   942   937   933   929   925   921   916   910   884

      874   954   962   959   954   950   946   942   938   933   929   925   921   916   911   898   825
         939   962   961   956   952   948   944   940   935   931   927   923   919   914   908   882

   875   956   964   961   957   952   948   944   940   935   931   927   923   919   914   909   895   823
      941   964   963   959   954   950   946   942   938   933   929   925   921   916   912   906   880

876   957   966   963   959   954   950   946   942   938   933   929   925   921   917   912   907   893   822
   938   966   965   961   957   952   948   944   940   936   931   927   923   919   914   910   903   874
861                                                                                                        811
   938   966   965   961   957   952   948   944   940   936   931   927   923   919   914   910   903   874
875   957   966   963   959   955   950   946   942   938   933   929   925   921   917   912   907   893   824

      941   964   963   959   955   950   946   942   938   933   929   925   921   917   912   906   880
   875   956   964   961   957   952   948   944   940   936   931   927   923   919   914   910   896   827

         940   962   961   957   952   948   944   940   936   931   927   923   919   914   908   883
      875   955   962   959   955   950   946   942   938   934   929   925   921   917   912   898   828

            938   960   959   955   950   946   942   938   934   929   925   921   917   910   885
         874   953   960   957   953   948   944   940   936   931   927   923   919   914   900   830

               936   958   957   953   948   944   940   936   932   927   923   919   912   886
            873   951   958   955   950   946   942   938   934   929   925   921   916   902   831

                  934   956   955   950   946   942   938   934   929   925   921   915   888
               872   945   956   953   948   944   940   936   932   927   923   919   904   833

                     933   954   952   948   944   940   936   932   927   923   917   890
                  870   947   954   950   946   942   938   934   929   925   920   906   834

                        930   952   950   946   941   937   933   929   924   918   892
                     869   944   950   946   942   938   933   929   925   920   907   835

                           924   940   937   933   929   925   921   916   911   890
                        867   922   923   919   916   912   908   904   900   892   836

                        850   861   859   856   854   851   848   844   841   836   826
```

Fig. 53. 2σ Clad Mid-Wall Temperatures at Mid-Plane

```
AXIAL DIST (IN)     2-SIGMA BUNDLE AVG M.W.     2-SIGMA PEAK M.W.
     55.00                 1063.2                     1145.4

CLAD TEMPERATURE BY SUBCHANNEL

                         943   951   948   944   940   935   930   926   922   918   911

                         951  1034  1044  1040  1034  1029  1023  1017  1010   993   919
                           1035  1074  1074  1068  1062  1056  1051  1044  1034   992

                      956  1079  1107  1106  1100  1094  1087  1081  1074  1064  1029   919
                        1053  1110  1116  1111  1105  1098  1092  1085  1078  1061  1003

                   960  1088  1122  1123  1117  1111  1104  1098  1091  1084  1072  1032   917
                     1058  1118  1126  1121  1115  1109  1102  1096  1089  1081  1063  1001

                964  1091  1127  1128  1122  1116  1109  1103  1097  1090  1083  1070  1029   915
                  1061  1121  1130  1125  1119  1113  1106  1100  1093  1087  1079  1060   999

             968  1095  1130  1131  1126  1119  1113  1106  1100  1094  1087  1080  1067  1026   913
               1065  1125  1133  1129  1123  1116  1110  1103  1097  1090  1084  1075  1057   996

          971  1098  1133  1134  1129  1123  1116  1110  1103  1097  1090  1084  1077  1064  1023   911
            1068  1128  1136  1132  1126  1119  1113  1107  1100  1094  1087  1081  1072  1054   994

       974  1101  1136  1138  1132  1126  1119  1113  1107  1100  1094  1087  1081  1074  1061  1020   909
         1071  1131  1140  1135  1129  1123  1116  1110  1103  1097  1091  1084  1077  1069  1051   991

    976  1104  1140  1141  1136  1129  1123  1116  1110  1103  1097  1091  1084  1078  1070  1058  1017   908
      1072  1134  1143  1139  1132  1126  1120  1113  1107  1100  1094  1087  1081  1074  1066  1047   987

 977  1101  1141  1144  1139  1132  1126  1120  1113  1107  1100  1094  1087  1081  1074  1067  1053  1010   908
   1060  1132  1145  1142  1136  1129  1123  1116  1110  1104  1097  1091  1084  1078  1071  1062  1041   974
968                                                                                                          905
   1059  1132  1145  1142  1136  1129  1123  1116  1110  1104  1097  1091  1084  1078  1071  1062  1041   976
 974  1101  1142  1144  1139  1133  1126  1120  1113  1107  1100  1094  1088  1081  1075  1067  1054  1012   914

      1072  1134  1143  1139  1133  1126  1120  1113  1107  1100  1094  1088  1081  1074  1066  1048   991
    976  1104  1140  1141  1136  1129  1123  1117  1110  1104  1097  1091  1084  1078  1071  1058  1019   917

         1072  1132  1140  1136  1129  1123  1117  1110  1104  1097  1091  1084  1078  1070  1052   995
       977  1102  1137  1138  1133  1126  1120  1113  1107  1101  1094  1088  1081  1074  1061  1023   919

            1071  1129  1137  1133  1126  1120  1113  1107  1101  1094  1088  1081  1073  1055   997
          978  1100  1134  1135  1129  1123  1117  1110  1104  1097  1091  1084  1077  1065  1026   921

               1069  1126  1134  1129  1123  1117  1110  1104  1097  1091  1084  1076  1058  1000
             978  1097  1131  1132  1126  1120  1114  1107  1101  1094  1088  1080  1068  1028   923

                  1066  1123  1130  1126  1120  1113  1107  1101  1094  1088  1079  1061  1003
                977  1094  1128  1128  1123  1117  1110  1104  1097  1091  1084  1071  1031   925

                     1064  1119  1127  1122  1116  1109  1103  1097  1090  1082  1064  1005
                   976  1091  1123  1124  1118  1111  1105  1099  1092  1085  1073  1034   927

                        1060  1112  1117  1112  1106  1100  1093  1087  1079  1063  1007
                      975  1083  1109  1107  1102  1095  1089  1083  1076  1066  1032   929

                           1043  1077  1077  1072  1067  1061  1055  1049  1039   998
                         971  1040  1049  1046  1041  1036  1031  1026  1019  1002   931

                         961   963   961   959   956   953   949   945   940   931   930
```

Fig. 54. 2σ Clad Mid-Wall Temperatures at the Top of Core

AXIAL DIST (IN)   2-SIGMA BUNDLE AVG M.W.   2-SIGMA PEAK M.W.
70.00   1024.7   1101.6

CLAD TEMPERATURE BY SUBCHANNEL

924 926 924 920 916 912 908 905 902 899 899

926 973 986 984 980 975 970 965 958 940 901
974 1009 1013 1009 1004 999 993 987 975 940

930 1013 1049 1052 1048 1042 1037 1031 1024 1011 973 901
993 1051 1065 1062 1057 1051 1045 1039 1031 1009 953

935 1025 1070 1078 1075 1069 1063 1057 1051 1043 1026 978 900
1000 1063 1081 1080 1075 1069 1063 1057 1050 1040 1014 953

939 1029 1077 1086 1083 1077 1071 1065 1059 1053 1045 1026 977 899
1004 1067 1086 1086 1081 1075 1069 1063 1057 1050 1039 1013 952

943 1033 1080 1090 1087 1081 1075 1069 1063 1057 1051 1042 1023 974 898
1007 1070 1090 1090 1084 1079 1072 1066 1060 1054 1048 1037 1010 949

947 1036 1083 1093 1090 1085 1079 1073 1067 1061 1054 1048 1039 1020 972 897
1010 1074 1093 1093 1088 1082 1076 1070 1064 1058 1051 1045 1034 1007 947

950 1039 1086 1096 1093 1088 1082 1076 1070 1064 1058 1052 1045 1037 1018 969 896
1013 1076 1096 1096 1091 1085 1079 1073 1067 1061 1055 1048 1042 1031 1005 945

953 1040 1089 1099 1096 1091 1085 1079 1073 1067 1061 1055 1049 1042 1034 1015 966 897
1013 1078 1099 1099 1094 1088 1082 1076 1070 1064 1058 1052 1046 1039 1028 1001 942

953 1034 1088 1101 1099 1094 1088 1082 1076 1070 1064 1058 1052 1046 1039 1030 1009 958 898
998 1072 1099 1101 1097 1091 1085 1079 1073 1067 1061 1055 1049 1043 1035 1023 992 929
951 901
997 1072 1099 1102 1097 1091 1085 1079 1073 1067 1061 1055 1049 1043 1036 1023 992 931
952 1034 1088 1102 1099 1094 1088 1082 1076 1070 1064 1059 1052 1046 1039 1030 1010 960 904

1013 1078 1099 1099 1094 1088 1082 1076 1070 1064 1058 1052 1046 1039 1028 1002 947
954 1041 1089 1099 1097 1091 1085 1079 1073 1067 1061 1055 1049 1042 1034 1015 970 907

1015 1077 1096 1096 1091 1085 1079 1073 1067 1061 1055 1049 1042 1031 1006 951
956 1041 1087 1097 1094 1088 1082 1076 1070 1064 1058 1052 1045 1037 1019 974 910

1015 1075 1093 1093 1088 1082 1076 1070 1064 1058 1052 1045 1034 1009 954
958 1039 1084 1094 1091 1085 1079 1073 1067 1061 1055 1049 1040 1022 976 912

1014 1073 1091 1090 1085 1079 1073 1067 1061 1055 1048 1037 1012 956
959 1038 1082 1091 1088 1082 1076 1070 1064 1058 1052 1043 1025 979 914

1013 1070 1087 1087 1082 1076 1070 1064 1058 1051 1040 1015 959
960 1035 1078 1087 1084 1078 1072 1066 1060 1054 1045 1027 981 916

1011 1066 1082 1081 1076 1070 1064 1058 1051 1041 1016 961
960 1032 1073 1080 1076 1070 1064 1058 1052 1044 1027 983 918

1006 1055 1067 1065 1059 1054 1048 1042 1033 1012 961
959 1022 1052 1055 1051 1046 1040 1035 1028 1015 979 920

989 1017 1020 1017 1012 1008 1003 997 985 952
956 986 997 996 993 989 985 980 973 956 923

953 949 948 946 944 942 939 936 931 923 928

Fig. 55. 2σ Clad Mid-Wall Temperatures at the Outlet

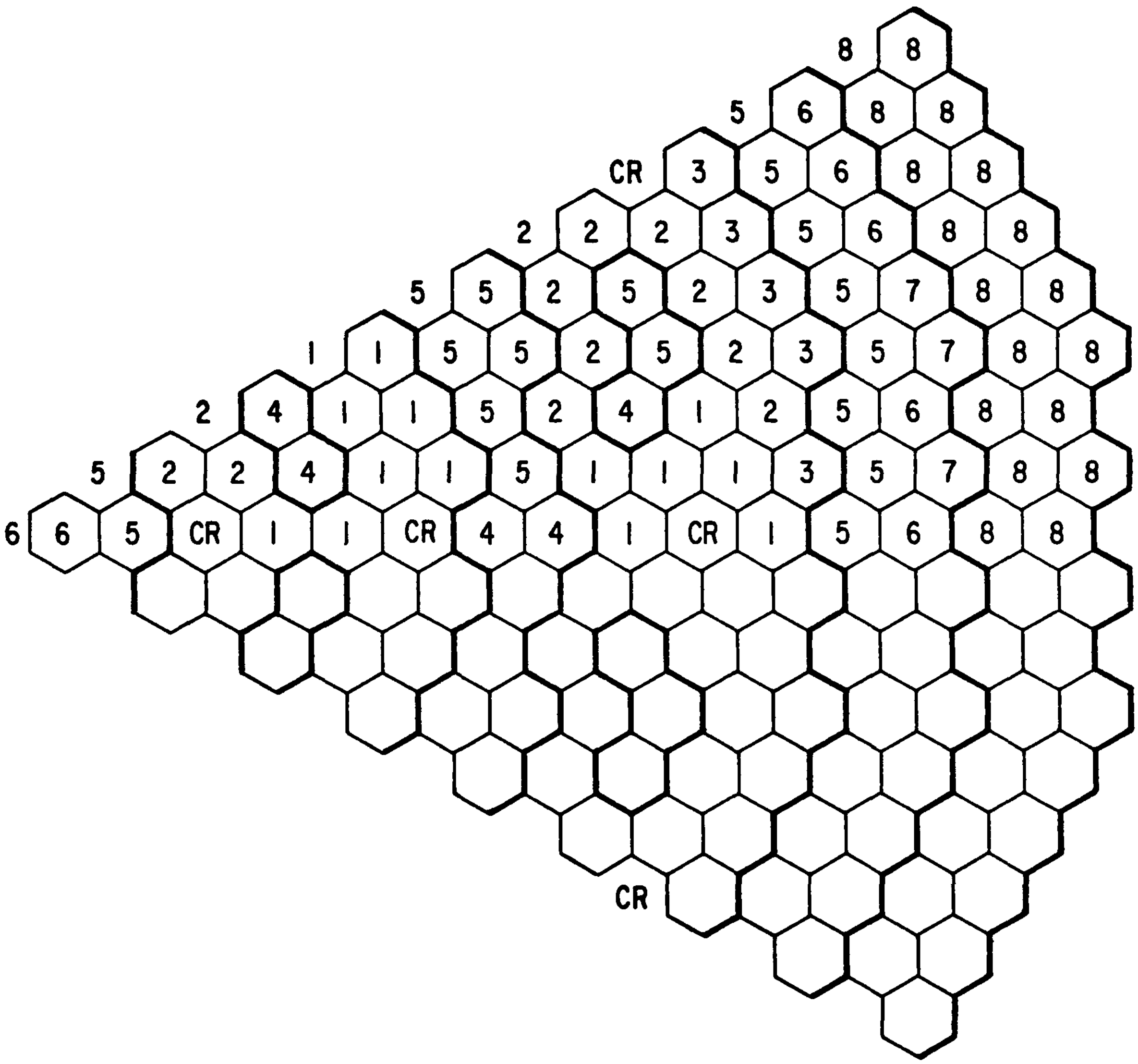

Fig. 56. Orificing Scheme of Configuration A with Equal Peak Clad Temperature at EOEC

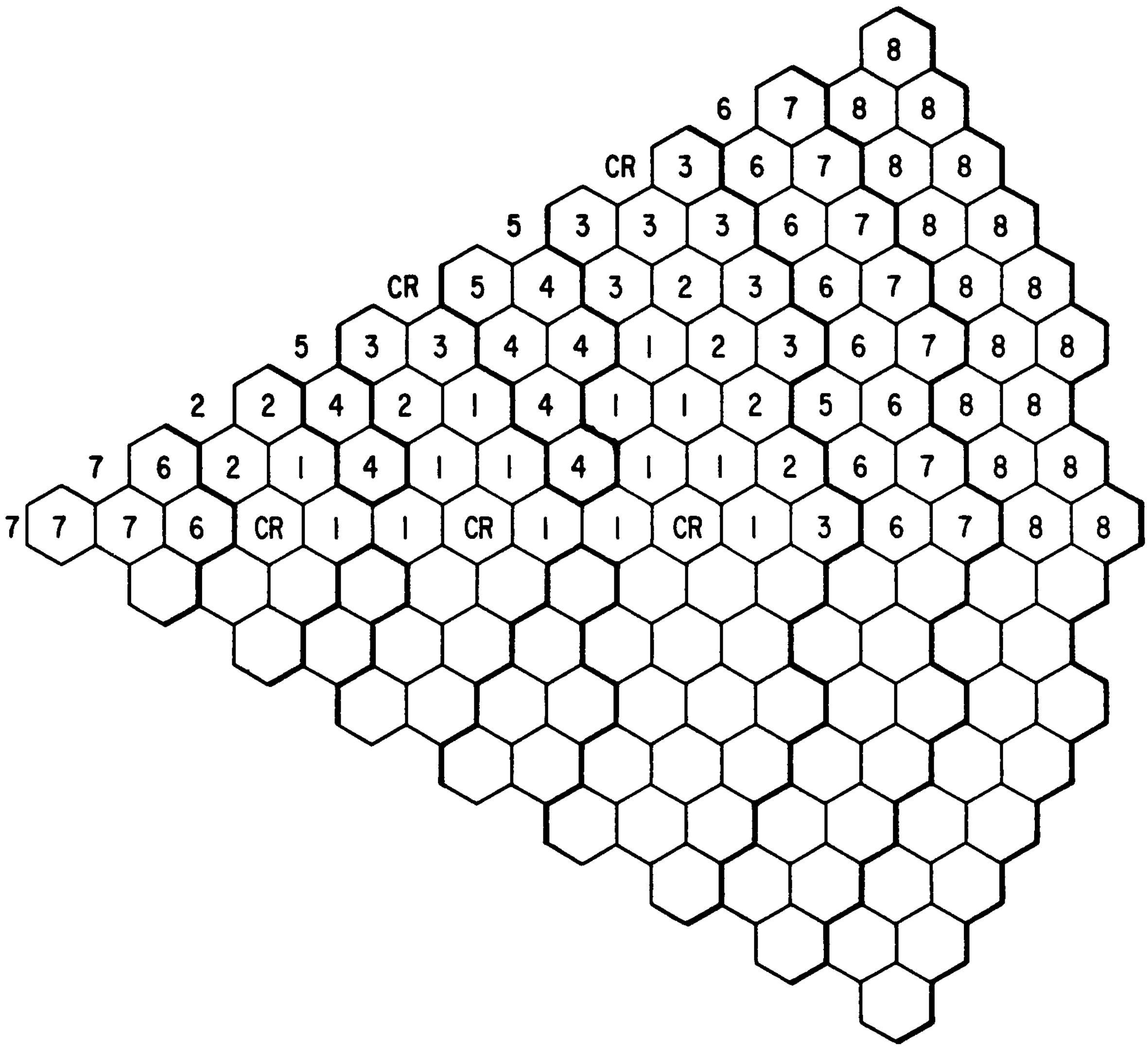

Fig. 57. Orificing Scheme of Configuration B with Equal Peak Clad Temperatures at BOL in the Core and at EOL in the Internal Blankets

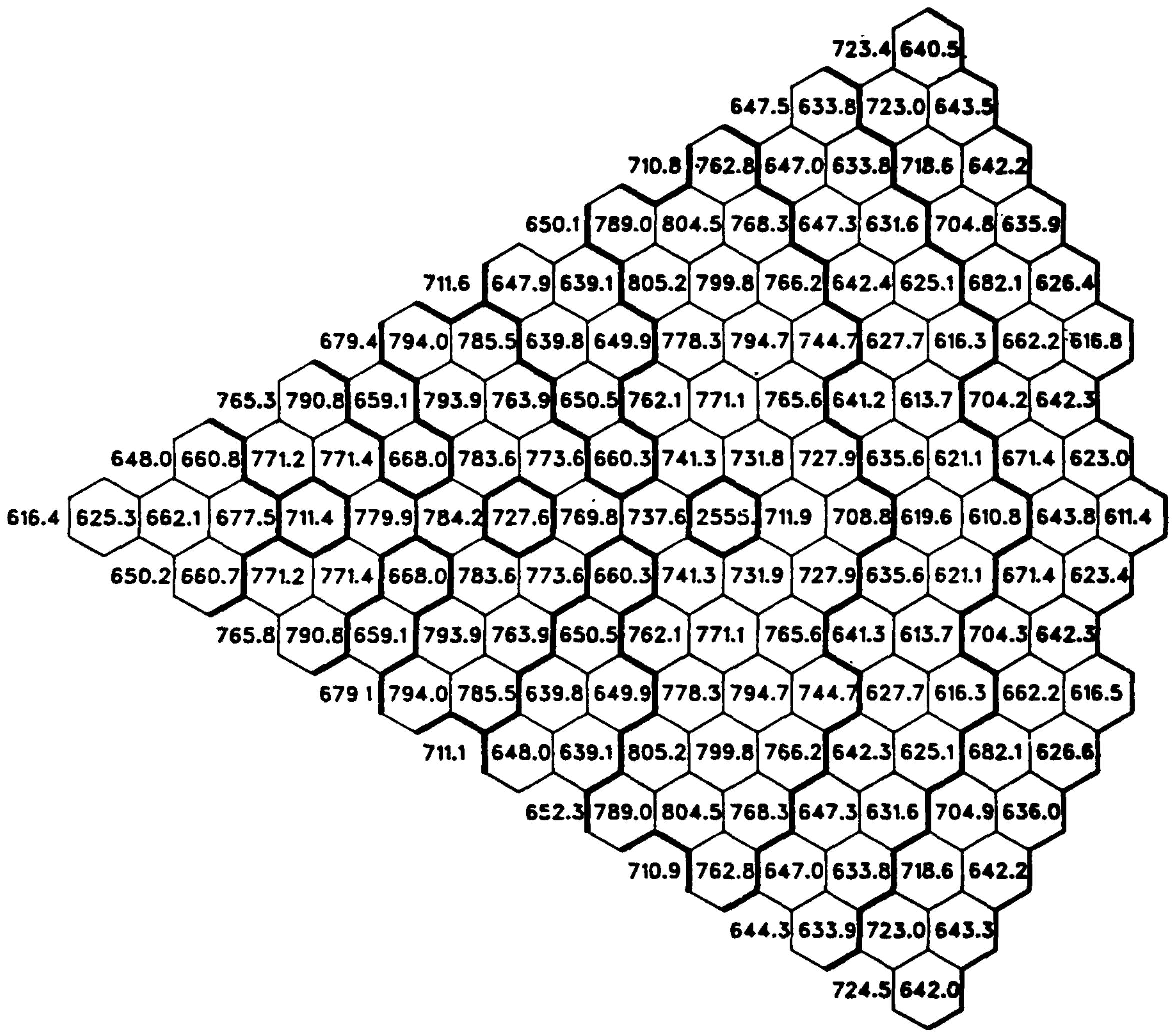

Fig. 58. Configuration B BOL Average Coolant Temperature at Core Mid-Plane (Orificed for Minimum Peak Temperature)

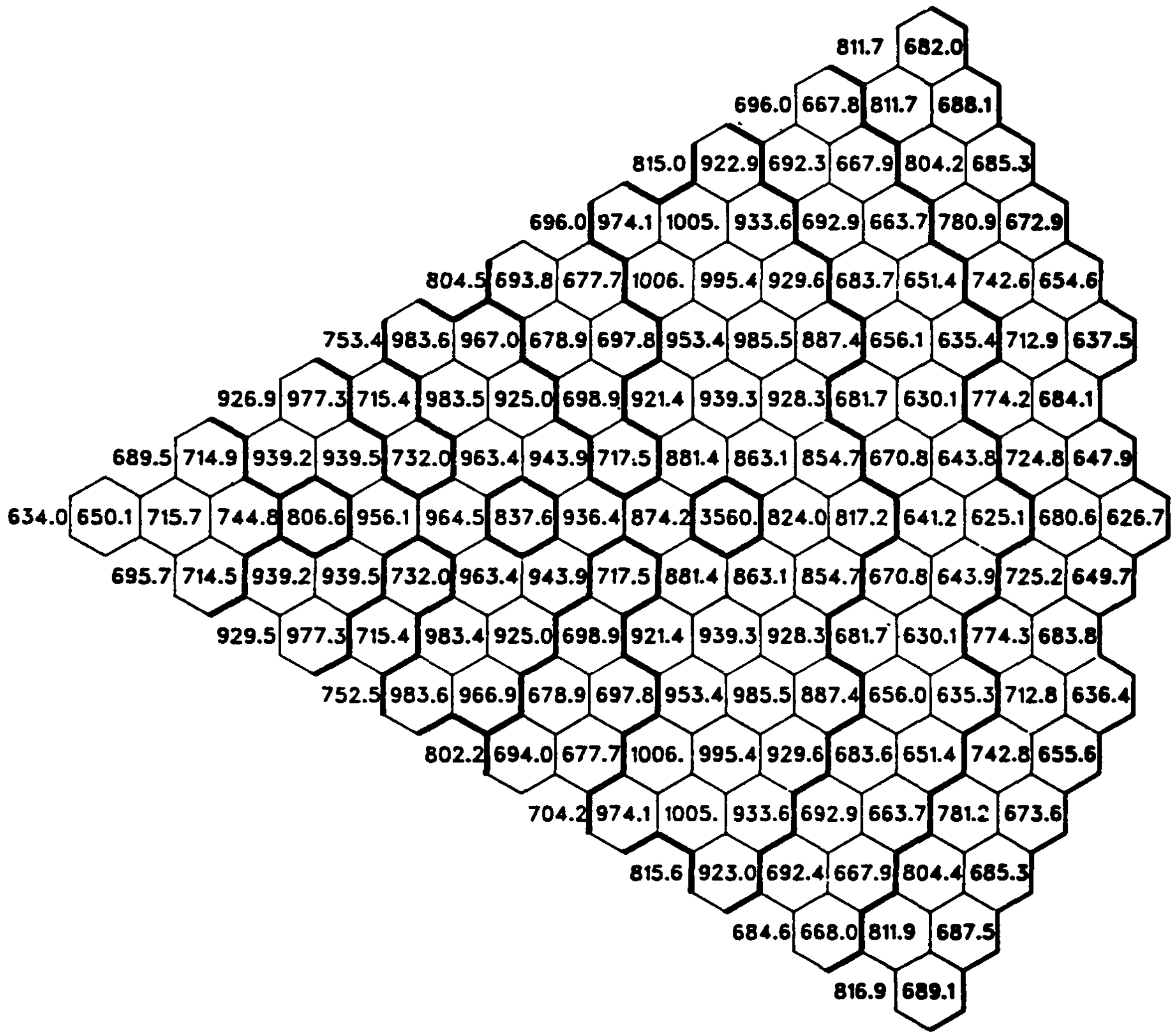

Fig. 59. Configuration B BOL Average Coolant Temperature at Top of Core (Orificed for Minimum Peak Temperature)

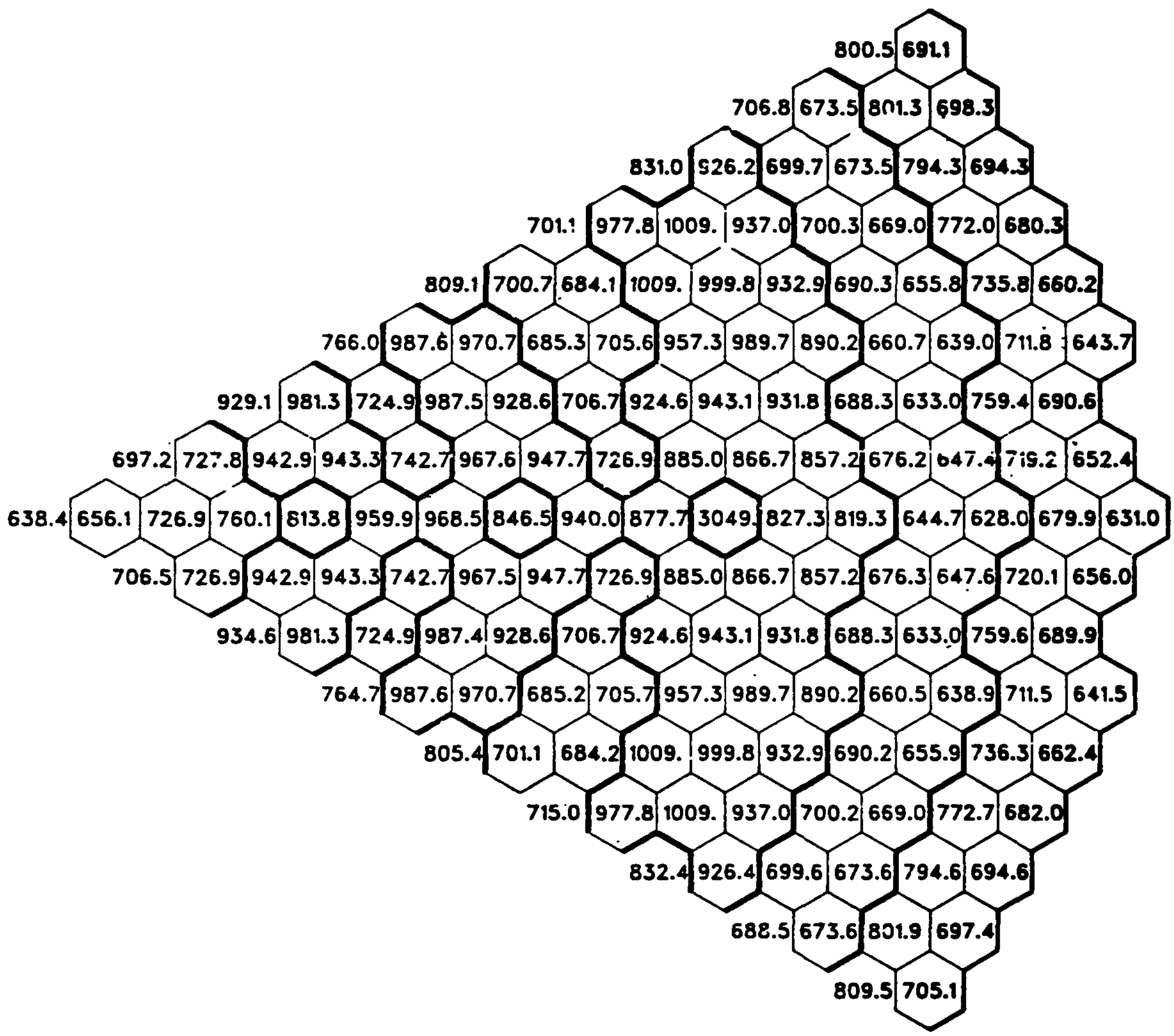

Fig. 60. Configuration B BOL Average Coolant Temperature at Outlet (Orificed for Minimum Peak Temperature)

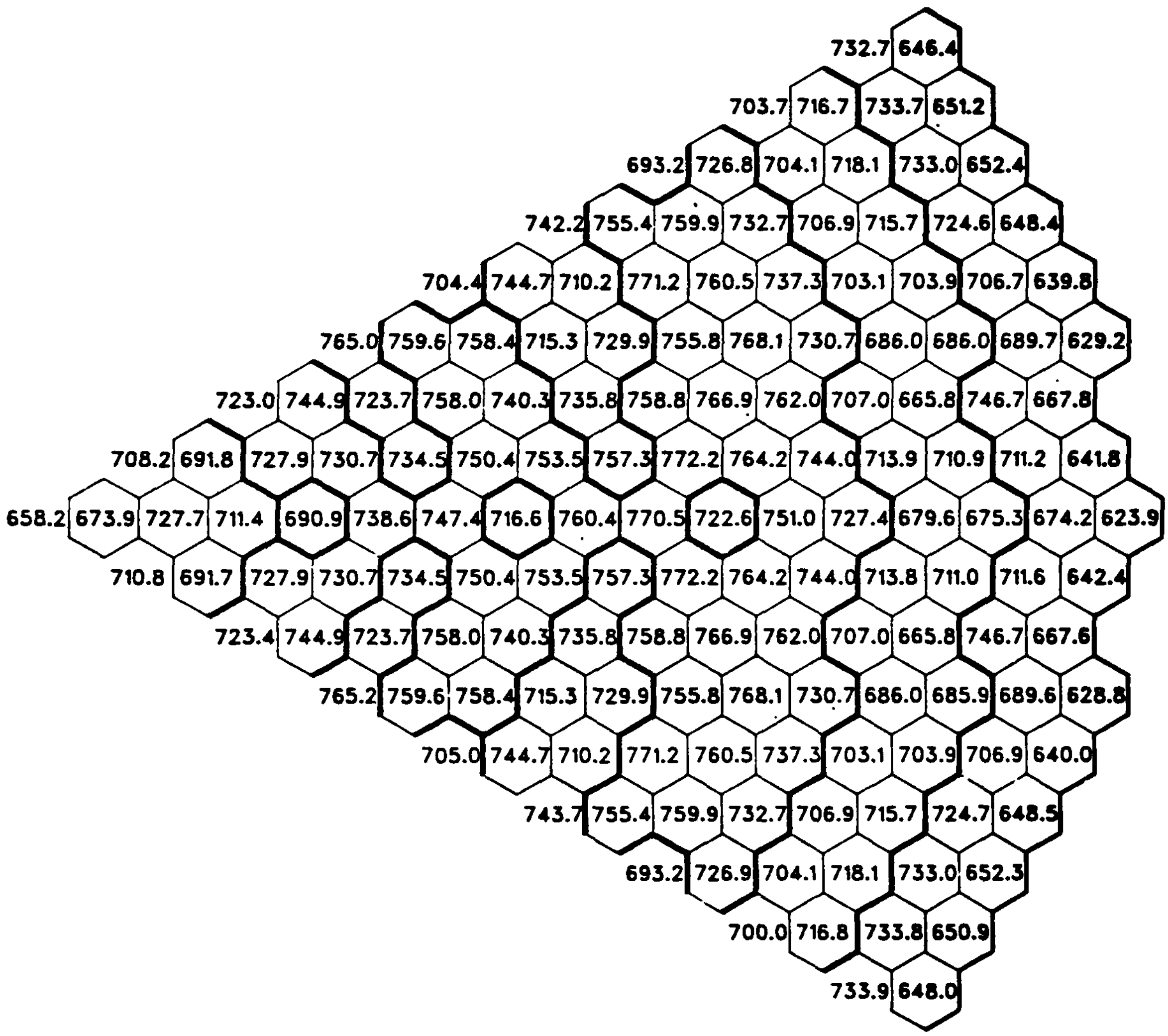

Fig. 61. Configuration B EOEC Average Coolant Temperature at Core Mid-Plane (Orificed for Minimum Peak Temperature)

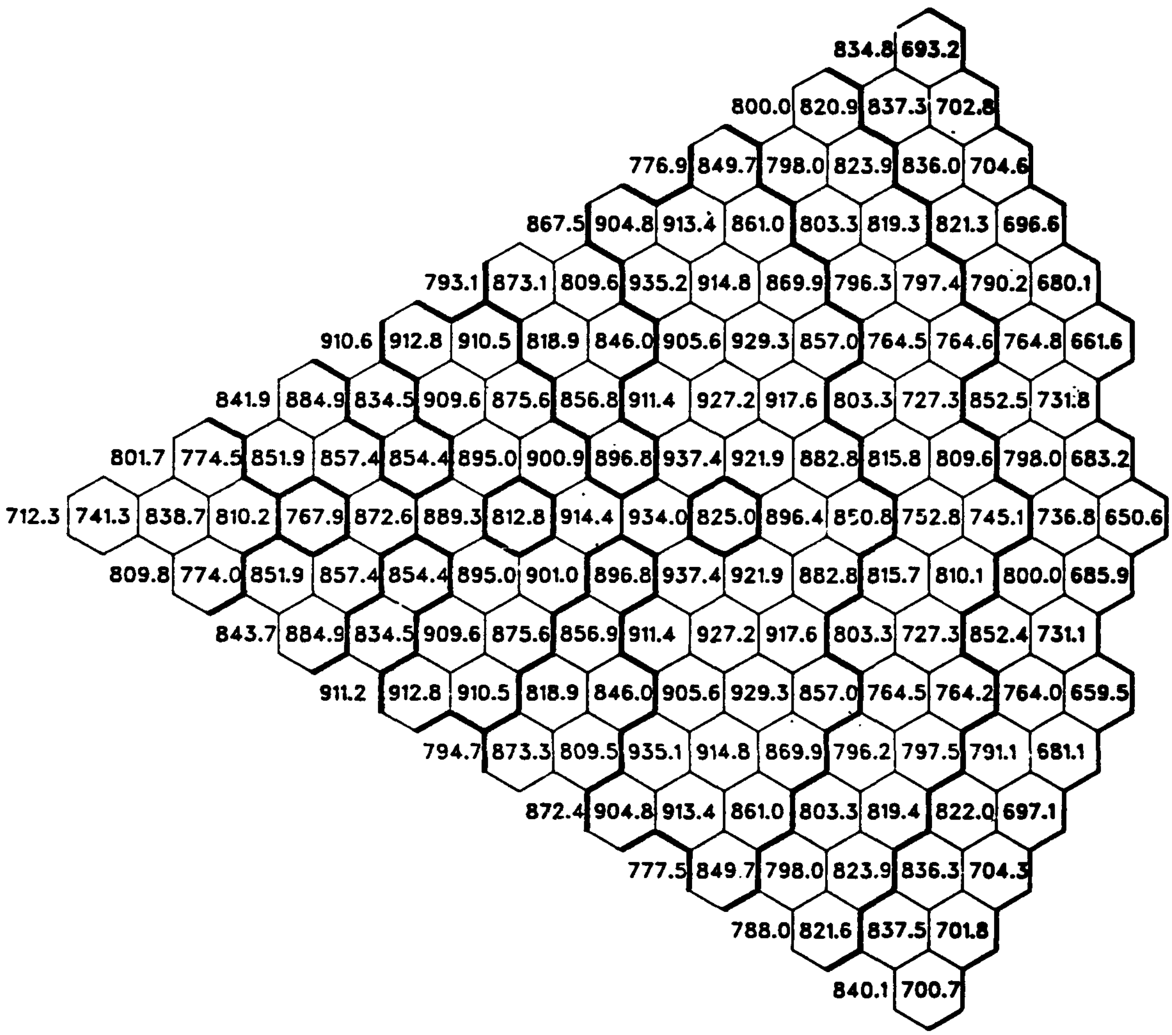

Fig. 62. Configuration B EOEC Average Coolant Temperature at Top of Core (Orificed for Minimum Peak Temperature)

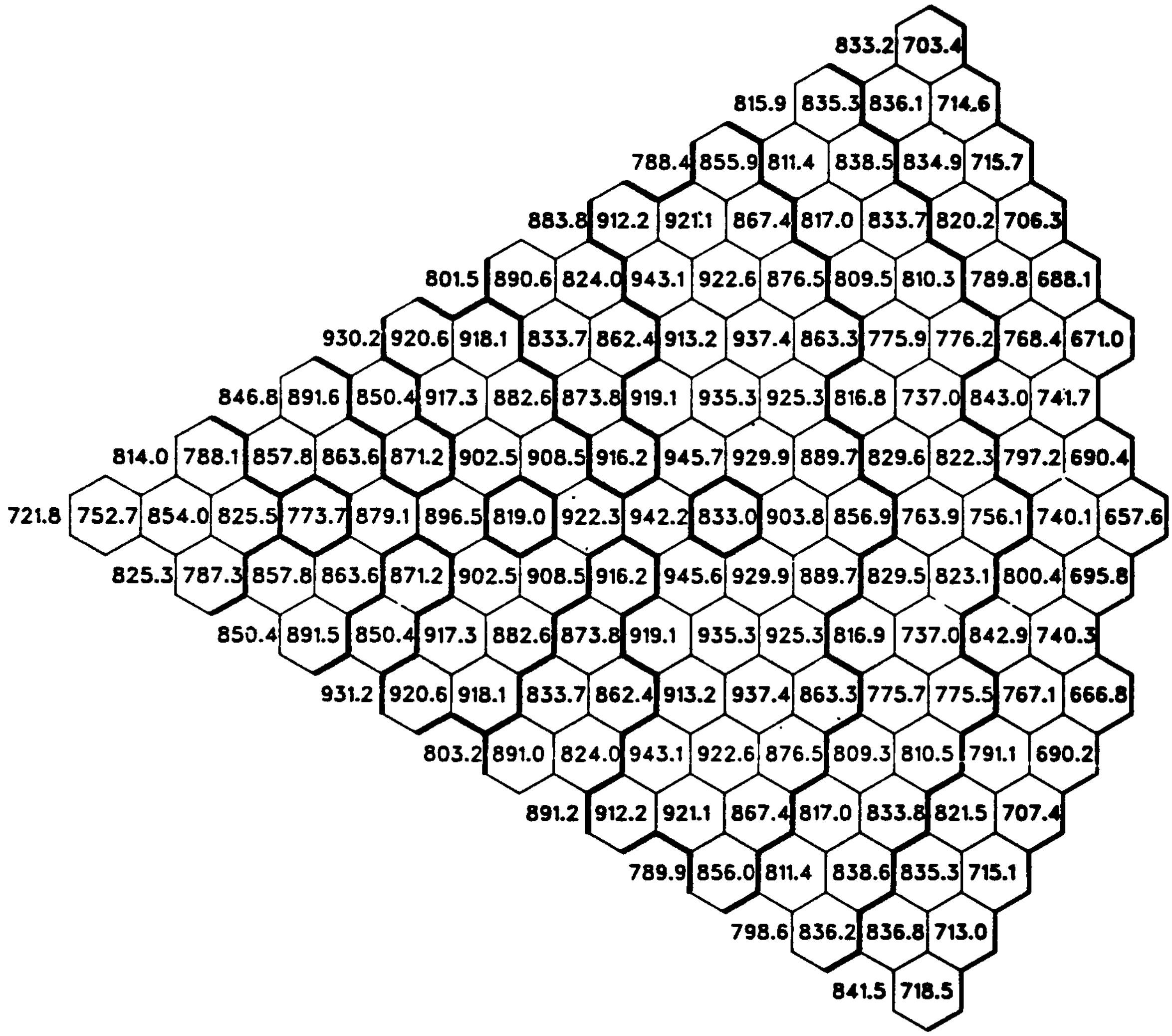

Fig. 63. Configuration B EOEC Average Coolant Temperature at Outlet (Orificed for Minimum Peak Temperature)

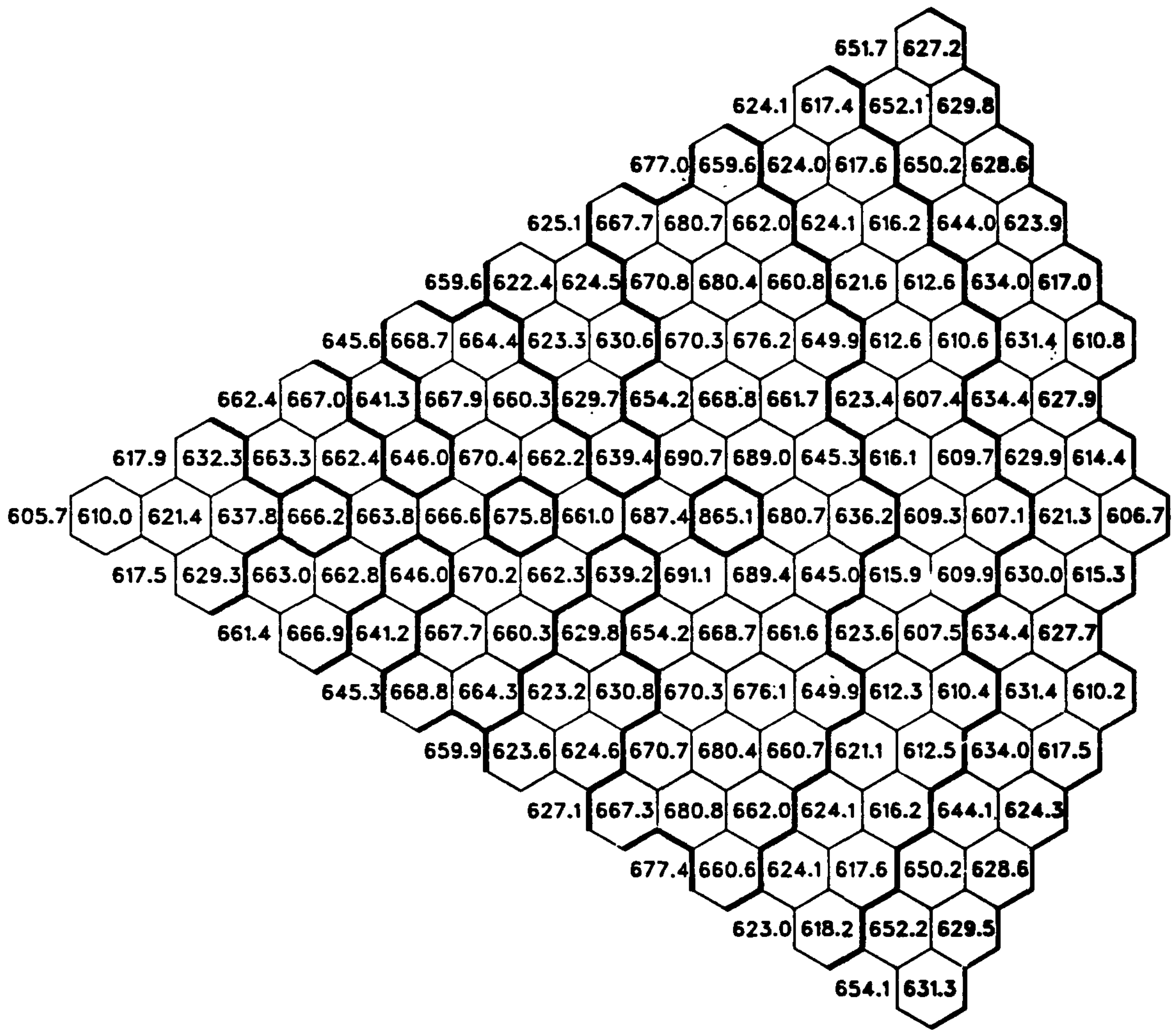

Fig. 64. Configuration B BOL Average Duct Wall Temperature at Core Mid-Plane (Orificed for Minimum Peak Temperature)

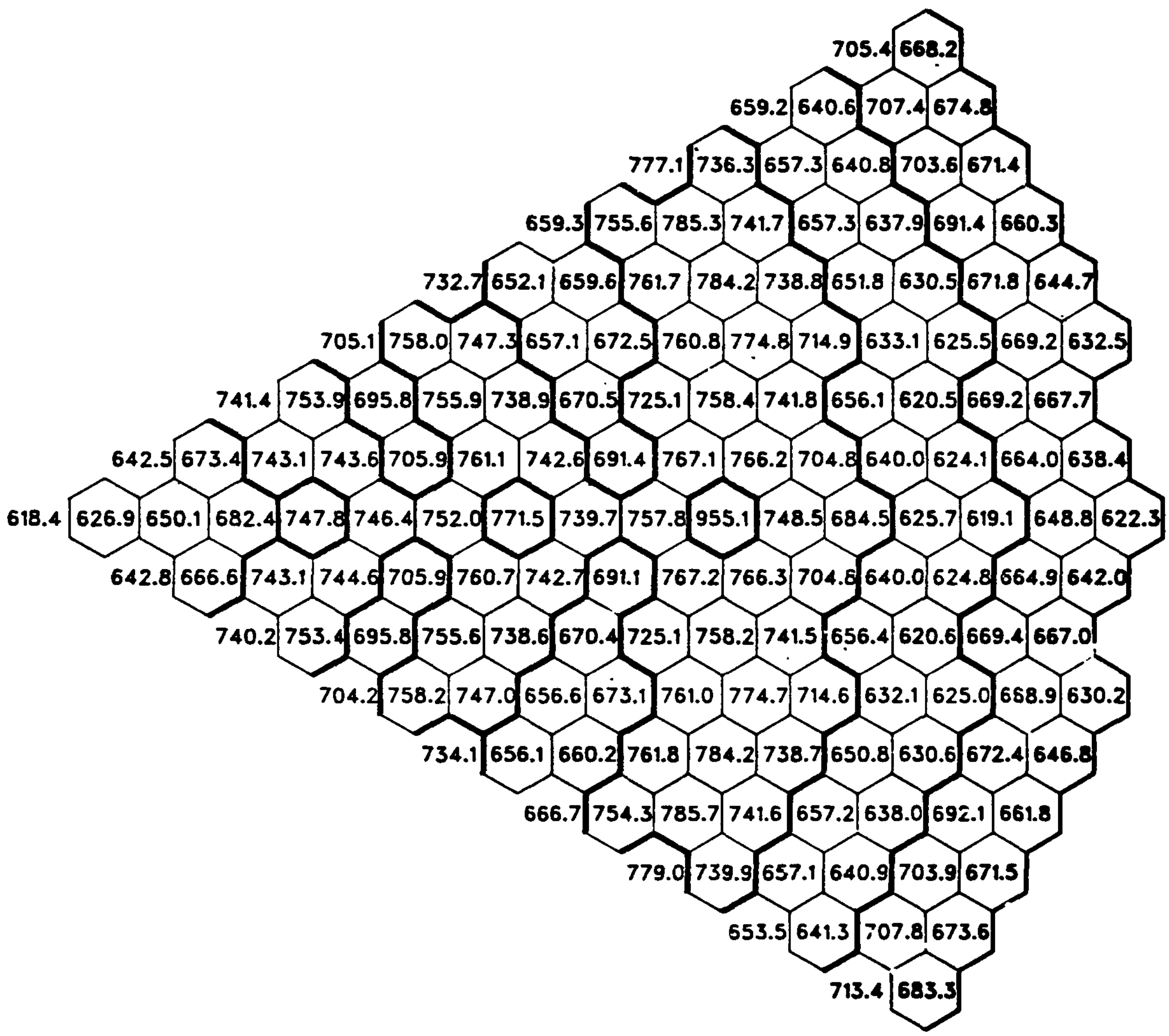

Fig. 65. Configuration B BOL Average Duct Wall Temperature at Top of Core (Orificed for Minimum Peak Temperature)

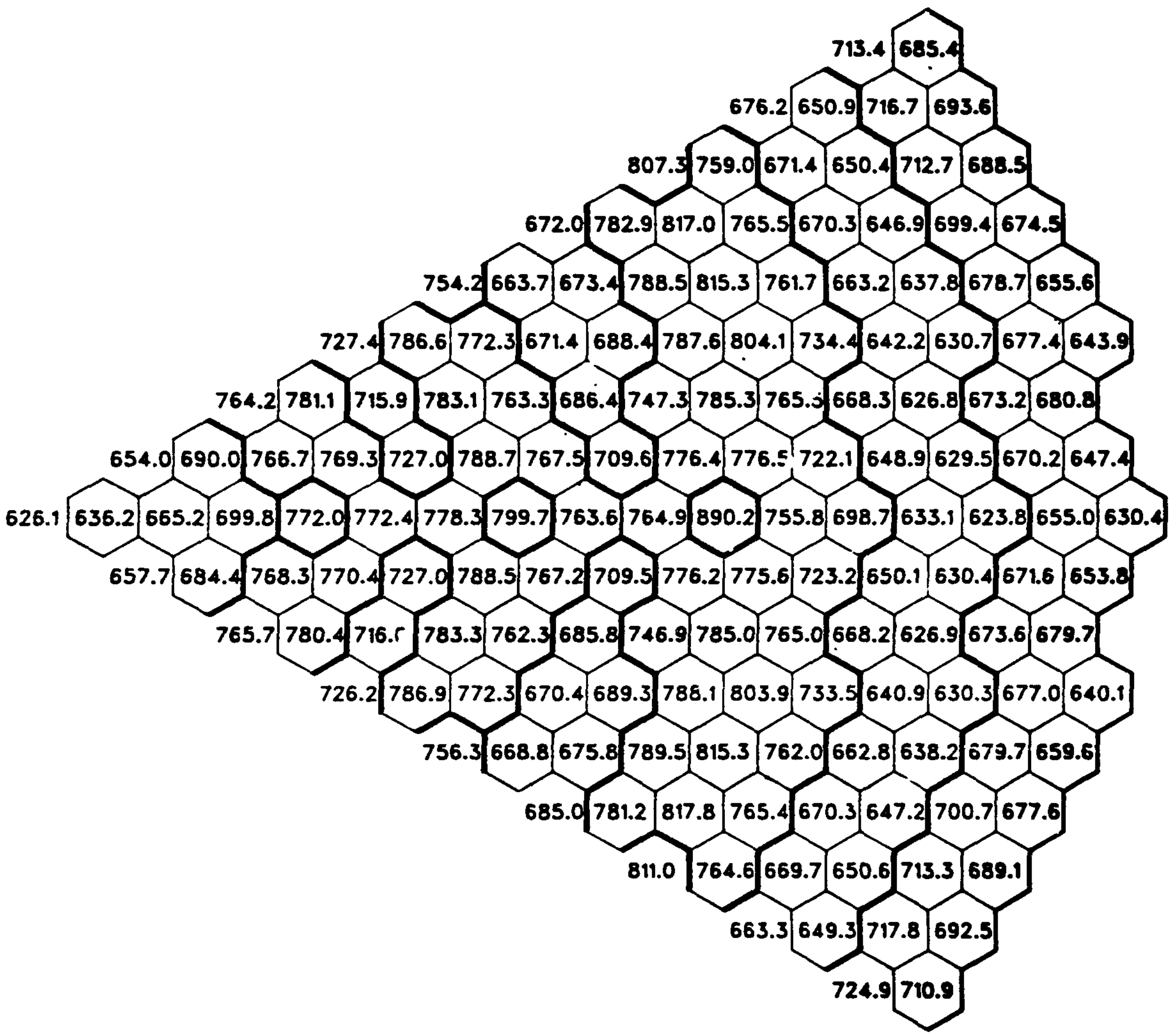

Fig. 66. Configuration B BOL Average Duct Wall Temperature at Outlet (Orificed for Minimum Peak Temperature)

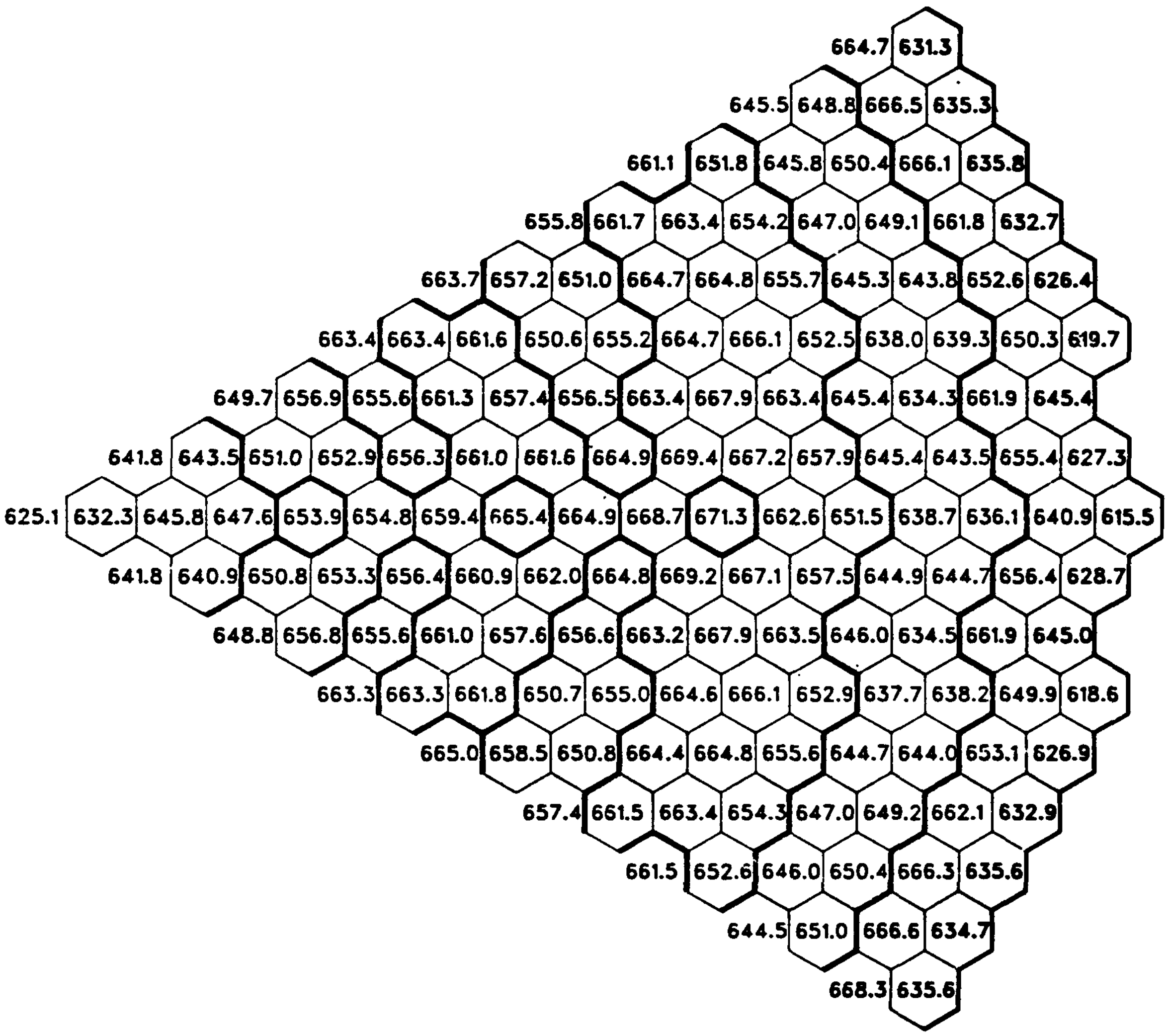

Fig. 67. Configuration B EOEC Average Duct Wall Temperature at Core Mid-Plane (Orificed for Minimum Peak Temperature)

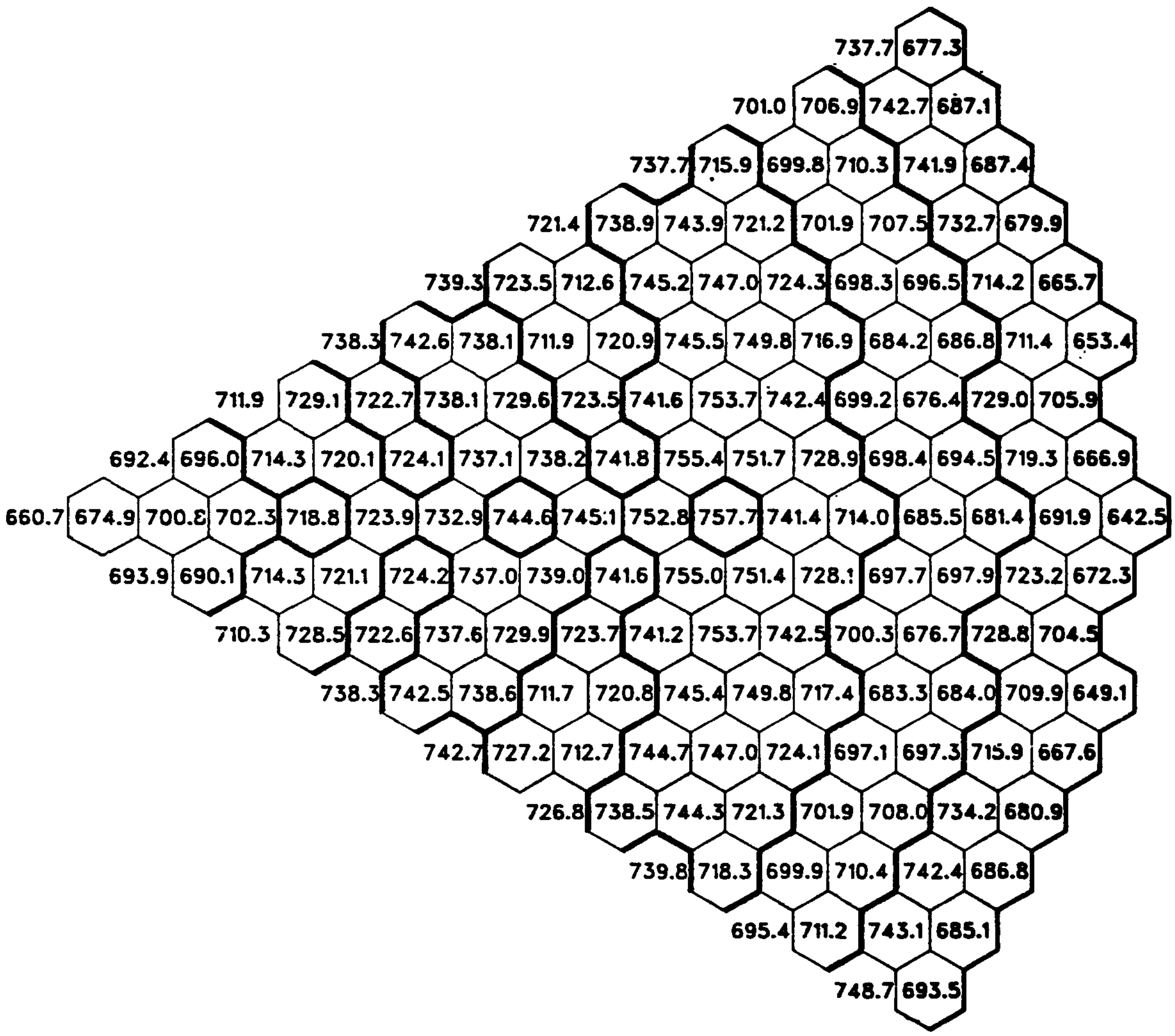

Fig. 68. Configuration B EOEC Average Duct Wall Temperature at Top of Core (Orificed for Minimum Peak Temperature)

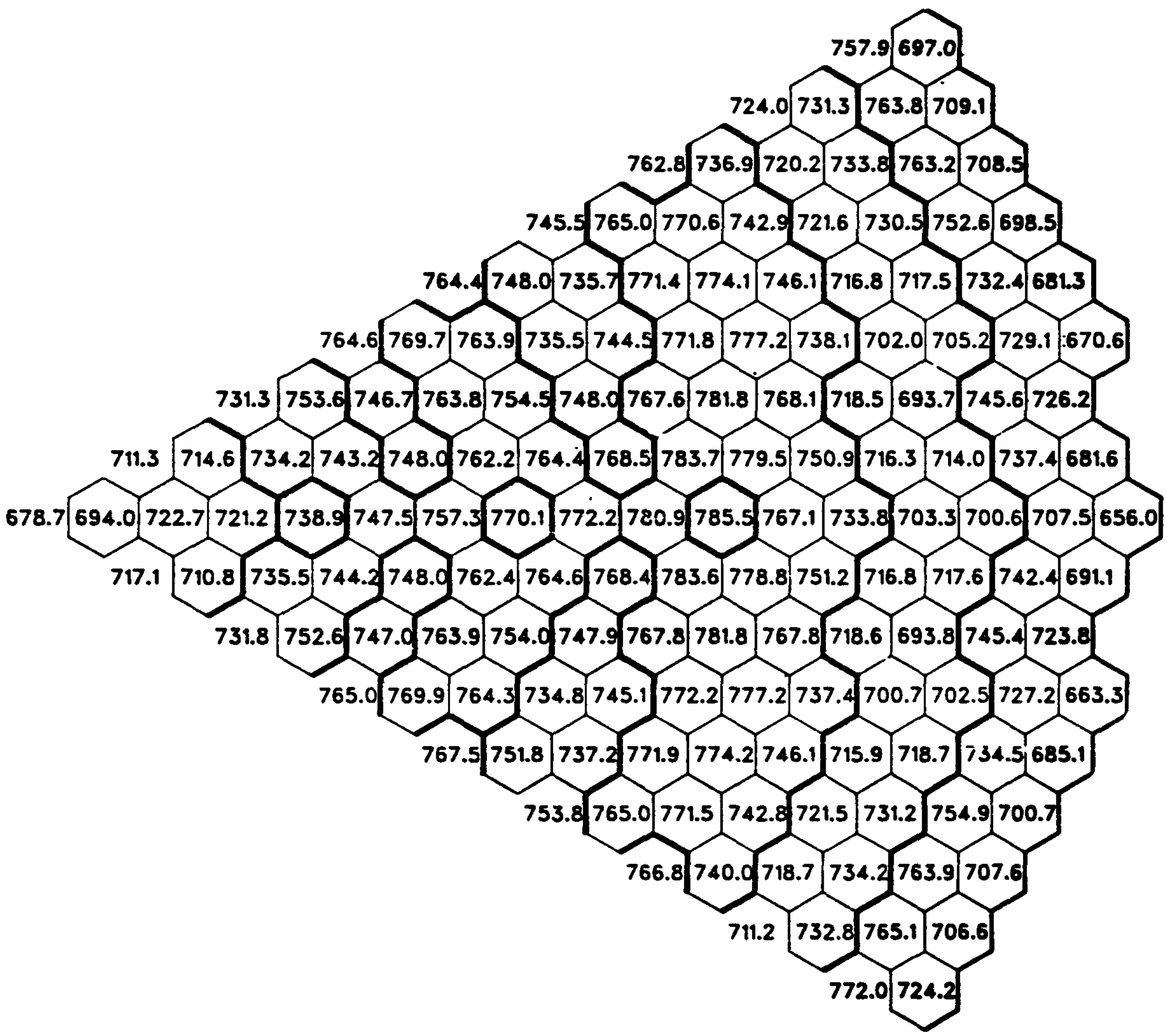

Fig. 69. Configuration B EOEC Average Duct Wall Temperature at Outlet (Orificed for Minimum Peak Temperature)

```
AXIAL DIST (IN)      ESTAR          ALPSTA       AVERAGE TEMP      AVERAGE WALL TEMP
    34.00         1.4167E 02     1.2391E-03        776.6                709.0

CCOLANT TEMPERATURE BY SUBCHANNEL

712 714 713 712 711 710 709 708 707 705 704 702

713 778 780 778 777 775 774 772 770 769 764 704
778 794 793 791 789 788 786 784 783 780 763

715 795 801 800 798 796 794 793 791 789 787 779 704
783 802 802 800 798 796 795 793 791 789 786 766

716 797 803 802 800 798 797 795 793 791 789 787 778 703
783 803 803 801 799 797 796 794 792 790 788 785 765

716 797 804 803 801 799 797 795 794 792 790 788 786 777 703
784 804 803 802 800 798 796 794 793 791 789 787 784 764

717 798 805 803 801 800 798 796 794 793 791 789 787 785 776 702
785 804 804 802 800 799 797 795 793 792 790 788 786 783 763

717 799 805 804 802 800 798 797 795 793 791 790 788 786 784 775 701
785 805 805 803 801 799 798 796 794 792 790 789 787 785 782 762

718 799 806 805 803 801 799 797 796 794 792 790 788 787 785 783 774 701
786 806 805 804 802 800 798 796 795 793 791 789 787 786 784 781 761

718 800 807 805 803 802 800 798 796 794 793 791 789 787 786 784 782 773 700
786 806 806 804 802 801 799 797 795 793 792 790 788 786 785 783 780 760

719 800 807 806 804 802 800 799 797 795 793 791 790 788 786 784 783 780 771 699
787 807 807 805 803 801 799 798 796 794 792 791 789 787 785 783 782 778 758

719 800 808 806 805 803 801 799 797 796 794 792 790 789 787 785 783 781 779 770 698
784 807 807 806 804 802 800 798 797 795 793 791 789 788 786 784 782 780 777 754
716                                                                              698
783 807 807 805 804 802 800 798 796 795 793 791 789 787 786 784 782 780 777 755
717 800 807 806 804 803 801 799 797 795 794 792 790 788 786 785 783 781 779 770 700

786 806 806 804 802 801 799 797 795 793 792 790 788 786 784 783 781 778 758
718 800 806 805 803 801 800 798 796 794 792 791 789 787 785 784 782 780 771 700

785 805 805 803 801 799 798 796 794 792 790 789 787 785 783 782 778 759
718 799 805 804 802 800 798 797 795 793 791 789 788 786 784 782 780 771 701

785 804 804 802 800 798 796 795 793 791 789 788 786 784 782 779 759
718 797 804 803 801 799 797 795 794 792 790 788 787 785 783 781 772 701

784 803 802 801 799 797 795 794 792 790 788 786 785 783 780 760
717 796 803 801 800 798 796 794 793 791 789 787 785 784 781 773 702

783 802 801 800 798 796 794 792 791 789 787 785 783 780 760
717 795 802 800 799 797 795 793 791 790 788 786 784 782 773 702

782 800 800 798 797 795 793 791 789 788 786 784 781 761
716 794 800 799 797 796 794 792 790 788 787 785 783 774 702

780 799 799 797 795 794 792 790 788 787 785 782 762
716 793 799 798 796 794 793 791 789 787 785 783 774 702

779 798 797 796 794 792 790 789 787 785 782 762
715 791 797 795 794 792 790 788 787 785 783 774 702

775 789 788 787 785 783 782 780 778 776 759
714 774 776 775 773 771 770 768 767 765 760 702

712 712 711 711 710 709 708 707 706 705 702 702
```

Fig. 70. Coolant Temperature at Midplane

AXIAL DIST (IN)	ZSTAR	ALPSTA	AVERAGE TEMP	AVERAGE WALL TEMP
52.00	2.1667E 02	1.1723E-03	956.3	843.6

COOLANT TEMPERATURE BY SUBCHANNEL

```
848 851 850 848 845 843 940 838 835 832 830 829
850 933 942 940 937 934 931 928 924 920 907 831
933 969 969 966 963 960 956 953 950 943 906
852 971 995 995 991 988 984 981 977 974 968 940 831
946 997 1002 999 995 992 988 985 981 977 966 916
855 976 1005 1006 1002 999 995 992 988 984 981 973 942 830
949 1001 1007 1005 1001 998 994 990 987 983 979 966 915
857 978 1007 1008 1005 1001 998 994 990 987 983 979 972 940 828
951 1002 1039 1006 1003 999 996 992 989 985 981 977 964 911
859 979 1008 1009 1006 1003 999 995 992 988 985 981 977 969 938 827
952 1004 1010 1008 1004 1001 997 993 990 986 983 979 974 962 911
861 981 1009 1011 1007 1004 1000 997 993 989 986 982 979 975 967 935 825
953 1005 1011 1009 1005 1002 998 995 991 988 984 980 977 972 960 909
862 982 1011 1012 1009 1005 1002 998 994 991 987 984 980 976 972 965 933 824
955 1006 1013 1010 1097 1003 1000 996 992 989 985 982 978 974 970 958 907
863 983 1012 1013 1010 1006 1003 999 996 992 988 985 981 978 974 970 962 931 823
956 1007 1014 1012 1008 1004 1001 997 994 990 987 983 979 976 972 968 955 905
864 984 1013 1014 1011 1008 1004 1000 997 993 990 986 983 979 975 972 968 960 929 821
956 1008 1015 1013 1009 1006 1002 999 995 991 988 984 981 977 973 970 965 953 902
863 981 1014 1016 1013 1009 1005 1002 998 995 991 987 984 980 977 973 970 965 957 924 821
945 1007 1016 1014 1011 1007 1003 1000 996 993 989 985 982 978 975 971 967 963 948 891
860                                                                                        821
944 1006 1016 1014 1010 1007 1003 999 996 992 989 985 982 978 974 971 967 962 948 892
860 980 1013 1015 1012 1008 1005 1001 997 994 990 987 983 980 976 972 969 965 957 924 825
954 1007 1014 1011 1008 1004 1001 997 994 990 986 983 979 976 972 968 964 952 903
862 983 1012 1013 1010 1006 1002 999 995 992 988 984 981 977 974 970 966 959 928 827
954 1005 1012 1009 1006 1002 998 995 991 988 984 981 977 973 970 965 953 905
863 981 1009 1010 1007 1004 1000 996 993 989 986 982 979 975 971 967 960 930 827
953 1003 1009 1007 1003 1000 996 993 989 985 982 978 975 971 966 955 906
863 979 1007 1008 1005 1001 998 994 991 987 983 980 976 973 969 961 931 828
951 1001 1007 1005 1001 997 994 990 987 983 980 976 972 968 956 907
863 977 1005 1006 1003 999 995 992 988 985 981 978 974 970 962 932 829
950 999 1005 1002 999 995 992 988 984 981 977 974 969 957 908
862 975 1002 1003 1000 997 993 990 986 982 979 975 971 964 933 829
948 996 1002 1000 996 993 989 986 982 978 975 970 958 909
862 973 1000 1001 998 994 991 987 984 980 976 972 965 934 830
946 994 1000 997 994 990 986 983 979 976 971 959 910
861 971 997 998 995 991 987 984 980 977 973 966 935 830
943 989 993 991 987 984 980 976 973 969 958 910
859 965 987 986 983 980 976 973 969 966 960 933 831
930 961 962 959 956 953 950 946 943 936 901
857 928 936 934 932 929 926 923 920 917 903 831
853 851 850 849 848 846 845 843 841 837 831 834
```

Fig. 71. Coolant Temperatures at Top of Core

AXIAL DIST (IN)	ZSTAR	ALPSTA	AVERAGE TEMP	AVERAGE WALL TEMP
68.00	2.8333E 02	1.1696E-03	960.7	872.2

COOLANT TEMPERATURE BY SUBCHANNEL

```
                         874  876  875  873  870  867  864  862  859  857  855  855

                         875  917  929  929  926  923  920  916  913  908  894  857
                            918  949  953  951  948  945  941  938  934  925  893

                      878  951  983  986  984  980  977  974  970  966  956  923  857
                         933  984  996  995  992  988  985  981  978  972  955  905

                   880  960  999 1006 1004 1001  997  993  990  986  981  968  928  855
                      937  992 1008 1008 1004 1001  997  994  990  986  979  959  905

                883  962 1003 1011 1009 1006 1002  998  995  991  987  982  968  926  854
                   939  994 1011 1011 1008 1004 1000  997  993  989  985  978  958  904

             885  964 1004 1013 1011 1008 1004 1000  997  993  989  986  980  966  924  853
                941  996 1012 1012 1009 1006 1002  998  995  991  987  983  976  956  902

          888  965 1006 1014 1012 1009 1005 1002  998  994  991  987  983  978  964  922  851
             942  997 1013 1014 1010 1007 1003 1000  996  992  989  985  981  974  953  900

       890  966 1007 1015 1014 1010 1007 1003  999  996  992  988  985  981  976  962  920  850
          944  999 1015 1015 1012 1008 1005 1001  997  994  990  986  983  979  972  951  898

    892  968 1008 1017 1015 1011 1008 1004 1001  997  993  990  986  992  979  973  960  918  850
       945 1000 1016 1016 1013 1010 1006 1002  999  995  991  988  984  980  976  969  949  896

 893  968 1009 1018 1016 1013 1009 1006 1002  998  995  991  987  984  980  976  971  957  916  849
    944 1000 1017 1018 1014 1011 1007 1004 1000  996  993  989  985  982  978  974  967  946  893

892  962 1008 1019 1017 1014 1010 1007 1003 1000  996  992  989  985  981  978  974  968  953  909  850
   930  994 1017 1015 1016 1012 1008 1005 1001  998  994  990  987  983  979  976  971  963  938  881
890                                                                                                     851
   930  994 1017 1018 1015 1012 1008 1004 1001  997  994  990  986  983  979  975  971  963  938  882
890  961 1008 1018 1017 1013 1010 1006 1002  999  995  992  988  984  981  977  973  968  953  910  854

    942  999 1016 1016 1013 1009 1006 1002  998  995  991  988  984  980  977  973  966  946  895
 891  967 1008 1016 1014 1011 1007 1004 1000  996  993  989  986  982  978  975  969  956  917  856

       944  998 1014 1014 1011 1007 1003 1000  996  993  989  985  982  978  974  967  947  898
    892  966 1006 1014 1012 1009 1005 1001  998  994  991  987  983  980  976  971  957  918  857

          943  996 1011 1011 1008 1005 1001  997  994  990  987  983  979  975  968  949  899
       893  965 1004 1012 1010 1006 1003  999  995  992  988  985  981  977  972  959  920  858

             942  994 1009 1009 1006 1002  999  995  991  988  984  981  976  970  950  900
          893  963 1002 1009 1007 1004 1000  997  993  989  986  982  978  973  960  921  858

                941  992 1007 1007 1004 1000  996  993  989  986  982  978  971  951  901
             893  962  999 1007 1005 1002  998  994  991  987  983  980  974  961  922  859

                   940  989 1004 1004 1001  997  994  990  987  983  979  972  952  902
                893  960  997 1004 1002  999  995  992  988  984  981  975  962  923  860

                      938  987 1000 1000  997  993  990  986  983  979  972  953  903
                   893  957  992  999  996  993  989  986  982  979  974  961  923  861

                         934  978  989  987  984  981  977  974  970  965  948  902

                   892  949  976  979  977  973  970  967  963  959  950  919  862

                         919  945  948  947  944  941  938  935  931  922  893
                      889  917  927  927  925  923  920  918  915  910  895  864

                      887  883  882  881  880  879  877  876  873  870  864  867
```

Fig. 72. Coolant Temperatures at Outlet

AXIAL DIST (IN)	2-SIGMA BUNDLE AVG H.W.	2-SIGMA PEAK H.W.
52.00	1088.7	1164.5

CLAD TEMPERATURE BY SUBCHANNEL

957 966 965 961 958 954 951 947 943 940 936 929

965 1062 1073 1070 1066 1062 1057 1053 1049 1043 1026 938
1063 1106 1106 1102 1097 1093 1089 1084 1079 1070 1026

968 1109 1138 1137 1132 1128 1123 1118 1114 1109 1101 1067 937
1079 1140 1145 1142 1137 1132 1127 1123 1118 1112 1098 1037

972 1115 1150 1150 1146 1141 1136 1132 1127 1122 1117 1107 1068 935
1082 1145 1152 1149 1144 1139 1135 1130 1125 1120 1114 1099 1035

975 1118 1152 1153 1149 1144 1139 1135 1130 1125 1120 1115 1105 1066 933
1084 1147 1155 1151 1146 1142 1137 1132 1127 1122 1118 1112 1096 1032

977 1119 1154 1155 1151 1146 1141 1136 1132 1127 1122 1117 1112 1102 1063 931
1086 1149 1156 1153 1148 1143 1139 1134 1129 1124 1119 1115 1108 1093 1030

979 1121 1156 1157 1153 1148 1143 1138 1133 1129 1124 1119 1114 1109 1099 1060 929
1088 1151 1158 1155 1150 1145 1140 1136 1131 1126 1121 1116 1111 1105 1090 1027

981 1123 1158 1159 1154 1149 1145 1140 1135 1130 1125 1121 1116 1111 1106 1096 1057 927
1090 1152 1160 1156 1152 1147 1142 1137 1132 1128 1123 1118 1113 1108 1102 1087 1024

983 1124 1159 1160 1156 1151 1146 1142 1137 1132 1127 1122 1118 1113 1108 1103 1093 1054 925
1091 1154 1162 1158 1153 1149 1144 1139 1134 1129 1125 1120 1115 1110 1105 1099 1084 1022

984 1126 1161 1162 1158 1153 1148 1143 1138 1134 1129 1124 1119 1115 1110 1105 1100 1090 1051 923
1091 1155 1163 1160 1155 1150 1145 1141 1136 1131 1126 1121 1117 1112 1107 1102 1096 1081 1018

983 1122 1162 1164 1159 1155 1150 1145 1140 1135 1131 1126 1121 1116 1111 1107 1102 1096 1086 1044 922
1078 1153 1164 1162 1157 1152 1147 1142 1138 1133 1128 1123 1118 1114 1109 1104 1099 1093 1075 1004
973 917
1077 1153 1164 1161 1156 1152 1147 1142 1137 1132 1128 1123 1118 1113 1108 1104 1099 1092 1074 1005
979 1121 1161 1163 1159 1154 1149 1144 1139 1134 1130 1125 1120 1115 1111 1106 1101 1096 1085 1045 927

1089 1154 1161 1158 1153 1148 1144 1139 1134 1129 1124 1120 1115 1110 1105 1100 1094 1079 1019
981 1124 1155 1160 1155 1151 1146 1141 1136 1131 1127 1122 1117 1112 1107 1103 1097 1088 1050 929

1089 1151 1158 1155 1150 1145 1141 1136 1131 1126 1121 1117 1112 1107 1102 1096 1081 1021
981 1122 1156 1157 1152 1148 1143 1138 1133 1128 1124 1119 1114 1109 1104 1099 1089 1052 930

1087 1148 1155 1152 1147 1142 1137 1133 1128 1123 1118 1113 1109 1104 1098 1083 1023
982 1119 1153 1154 1149 1144 1140 1135 1130 1125 1120 1116 1111 1106 1101 1091 1054 931

1085 1145 1152 1149 1144 1139 1134 1130 1125 1120 1115 1110 1105 1100 1084 1024
981 1116 1150 1150 1146 1141 1137 1132 1127 1122 1117 1113 1108 1102 1093 1055 932

1083 1142 1149 1146 1141 1136 1131 1126 1122 1117 1112 1107 1101 1086 1026
980 1114 1147 1147 1143 1138 1133 1129 1124 1119 1114 1109 1104 1094 1057 933

1080 1139 1146 1142 1138 1133 1128 1123 1119 1114 1109 1103 1088 1027
979 1111 1143 1144 1140 1135 1130 1125 1121 1116 1111 1106 1096 1058 934

1078 1136 1142 1139 1134 1129 1125 1120 1115 1110 1104 1089 1028
978 1108 1140 1140 1135 1131 1126 1121 1116 1112 1106 1097 1059 935

1074 1129 1134 1131 1126 1121 1116 1112 1107 1101 1088 1028

976 1100 1127 1126 1121 1117 1112 1107 1103 1098 1090 1057 935

1057 1095 1096 1092 1088 1083 1079 1075 1070 1061 1018
972 1054 1064 1062 1058 1055 1051 1047 1043 1038 1021 936

961 964 963 961 959 957 954 952 948 944 936 934

Fig. 73. Nominal Clad Temperatures at Mid-Plane

```
AXIAL DIST (IN)     NOMINAL BUNDLE AVG M.W.     NOMINAL PEAK M.W.
    34.00                  830.9                      864.9

CLAD TEMPERATURE BY SUBCHANNEL

                      767  775  774  772  771  769  768  766  764  763  761  753

                      775  834  836  834  832  830  828  826  824  821  816  761
                         835  850  848  846  844  842  840  838  835  833  815

                   777  852  857  855  853  851  849  846  844  842  839  830  760
                      839  858  857  855  853  851  848  846  844  842  838  817

                778  853  859  857  855  853  851  848  846  844  842  839  830  759
                   840  859  858  856  854  852  850  847  845  843  841  837  816

             779  854  860  858  856  854  852  849  847  845  843  840  838  828  758
                841  860  859  857  855  853  850  848  846  844  841  839  836  815

          779  855  861  859  857  855  852  850  948  846  843  841  839  836  827  757
             842  861  860  858  856  853  851  849  847  844  842  840  838  834  814

       780  856  862  860  858  855  853  851  849  846  844  842  840  838  835  825  756
          843  862  861  859  856  854  852  850  847  845  843  841  839  836  833  812

    781  856  863  861  858  856  854  852  850  847  845  843  841  838  836  833  824  755
       843  862  862  860  857  855  853  851  848  846  844  842  839  837  835  831  811

 781  857  863  862  859  857  855  853  850  848  846  844  841  839  837  835  832  823  754
    844  863  863  860  858  856  854  851  849  847  845  842  840  838  836  833  830  809

782  858  864  862  860  858  856  853  851  849  947  844  842  840  838  835  833  831  821  753
   845  864  863  861  859  857  854  852  850  848  845  843  841  839  836  834  832  828  808

782  858  865  863  861  859  856  854  852  850  847  845  843  841  838  836  834  832  829  819  752
   842  865  864  862  860  857  855  853  851  848  846  844  842  840  837  835  833  830  827  804
773                                                                                                746
   842  864  864  862  859  857  855  853  850  848  946  844  842  839  837  835  833  830  827  804
780  858  864  863  860  858  856  854  851  849  847  845  843  840  838  836  834  831  829  819  753

   844  863  862  860  858  856  854  851  849  847  845  842  840  838  836  833  831  828  808
781  857  863  861  859  857  855  852  850  848  846  843  841  839  837  834  832  830  820  754

    843  862  861  859  857  854  852  850  848  845  843  841  839  836  834  832  828  808
 781  856  862  860  858  855  853  851  849  846  844  842  840  837  835  833  830  821  755

       842  860  860  857  855  853  851  848  846  844  842  839  837  835  833  829  809
    780  854  860  858  856  854  852  849  847  845  843  840  838  836  834  831  822  755

          840  859  858  856  854  851  849  847  845  842  840  838  836  833  830  810
       779  853  859  857  855  852  850  848  846  843  841  839  837  835  832  823  756

             839  857  857  854  852  850  848  846  843  841  839  837  834  831  811
          779  851  857  855  853  851  849  847  944  842  840  838  835  833  823  756

                838  856  855  853  851  849  846  844  842  940  837  835  832  811
             778  850  856  854  852  850  847  845  843  841  838  836  834  824  757

                   836  855  854  852  849  847  845  843  840  838  836  832  812
                777  849  854  853  850  848  846  844  841  839  837  834  825  757

                      835  853  852  850  847  845  843  841  839  836  833  813

                776  847  852  850  847  845  843  841  839  836  834  825  757

                   830  844  843  841  839  836  834  832  830  827  810
                774  829  831  829  827  825  823  821  819  817  811  757

                   766  771  770  769  768  766  765  763  762  760  757  752
```

Fig. 74. Nominal Clad Temperatures at Top of Core

AXIAL DIST (IN) NOMINAL BUNDLE AVG N.W. NOMINAL PEAK N.W.

52.00 979.8 1040.7

CLAD TEMPERATURE BY SUBCHANNEL

872 878 877 874 872 869 866 863 860 857 855 851

877 958 966 964 961 958 954 951 948 943 930 856

958 993 994 990 987 983 980 976 972 966 929

880 996 1019 1019 1015 1011 1008 1004 1000 997 990 963 856

971 1021 1026 1023 1019 1015 1011 1008 1004 1000 988 938

882 1001 1029 1030 1026 1022 1019 1015 1011 1007 1003 996 964 854

974 1025 1031 1029 1025 1021 1017 1014 1010 1006 1001 989 937

884 1003 1031 1032 1029 1025 1021 1017 1014 1010 1006 1002 994 962 853

975 1027 1033 1030 1027 1023 1019 1015 1012 1008 1004 999 987 935

886 1004 1032 1033 1030 1026 1022 1019 1015 1011 1007 1004 999 992 960 851

977 1028 1034 1032 1028 1024 1020 1017 1013 1009 1005 1002 997 984 933

888 1005 1034 1035 1031 1028 1024 1020 1016 1013 1009 1005 1001 997 989 958 849

978 1029 1036 1033 1029 1026 1022 1018 1014 1010 1007 1003 999 994 982 931

889 1007 1035 1036 1033 1029 1025 1021 1018 1014 1010 1006 1003 999 995 987 955 848

980 1031 1037 1034 1031 1027 1023 1019 1016 1012 1008 1004 1000 997 992 979 929

891 1008 1036 1037 1034 1030 1027 1023 1019 1015 1011 1008 1004 1000 996 992 984 953 846

981 1032 1038 1036 1032 1028 1024 1021 1017 1013 1009 1006 1002 998 994 989 977 926

892 1009 1038 1039 1035 1032 1028 1024 1020 1017 1013 1009 1005 1001 998 994 990 982 951 845

981 1033 1040 1037 1033 1030 1026 1022 1018 1015 1011 1007 1003 999 996 992 987 975 924

891 1006 1038 1040 1037 1033 1029 1025 1022 1018 1014 1010 1007 1003 999 995 991 987 979 945 844

970 1031 1041 1038 1035 1031 1027 1023 1020 1016 1012 1008 1005 1001 997 993 989 984 970 912

885 842

969 1031 1040 1038 1034 1031 1027 1023 1019 1015 1012 1008 1004 1000 997 993 989 984 970 913

888 1005 1038 1039 1036 1032 1029 1025 1021 1017 1013 1010 1006 1002 998 995 991 987 978 945 848

979 1032 1038 1036 1032 1028 1024 1021 1017 1013 1009 1006 1002 998 994 990 986 973 924

889 1007 1036 1037 1034 1030 1026 1022 1019 1015 1011 1007 1003 1000 996 992 988 980 950 850

979 1030 1036 1033 1030 1026 1022 1018 1014 1011 1007 1003 999 996 992 987 975 926

890 1006 1034 1035 1031 1027 1024 1020 1016 1012 1009 1005 1001 997 993 989 982 951 851

978 1027 1033 1031 1027 1023 1020 1016 1012 1008 1004 1001 997 993 988 976 928

890 1004 1031 1032 1029 1025 1021 1017 1014 1010 1006 1002 999 995 991 983 953 852

976 1025 1031 1028 1025 1021 1017 1013 1010 1006 1002 998 994 990 978 929

890 1002 1029 1030 1026 1023 1019 1015 1011 1007 1004 1000 996 992 984 954 852

974 1023 1029 1026 1022 1018 1015 1011 1007 1003 1000 996 991 979 930

889 1000 1026 1027 1024 1020 1016 1013 1009 1005 1001 998 993 936 955 853

972 1020 1026 1023 1020 1016 1012 1008 1005 1001 997 992 980 931

888 997 1024 1025 1021 1018 1014 1010 1006 1003 999 995 987 956 854

970 1018 1023 1021 1017 1013 1009 1006 1002 998 993 981 932

887 995 1021 1021 1018 1014 1010 1007 1003 999 995 988 957 854

967 1013 1017 1014 1010 1007 1003 999 995 991 980 932

886 989 1011 1010 1006 1003 999 995 992 988 982 955 855

954 985 985 982 979 976 972 969 965 959 923

883 952 960 958 955 952 949 946 943 939 926 856

876 877 876 875 873 872 870 868 865 862 856 855

Fig. 75. Nominal Clad Temperatures at Outlet

AXIAL DIST (IN)	2-SIGMA BUNDLE AVG H.W.	2-SIGMA PEAK H.W.
34.00	930.7	974.7

CLAD TEMPERATURE BY SUBCHANNEL

```
                      853  868  866  864  862  860  857  855  852  849  847  832

                      868  937  938  935  933  930  927  924  921  919  911  847
                         938  955  953  950  947  944  941  938  935  931  910

                   870  958  964  961  958  955  952  949  946  943  939  928  846
                      943  965  964  961  958  955  952  949  945  942  938  912

                872  960  967  964  961  958  955  952  949  946  942  939  927  844
                   944  967  966  963  960  956  953  950  947  944  941  936  910

             873  961  968  965  962  959  956  953  950  947  944  941  937  925  843
                946  968  967  964  961  958  954  951  948  945  942  939  934  908

          874  962  969  967  963  960  957  954  951  948  945  942  939  935  923  841
             947  969  968  965  962  959  956  952  949  946  943  940  937  932  907

       875  963  970  968  965  961  958  955  952  949  946  943  940  937  933  921  840
          948  970  969  966  963  960  957  954  950  947  944  941  938  935  930  905

    876  964  971  969  966  963  959  956  953  950  947  944  941  938  935  931  919  838
       949  971  970  967  964  961  958  955  952  948  945  942  939  936  933  928  903

 877  965  973  970  967  964  961  957  954  951  948  945  942  939  936  933  929  917  836
    950  973  971  968  965  962  959  956  953  950  946  943  940  937  934  931  926  901

878  966  974  971  968  965  962  959  955  952  949  946  943  940  937  934  931  927  915  835
   951  974  972  969  966  963  960  957  954  951  948  944  941  938  935  932  929  924  899

878  967  975  972  969  966  963  960  957  953  950  947  944  941  938  935  932  929  925  913  833
   947  974  974  971  967  964  961  958  955  952  949  946  942  939  936  933  930  927  922  893
862                                                                                                  820
   947  974  973  970  967  964  961  958  955  951  948  945  942  939  936  933  930  926  921  894
876  966  974  972  968  965  962  959  956  953  950  947  944  940  937  934  931  928  924  912  835

   949  973  971  968  965  962  959  956  953  949  946  943  940  937  934  931  928  923  898
876  965  972  970  966  963  960  957  954  951  948  945  942  938  935  932  929  925  914  836

    948  971  969  966  963  960  957  954  951  947  944  941  939  935  932  929  924  899
 876  963  970  968  964  961  958  955  952  949  946  943  940  936  933  930  927  915  837

       946  969  967  964  961  958  955  952  949  945  942  939  936  933  930  925  900
    875  961  968  966  962  959  956  953  950  947  944  941  938  934  931  928  916  838

          944  966  965  962  959  956  953  950  947  943  940  937  934  931  926  901
       874  959  966  964  960  957  954  951  948  945  942  939  936  932  929  917  838

             943  964  963  960  957  954  951  948  945  941  938  935  932  927  902
          873  957  964  962  958  955  952  949  946  943  940  937  933  930  918  839

                941  962  961  958  955  952  949  946  943  939  936  933  929  903
             871  955  962  960  956  953  950  947  944  941  938  935  931  919  840

                   939  960  959  956  953  950  947  944  941  937  934  930  904
                870  953  960  957  954  951  948  945  942  939  936  932  920  840

                      937  958  957  954  950  947  944  941  938  935  930  905

                868  951  956  954  951  948  944  941  938  935  932  921  841

                      931  947  945  942  939  936  933  930  927  923  903
                   866  929  931  928  925  922  919  917  914  911  904  841

                   850  862  860  858  856  854  852  850  847  845  841  829
```

Fig. 76. 2σ Mid-Wall Clad Temperatures at Mid-Plane

```
AXIAL DIST (IN)     NOMINAL BUNDLE AVG S.W.     NOMINAL PEAK S.W.
    68.00                   960.9                     1019.0

CLAD TEMPERATURE BY SUBCHANNEL

                    875   876   875   873   870   867   865   862   860   857   855   855

                    876   918   930   929   926   923   920   917   913   908   894   857
                       918   950   954   951   948   945   942   938   934   925   894

                 878   951   983   987   984   981   977   974   970   966   957   923   857
                    933   984   997   995   992   989   985   981   978   972   955   905

              881   960   999  1006  1004  1001   997   994   990   986   981   969   928   856
                 937   992  1008  1008  1005  1001   997   994   990   986   980   959   905

           883   962  1003  1011  1009  1006  1002   999   995   991   988   982   969   927   854
              939   995  1011  1011  1008  1004  1001   997   993   990   986   979   958   904

        886   964  1005  1013  1011  1008  1004  1000   997   993   990   986   980   967   925   853
           941   996  1012  1013  1009  1006  1002   999   995   991   988   983   976   956   902

     888   965  1006  1014  1013  1009  1005  1002   998   995   991   987   983   978   964   923   852
        943   997  1014  1014  1011  1007  1003  1000   996   993   989   985   981   974   954   900

  890   967  1007  1015  1014  1010  1007  1003   999   996   992   989   985   981   976   962   921   851
     944   999  1015  1015  1012  1008  1005  1001   997   994   990   987   983   979   972   951   898

892   968  1009  1017  1015  1012  1008  1004  1001   997   994   990   986   983   979   973   960   919   850
   945  1000  1016  1016  1013  1010  1006  1002   999   995   992   988   984   981   977   970   949   896

893   968  1010  1018  1016  1013  1009  1006  1002   998   995   991   988   984   980   976   971   957   916   850
   944  1000  1017  1018  1015  1011  1007  1004  1000   996   993   989   986   982   978   974   967   946   893

892   962  1009  1019  1018  1014  1011  1007  1003  1000   996   992   989   985   982   978   974   968   953   909   850
   931   995  1017  1019  1016  1012  1009  1005  1001   998   994   990   987   983   980   976   972   964   939   881
891                                                                                                                   852
   930   994  1017  1018  1016  1012  1008  1005  1001   997   994   990   987   983   979   976   971   963   939   883
890   961  1008  1018  1017  1014  1010  1006  1003   999   995   992   988   985   981   977   973   968   953   910   854

   943   999  1016  1016  1013  1010  1006  1002   999   995   991   988   984   981   977   973   966   946   896
891   967  1008  1016  1015  1011  1008  1004  1000   997   993   989   986   982   979   975   969   956   917   856

   944   998  1014  1014  1011  1007  1004  1000   996   993   989   985   982   978   974   967   948   899
892   966  1006  1014  1012  1009  1005  1002   998   994   991   987   984   980   976   971   958   919   857

   944   996  1012  1012  1009  1005  1001   998   994   990   987   983   979   975   969   949   900
693   965  1004  1012  1010  1007  1003   999   996   992   988   985   981   977   972   959   920   858

   943   994  1009  1009  1006  1003   999   995   992   988   984   981   977   970   950   901
894   964  1002  1009  1008  1004  1001   997   993   990   986   982   979   973   960   921   859

   941   992  1007  1007  1004  1000   997   993   989   986   982   978   971   951   902
894   962   999  1007  1005  1002   998   995   991   987   984   980   975   961   922   859

   940   990  1004  1004  1001   998   994   990   987   983   979   972   952   902
894   960   997  1004  1002   999   995   992   988   985   981   976   962   923   860

   938   987  1001  1000   997   994   990   986   983   979   972   953   903
893   957   993   999   997   993   990   986   982   979   974   962   923   861

      935   978   989   988   984   981   977   974   970   965   948   903
892   949   976   979   977   974   970   967   964   959   950   919   863

   920   945   949   947   944   941   938   935   932   923   893
889   917   927   927   925   923   920   918   915   910   896   864

887   884   883   881   880   879   978   876   874   870   864   868
```

Fig. 77. 2σ Mid-Wall Clad Temperatures at Mid-Plane

```
AXIAL DIST (IN)     2-SIGMA BUNDLE AVG M.W.     2-SIGMA PEAK M.W.
     68.00                 1046.0                    1117.5

CLAD TEMPERATURE BY SUBCHANNEL

                                 940   942   941   938   934   931   927   924   921   918   916   916

                                 941   993  1007  1006  1003   999   995   991   987   981   963   918
                                    993  1032  1037  1034  1030  1026  1022  1018  1013  1002   963

                              944  1034  1073  1078  1075  1070  1066  1062  1057  1052  1041  1000   918
                                 1012  1075  1090  1088  1084  1080  1076  1071  1067  1060  1039   977

                           947  1045  1093  1102  1099  1095  1091  1086  1082  1077  1071  1056  1005   916
                              1017  1085  1104  1104  1100  1095  1091  1087  1082  1077  1069  1044   978

                        950  1048  1098  1108  1106  1101  1097  1093  1088  1084  1079  1072  1055  1004   914
                           1019  1088  1107  1108  1104  1099  1095  1090  1086  1081  1076  1068  1042   976

                     953  1050  1100  1110  1108  1104  1099  1095  1090  1086  1081  1077  1070  1053  1001   913
                        1022  1089  1109  1110  1106  1101  1097  1092  1088  1083  1079  1074  1065  1040   973

                  956  1051  1102  1112  1110  1105  1101  1096  1092  1087  1083  1078  1074  1067  1050   999   911
                     1023  1091  1111  1111  1107  1103  1098  1094  1089  1085  1081  1076  1071  1062  1037   971

               959  1053  1103  1113  1111  1107  1103  1098  1094  1089  1085  1080  1076  1071  1064  1047   996   910
                  1025  1093  1112  1113  1109  1105  1100  1096  1091  1087  1082  1078  1073  1068  1059  1034   969

            961  1055  1105  1115  1113  1109  1104  1100  1095  1091  1086  1082  1077  1073  1068  1061  1045   994   909
               1027  1094  1114  1114  1111  1106  1102  1097  1093  1088  1084  1079  1075  1070  1065  1057  1031   967

         962  1055  1106  1116  1114  1110  1106  1101  1097  1092  1088  1083  1079  1074  1070  1065  1059  1042   991   909
            1025  1095  1115  1116  1112  1108  1103  1099  1094  1090  1085  1081  1076  1072  1067  1062  1054  1028   963

      962  1048  1105  1118  1116  1112  1107  1103  1098  1094  1089  1085  1080  1076  1071  1067  1062  1055  1036   982   909
         1009  1088  1115  1117  1114  1109  1105  1100  1096  1091  1087  1082  1078  1074  1069  1064  1059  1049  1018   948
   959                                                                                                                           911
         1008  1087  1115  1117  1113  1109  1104  1100  1095  1091  1086  1082  1078  1073  1069  1064  1059  1049  1019   949
      959  1047  1104  1117  1115  1111  1106  1102  1097  1093  1089  1084  1080  1075  1071  1066  1061  1055  1036   983   914

            1023  1093  1114  1114  1110  1106  1102  1097  1093  1088  1084  1079  1075  1070  1066  1061  1052  1027   966
         960  1053  1104  1114  1112  1108  1104  1099  1095  1090  1086  1081  1077  1072  1068  1063  1057  1040   992   917

               1025  1092  1111  1111  1108  1103  1099  1094  1090  1085  1081  1076  1072  1067  1062  1054  1030   969
            961  1053  1102  1111  1109  1105  1101  1096  1092  1087  1083  1078  1074  1069  1065  1058  1042   994   918

                  1025  1089  1108  1109  1105  1100  1096  1091  1087  1082  1078  1073  1069  1064  1055  1031   971
               962  1051  1099  1109  1106  1102  1098  1093  1089  1084  1080  1075  1071  1066  1060  1043   995   919

                     1023  1087  1105  1106  1102  1097  1093  1088  1084  1079  1075  1070  1065  1057  1033   972
                  963  1049  1096  1106  1104  1099  1095  1090  1086  1081  1077  1073  1068  1061  1045   997   920

                        1022  1084  1103  1103  1099  1094  1090  1085  1081  1077  1072  1067  1059  1034   973
                     963  1047  1094  1103  1101  1096  1092  1087  1083  1079  1074  1069  1063  1046   998   921

                           1020  1081  1100  1100  1096  1091  1087  1082  1078  1073  1068  1060  1036   974
                        963  1045  1091  1099  1097  1093  1088  1084  1080  1075  1070  1064  1048   999   922

                              1018  1078  1095  1095  1091  1086  1082  1077  1073  1068  1060  1036   975
                           963  1042  1085  1093  1090  1086  1081  1077  1073  1068  1062  1047  1000   923

                                 1013  1067  1080  1079  1075  1071  1066  1062  1058  1051  1031   974

                           961  1031  1065  1069  1066  1062  1058  1053  1049  1044  1033   994   925

                                 995  1027  1031  1029  1025  1022  1018  1014  1010   999   963
                              958   992  1005  1004  1002   999   996   993   989   984   966   927

                              955   951   949   948   947   945   943   941   939   934   927   931

PEAK CLAD MID-WALL TEMPERATURE OF   1164.5 AT  52.00 INCHES
```

Fig. 78. 2σ Mid-Wall Clad Temperatures at Outlets

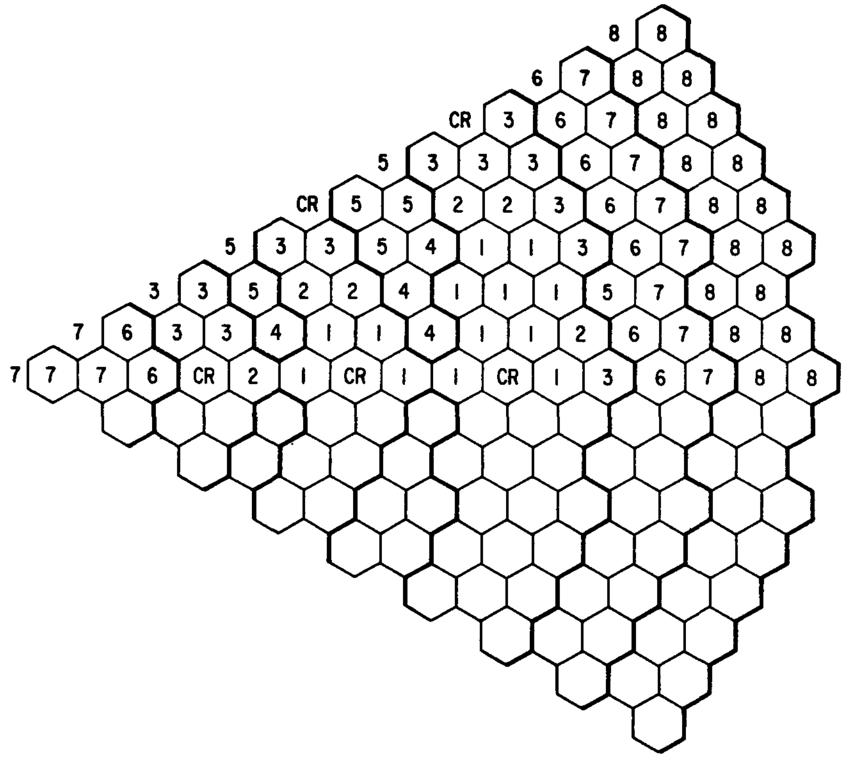

Fig. 79. Orificing Scheme of Configuration B with Peak Clad Temperature at EOEC

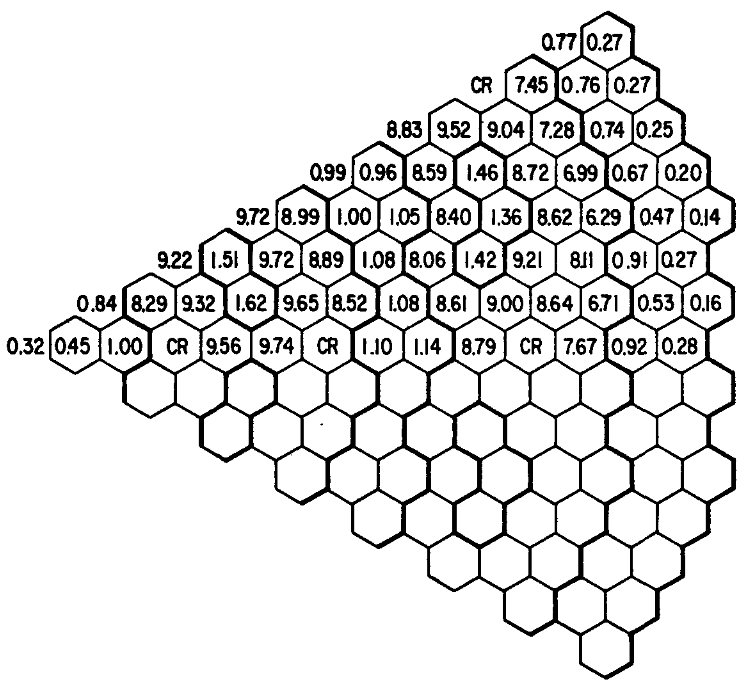

Fig. 80. Total Power Per Assembly (MWth) at BOL, Configuration A

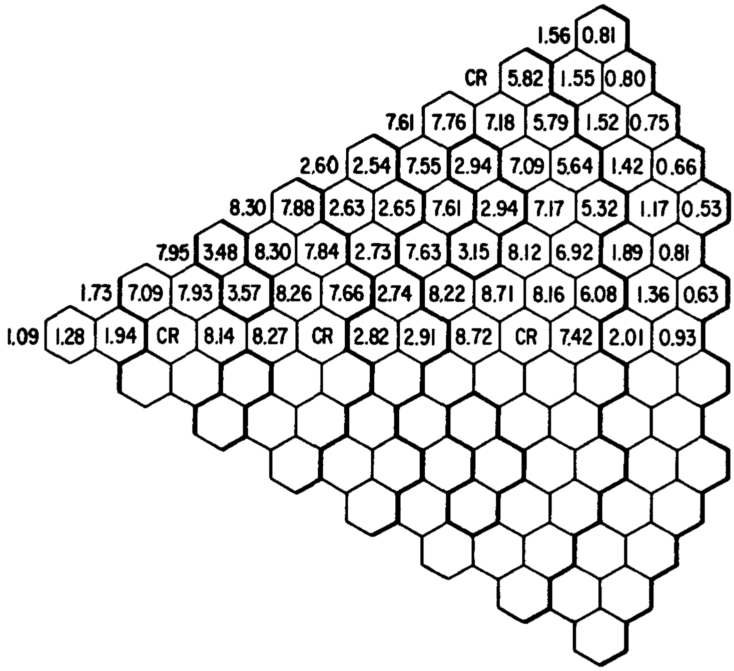

Fig. 81. Total Power Per Assembly (MWth) at EOEC, Configuration A

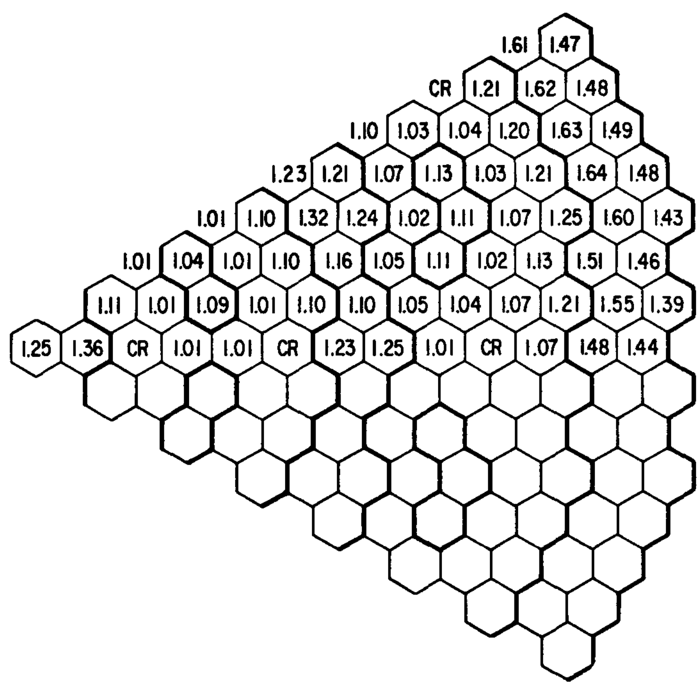

Fig. 82. Peak-to-Average Power Per Assembly at BOL, Configuration A

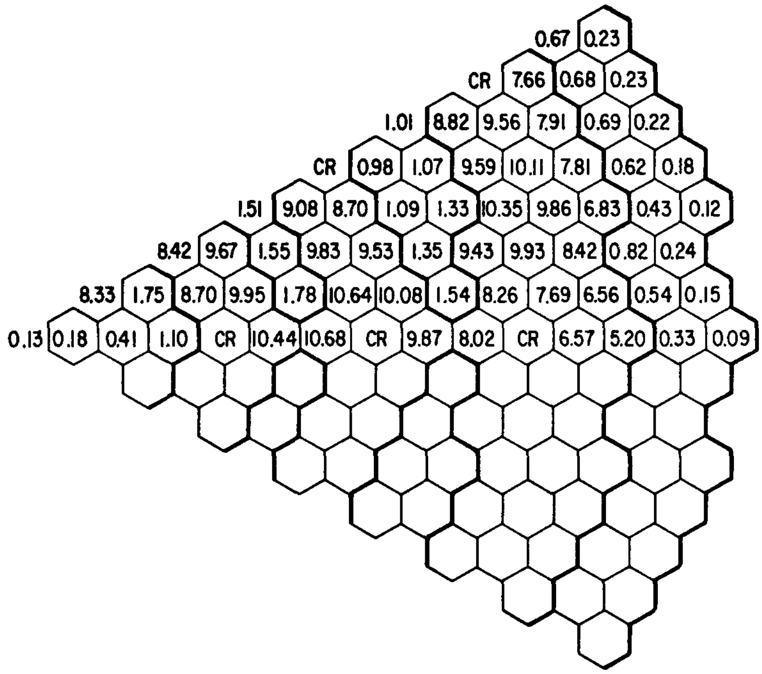

Fig. 83. Total Power Per Assembly (MWth) at BOL, Configuration B

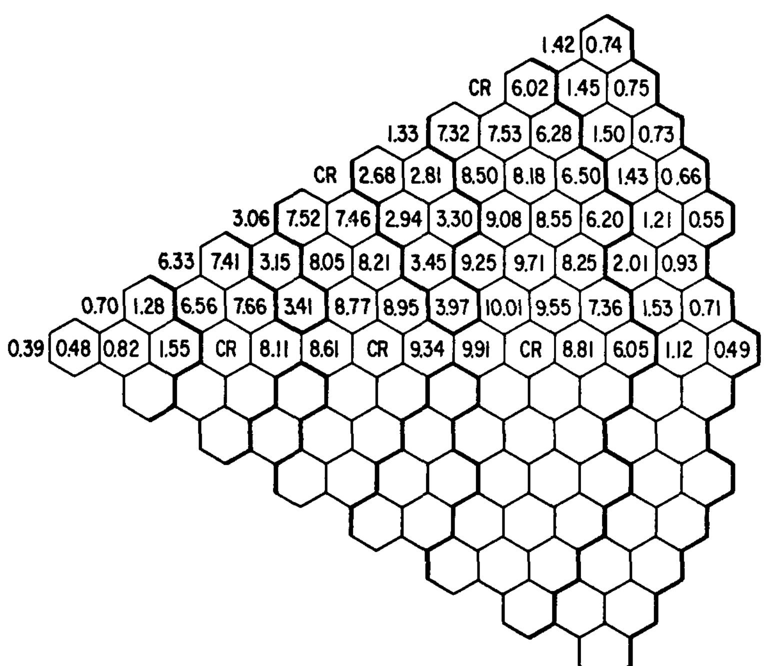

Fig. 84. Total Power Per Assembly (MWth) at EOEC, Configuration B

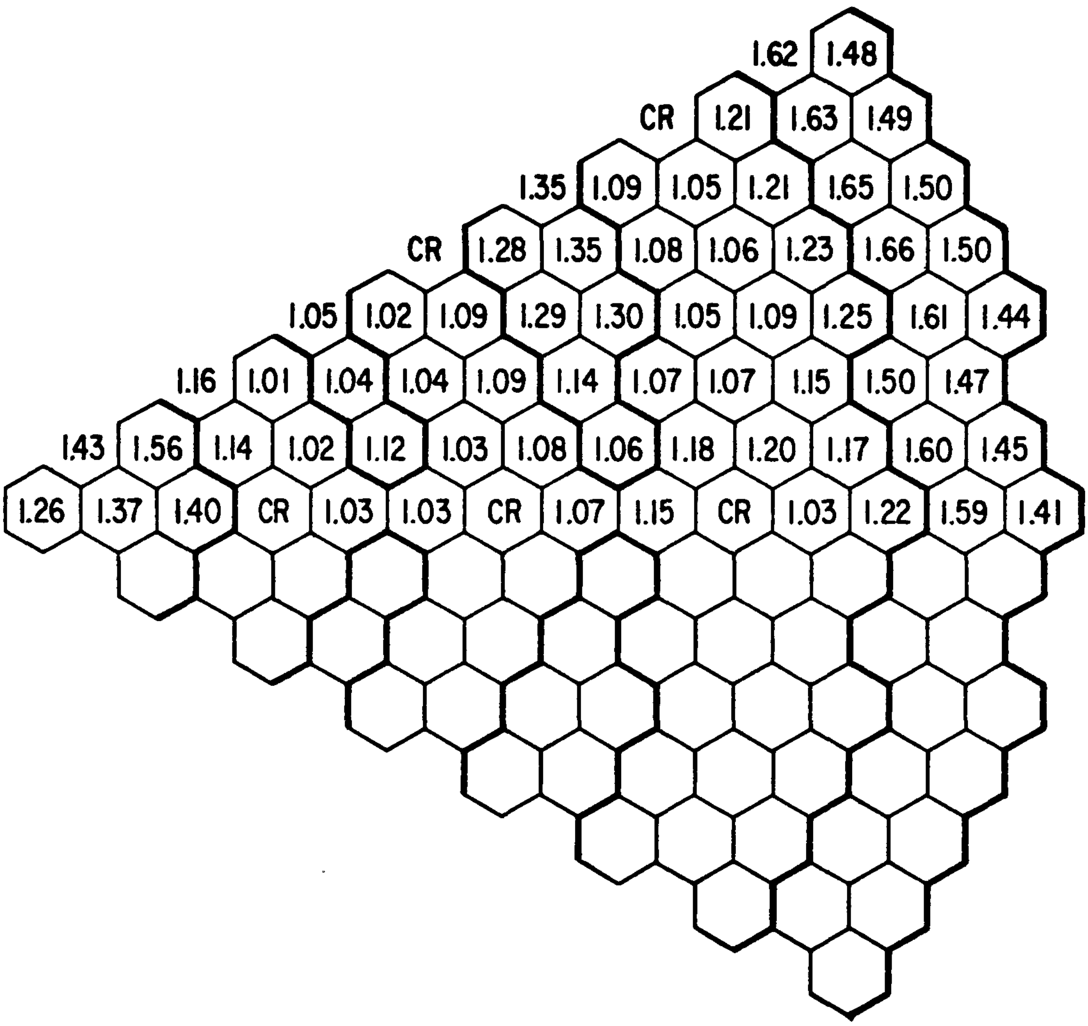

Fig. 85. Peak-to-Average Power Per Assembly at BOL, Configuration B

TABLE I. Number of Assemblies Per Region

Region	Configuration A	Configuration B
Inner Core	36	48
Middle Core	72	84
Outer Core	222	210
Core	330	342
Internal Blanket 1	19	37
Internal Blanket 2	24	30
Internal Blanket 3	78	78
Internal Blanket 4	36	-
Internal Blankets	157	145
Control Assemblies	24	30
Radial Blanket	174	174
Shield Assemblies	198	198

TABLE II. Fissile Inventories, kg

	Configuration A			Configuration B		
	BOL	BOEC	EOEC	BOL	BOEC	EOEC
Inner Core	415.7	397.7	363.7	566.7	537.3	480.7
Middle Core	831.4	794.1	724.1	942.4	894.4	802.9
Outer Core	2614.8	2514.0	2320.5	2281.6	2154.1	1979.9
Total Core	3861.9	3705.8	3408.3	3790.9	3585.8	3263.6
Internal Blanket 1	0.0	19.5	55.4	0.0	64.7	185.3
Internal Blanket 2	0.0	34.3	95.0	0.0	46.4	128.1
Internal Blanket 3 + 4[a]	0.0	143.5	401.4	0.0	107.7	300.0
Total Internal Blanket	0.0	197.3	551.8	0.0	218.8	520.7
Axial Blanket	0.0	55.3	161.4	0.0	74.7	216.9
Radial Blanket	0.0	310.0	453.5	0.0	334.1	488.5
Total Reactor	3861.9	4268.4	4575.0	3790.9	4213.4	4489.7

[a]Applies to configuration A only

TABLE III. Average Fissile Enrichment, % H.M.

	Configuration A			Configuration B		
	BOL	BOEC	EOEC	BOL	BOEC	EOEC
Inner Core	17.7	17.2	16.3	19.4	18.7	17.5
Middle Core	17.7	17.2	16.3	18.4	17.8	16.7
Outer Core	18.1	17.6	16.8	17.8	17.1	16.3
Internal Blanket 1	0.0	0.6	1.8	0.0	0.5	1.5
Internal Blanket 2	0.0	0.9	2.5	0.0	0.9	2.6
Internal Blanket 3 + 4[a]	0.0	0.7	2.2	0.0	0.8	2.3
Axial Blanket	0.0	0.3	0.9	0.0	0.4	1.2
Radial Blanket	0.0	1.1	1.6	0.0	1.2	1.7

[a]Applies only to Configuration A

TABLE IV. Discharge Burnups (MWD/Kg)

	Configuration A		Configuration B	
	Average	Peak	Average	Peak
Inner Core	62.44	81.34	73.82	88.34
Middle Core	65.06	83.26	74.05	95.31
Outer Core	54.63	83.90	58.64	100.7
Internal Blanket 1	4.88	12.78	3.44	9.86
Internal Blanket 2	9.66	19.41	10.60	19.61
Internal Blanket 3 + 4[a]	7.75	22.10	7.96	20.96
Axial Blanket	1.55	5.52	1.99	3.62
Radial Blanket	5.68	21.21	5.92	22.19

[a] Applies to Configuration A only

TABLE V. Primary and Secondary Control System Assignments

Configuration A			Configuration B		
Row	Primary System	Secondary System	Row	Primary System	Secondary System
4	-	6	5	-	6
7	6	-	8	6	-
11	6	-	9	-	6
13	-	6	11	6	-
Total	12	12	13	-	6
			Total	12	18

TABLE VI. Control Rod Worths

	Configuration A		Configuration B	
	Primary System	Secondary System	Primary System	Secondary System
Total Worth,[a] %Δk	4.28	3.01	4.95	3.81
Stuck Rod Worth, %Δk	0.39	0.27	0.44	0.21
Minimum Worth, %Δk	3.89	2.74	4.51	3.60

[a]-2σ values with unit bias of 1σ = 4%; all primary or secondary rods inserted simultaneously.

TABLE VII. Control Rod Requirements

	Configuration A	Configuration B
Primary Control Requirements, %Δk		
Hot-to-cold shift	0.94 ± 0.17	0.94 ± 0.17
Maximum reactivity fault	0.20	0.44
Excess reactivity at BOEC (nominal + uncertainty)	0.73	2.18
Criticality uncertainty	± 0.30	± 0.30
Fissile tolerance	± 0.30	± 0.30
Total	1.87 ± 0.46	3.56 ± 0.46
Maximum Requirement	2.33	4.02
Primary Control Worths, %Δk		
Total worth	4.65	5.38
-2σ values[a]	-0.37	-0.43
Stuck rod	-0.63	-0.71
Total	3.65	4.24
Secondary Control Requirements, %Δk		
Hot-to-cold shift	0.94 ± 0.17	0.94 ± 0.17
Maximum reactivity fault	0.20	0.44
Total	1.14 ± 0.17	1.38 ± 0.17
Maximum Requirement	1.31	1.55
Secondary Control Worths, %Δk		
Total	3.27	4.14
-2σ values[a]	-0.26	-0.33
Stuck rod	-0.43	-0.34
Total	2.58	3.47

[a]Unity bias, 1σ = 4%

TABLE VIII. Power Distribution

	Configuration A			Configuration B		
	BOL	BOEC	EOEC	BOL	BOEC	EOEC
Inner Core	10.4	9.4	9.3	13.9	13.2	12.6
Middler Core	21.6	19.8	19.2	24.2	23.2	22.2
Outer Core	57.9	54.4	47.1	51.6	48.5	41.9
Total Core	89.9	83.7	75.7	89.7	84.9	76.7
Internal Blanket 1	0.5	0.7	1.4	0.8	1.0	1.9
Internal Blanket 2	1.2	1.8	3.2	1.7	2.5	4.2
Internal Blanket 3 + 4[a]	4.8	7.4	12.1	3.3	4.8	8.5
Total Internal Blanket	6.5	10.0	16.8	5.8	8.3	14.6
Axial Blanket	1.3	1.6	2.4	2.0	2.2	3.3
Radial Blanket	2.1	4.3	4.7	2.4	4.3	4.9

[a]Applies only to configuration A

TABLE IX. (Peak/Average) Power Densitites

	Configuration A			Configuration B		
	BOL	BOEC	EOEC	BOL	BOEC	EOEC
Inner Core[a]	1.37	1.36	1.36	1.42	1.42	1.46
Middle Core[a]	1.41	1.34	1.32	1.41	1.39	1.43
Outer Core[a]	1.52	1.49	1.58	1.57	1.53	1.59
Internal Blanket 1[a]	3.72	3.15	2.79	5.17	3.96	3.47
Internal Blanket 2[a]	2.19	2.21	2.18	2.48	2.28	2.25
Internal Blanket[a] 3 + 4[c]	2.14	2.52	2.33	3.06	2.58	2.34
Axial Blanket[a]	3.66	3.36	3.35	3.65	3.21	3.07
Radial Blanket[a]	6.84	3.93	3.73	7.61	3.94	3.73
Core[b]	1.45	1.45	1.54	1.53	1.49	1.60

[a] zone peak value/zone average value
[b] excluding internal blanket regions
[c] applies to configuration A only

TABLE X. Nominal Peak Nuclear Linear Heat Rating, kW/ft

	Configuration A		Configuration B	
	BOL	EOL, Discharged	BOL	EOL, Discharged
Core	13.4	12.0	13.2	11.4
Internal Blanket	4.8	12.8	5.6	15.3
Radial Blanket	3.1	8.7	3.5	10.7

TABLE XI. Peak Fast Fluxes

	Peak Fast Flux × 10^{-15}			% Total Flux (> 0.1 MeV)			Peak Fast Fluence (× 10^{-23})
	BOL	BOEC	EOEC	BOL	BOEC	EOEC	
			Configuration A				
Core	3.39	3.32	3.26	58.1	58.0	57.6	1.45
Internal Blanket	2.92	2.91	2.91	51.8	52.5	53.6	1.28
Radial Blanket	1.52	1.60	1.61	43.7	46.2	46.9	0.71
			Configuration B				
Core	3.96	3.66	3.57	60.3	58.7	58.1	1.59
Internal Blanket	3.16	3.01	2.94	51.2	52.4	53.4	1.32
Radial Blanket	1.63	1.80	1.98	42.4	46.4	47.1	0.83

TABLE XII. Breeding Ratios

	Configuration A			Configuration B		
	BOL	BOEC	EOEC	BOL	BOEC	EOEC
Inner Core	0.065	0.060	0.062	0.078	0.074	0.076
Middle Core	0.135	0.125	0.128	0.145	0.139	0.143
Outer Core	0.350	0.324	0.307	0.305	0.296	0.277
Total Core	0.550	0.514	0.497	0.628	0.509	0.497
Internal Blanket 1	0.052	0.048	0.052	0.090	0.147	0.159
Internal Blanket 2	0.100	0.092	0.093	0.127	0.116	0.118
Internal Blanket 3 + 4[a]	0.414	0.387	0.378	0.307	0.269	0.268
Total Internal Blanket	0.566	0.527	0.523	0.52	0.458	0.466
Axial Blanket	0.144	0.138	0.139	0.217	0.174	0.178
Radial Blanket	0.227	0.220	0.202	0.260	0.219	0.205
Total Reactor	1.488	1.398	1.361	1.530	1.361	1.346

[a]Applies only to configuration A

TABLE XIII. Breeding Performance

Assembly Residence Time, yrs.					Configuration A	Configuration B
Core	Internal Blanket	Radial Blanket	Out-of-Pile Time, yrs.	Fuel Cycle Losses %	Compound System Doubling Time, yrs.	Compound System Doubling Time, yrs.
2	2	5	1	1	15.7	15.3
2	1	5	1	1	15.1	

TABLE XIV. Configuration A Sodium Void Reactivities[a] from Perturbation Calculations

Region	%Δk		$[b]	
	BOL	EOEC	BOL	EOEC
Core				
Zone 1	0.086	0.135	0.23	0.37
Zone 2	0.181	0.301	0.50	0.82
Zone 3	0.282	0.472	0.77	1.29
Total	0.549	0.908	1.50	2.48
Internal Blanket				
Zone 1	0.006	0.016	0.02	0.04
Zone 2	0.074	0.081	0.20	0.22
Zone 3	0.284	0.307	0.78	0.84
Total	0.364	0.404	1.00	1.10
Axial Blanket	-0.078	-0.074	-0.21	-0.20
Core + Upper Axial Blanket	0.510	0.871	1.40	2.38

[a]for voiding flowing sodium
[b]β_{eff} = 0.00365

TABLE XV. Configuration B Sodium Void Reactivities[a] from Perturbation Calculations

Region	%Δk		$[b]	
	BOL	EOEC	BOL	EOEC
Core				
Zone 1	0.071	0.164	0.19	0.45
Zone 2	0.174	0.347	0.48	0.96
Zone 3	0.108	0.348	0.29	2.38
Total	0.353	0.859	0.98	2.38
Internal Blanket				
Zone 1	-0.087	0.006	-0.24	0.02
Zone 2	0.086	0.112	0.24	0.31
Zone 3	0.162	0.190	0.45	0.52
Total	0.161	0.304	0.45	0.84
Axial Blanket	-0.112	-0.105	-0.31	-0.29
Core + Upper Axial Blanket	0.297	0.806	0.82	2.23

[a]for voiding flowing sodium
[b]β_{eff} = 0.003614

TABLE XVI. Isothermal Doppler Coefficients of Configuration A ($-T \frac{dk}{dT} \times 10^4$)

Region	Sodium - in BOL	Sodium - in EOEC	Sodium - out BOL	Sodium - out EOEC
Core				
Zone 1	6.74	6.47	4.31	4.00
Zone 2	14.42	13.66	7.19	8.83
Zone 3	31.98	25.76	19.78	16.13
Total	53.14	45.89	31.28	28.96
Internal Blanket				
Zone 1	2.10	3.71	1.99	3.17
Zone 2	8.70	10.31	6.10	6.64
Zone 3	28.61	34.27	22.68	25.87
Total	39.41	48.29	30.77	35.68
Radial Blanket	4.99	6.34	4.26	5.41
Axial Blanket	3.10	4.49	3.05	4.16

TABLE XVII. Isothermal Doppler Coefficients of Configuration B ($-T \frac{dk}{dT} \times 10^4$)

Region	Sodium - in BOL	Sodium - in EOEC	Sodium - out BOL	Sodium - out EOEC
Core				
Zone 1	6.82	6.56	4.88	4.36
Zone 2	14.18	14.23	9.69	9.03
Zone 3	29.76	25.27	16.91	14.79
Total	50.72	46.09	31.48	28.18
Internal Blanket				
Zone 1	2.04	3.28	2.17	3.16
Zone 2	8.39	10.47	7.00	7.72
Zone 3	16.06	24.15	13.27	17.82
Total	26.49	37.90	22.44	28.7
Radial Blanket	4.88	7.247	4.09	6.54
Axial Blanket	4.21	6.44	4.07	5.90

TABLE XVIII. Normalized Peak Power Density P(t)/P(0) for Configuration A in a 60¢ Step Insertion into the Outer Core

	Normalized Peak Power Density P(t)/P(0)		
Time, sec	Inner Core	Middle Core	Outer Core
0	1.000	1.000	1.000
0.3339-4	1.067	1.069	1.092
0.4014-4	1.098	1.103	1.131
0.5796-4	1.186	1.192	1.226
0.1293-3	1.492	1.499	1.544
0.6784-3	2.369	2.379	2.448
0.3460-2	2.501	2.511	2.570
0.1136-1	2.486	2.497	2.553
0.9079-1	2.283	2.294	2.345
0.2908	1.970	1.980	2.028
0.4908	1.782	1.791	1.838
0.6908	1.648	1.657	1.706
0.8908	1.548	1.556	1.606
1.0000	1.502	1.511	1.559

TABLE XIX. Normalized Peak Power Density P(t)/P(0) for Configuration A in a 60¢/500 ms Ramp into the Outer Core

	Normalized Peak Power Density P(t)/P(0)		
Time, sec	Inner Core	Middle Core	Outer Core
0	1.000	1.000	1.000
0.3339-4	1.000	1.000	1.000
0.1466	1.191	1.192	1.197
0.2670	1.413	1.413	1.429
0.3811	1.700	1.704	1.733
0.4871	2.056	2.064	2.113
0.5854	1.985	1.994	2.053
0.7854	1.791	1.800	1.856
1.0000	1.650	1.657	1.710

TABLE XX. Normalized Peak Power Density P(t)/P(0) for Configuration B in a 60¢ Step Insertion into the Outer Core

	Normalized Peak Power Density P(t)/P(0)		
Time, sec	Inner Core	Middle Core	Outer Core
0	1.000	1.000	1.000
0.325-4	1.073	1.079	1.101
0.564-4	1.194	1.202	1.235
0.130-3	1.515	1.525	1.564
0.589-3	2.326	2.340	2.388
0.162-2	2.485	2.499	2.549
0.121-1	2.490	2.503	2.553
0.1170	2.210	2.222	2.271
0.3167	1.911	1.922	1.969
0.5167	1.732	1.743	1.788
0.7167	1.608	1.618	1.664
1.0000	1.481	1.489	1.533

TABLE XXI. Normalized Peak Power Density P(t)/P(0) for Configuration B in a 60¢/500 ms Ramp into the Outer Core

	Normalized Peak Power Density P(t)/P(0)		
Time, sec	Inner Core	Middle Core	Outer Core
0	1.000	1.000	1.000
0.1379	1.167	1.169	1.171
0.3340	1.545	1.549	1.568
0.4239	1.804	1.811	1.843
0.5080	2.071	2.083	2.131
0.5940	1.961	1.974	2.025
0.7936	1.768	1.779	1.828
1.0000	1.631	1.642	1.687

TABLE XXII. Inlet and Outlet Temperatures of Configuration A at EOEC

	°K	°F
Core Inlet	586	595
Core Average Outlet	760	908
Core ΔT	174	313
(Core + Radial Blanket) Average Outlet	750	890
(Core + Radial Blanket) ΔT	164	295
Reactor Inlet	586	595
Reactor Outlet	741	875
Reactor ΔT	155	280

TABLE XXIII. Inlet and Outlet Temperatures of Configuration A Orificed for Equal Clad Temperatures at EOEC

Core Inlet	586	595
Core Average Outlet	756	902
Core ΔT	170	307
(Core + Radial Blanket) Average Outlet	750	890
(Core + Radial Blanket) ΔT	164	295
Reactor Inlet	586	595
Reactor Outlet	741	875
Reactor ΔT	155	280

TABLE XXIV. Orificing Scheme of Configuration A

Zone	Number Assemblies	Power MWt	Flow 10^6 lb/hr	Flow/ass'y lb/hr	Avg. ΔT deg. F	Velocity ft/sec
1	156	1265.4	45.140	289361	312.0	25.6
2	126	911.5	31.869	252928	318.3	22.4
3	48	272.0	10.121	210857	299.1	18.7
4	36	122.5	4.511	125333	302.2	17.5
5	108	285.1	11.570	107127	274.3	14.9
6	90	146.4	8.289	92105	196.6	12.8
7	97	75.3	4.608	47508	181.9	6.6
8	222	5.8	0.340	1538	189.6	-
Total	883	3084.0	116.448	--	294.7	----

TABLE XXV. Orificing Scheme of Configuration A
Orificed for Equal Clad Temperature at EOEC

Zone	Number Assemblies	Power MWt	Flow 10^6 lb/hr	Flow/ass'y lb/hr	Avg. ΔT deg. F	Velocity ft/sec
1	138	1123.1	40.854	296043	305.9	26.2
2	132	980.8	34.610	262197	315.4	23.2
3	60	345.0	13.435	223917	285.8	19.8
4	42	139.9	5.002	119095	311.3	16.5
5	180	400.1	17.696	98311	251.6	13.6
6	73	67.3	3.518	48192	212.8	6.7
7	36	22.0	0.945	26250	259.8	3.6
8	222	5.8	0.388	1748	166.3	-
Total	883	3084.0	116.448	------	294.7	----

TABLE XXVI. Nominal Cladding Temperature Axial Profiles For Design Limiting Fuel Pin, Configuration A

Distance From Bottom of Fuel (in.)	Beginning of Life				End of Life			
	Clad o.d. Temperature		Clad M.W. Temperature		Clad o.d. Temperature		Clad M.W. Temperature	
	(°F)	(°K)	(°F)	(°K)	(°F)	(°K)	(°F)	(°K)
8.	597	587	597	587	597	587	597	587
16.	618	599	633	607	615	597	628	604
24.	693	640	718	654	680	633	703	646
32.	790	694	820	711	766	681	792	696
40.	890	750	919	766	853	729	878	743
48.	972	795	993	807	925	769	944	780
56.	1006	814	1007	815	955	786	956	786
64.	1006	814	1007	815	955	786	955	786
72.	1006	814	1006	814	954	785	954	785

TABLE XXVII. 2σ Cladding Temperature Axial Profiles For Design Limiting Fuel Pin, Configuration A

Distance From Bottom of Fuel (in.)	Beginning of Life				End of Life			
	Clad o.d. Temperature		Clad M.W. Temperature		Clad o.d. Temperature		Clad M.W. Temperature	
	(°F)	(°K)	(°F)	(°K)	(°F)	(°K)	(°F)	(°K)
8.	598	588	599	588	597	587	598	588
16.	633	607	665	625	629	605	656	620
24.	733	663	786	692	717	654	763	679
32.	858	732	919	766	826	714	879	744
40.	982	801	1038	832	933	774	983	801
48.	1078	854	1119	877	1017	820	1054	841
56.	1103	868	1105	869	1039	833	1041	834
64.	1102	868	1103	868	1039	833	1039	833
72.	1101	867	1101	867	1038	832	1039	833

TABLE XXVIII. Peak Temperatures for the Assembly With the Hottest Fuel Pin, Configuration A

	Temperature, °F	
	Nominal	2σ
Cladding		
Outer Diameter	1015	1122
Mid Wall	1026	1145
Inner Diameter	1037	1178
Coolant[a]	1003	1098
Duct[a]	863	925

[a]Local peak values within the assembly.

TABLE XXIX. Inlet and Outlet Temperatures of Configuration B

	°K	°F
Core Inlet	586	595
Core Average Outlet	759	907
Core ΔT	173	312
(Core + Radial Blanket) Average Outlet	750	890
(Core + Radial Blanket) ΔT	164	295
Reactor Inlet	586	595
Reactor Outlet	741	875
Reactor ΔT	155	280

TABLE XXX. Inlet and Outlet Temperatures of Configuration B Orificed for Equal Clad Temperatures at EOEC

Core Inlet	586	595
Core Average Outlet	754	898
Core ΔT	168	303
(Core + Radial Blanket) Average Outlet	750	890
(Core + Radial Blanket) ΔT	164	295
Reactor Inlet	586	595
Reactor Outlet	741	875
Reactor ΔT	155	280

TABLE XXXI. Orificing Scheme of Configuration B

Zone	Number Assemblies	Power MWt	Flow 10^6 lb/hr	Flow/ass'y lb/hr	Avg. ΔT deg. F	Velocity ft/sec
1	138	1243.3	43.458	314911	318.4	25.6
2	90	690.7	24.795	275502	310.0	22.4
3	114	791.1	29.032	254666	303.3	20.7
4	84	276.4	11.461	136436	268.4	17.8
5	36	90.7	3.603	100096	280.2	13.1
6	102	137.2	7.567	74185	201.8	9.7
7	97	65.2	3.302	34041	219.7	4.5
8	228	5.4	0.318	1395	189.0	--
Total	889	3300.0	124.604	------	294.7	----

TABLE XXXII. Orificing Scheme of Configuration B Orificed for Equal Clad Temperatures at EOEC

1	132	1205.9	44.876	339969	299.1	27.6
2	66	527.0	18.567	281311	315.9	22.9
3	144	992.2	36.798	255543	300.1	20.8
4	48	169.6	6.521	135848	289.4	17.8
5	72	197.5	7.560	104993	290.7	13.8
6	90	126.0	5.831	64784	240.5	8.5
7	109	76.5	4.069	37329	209.2	4.9
8	228	5.4	0.381	1671	157.7	--
Total	889	3300.0	124.604	------	294.7	----

TABLE XXXIII. 2σ Cladding Temperature Axial Profiles for Design Limiting Fuel Pin, Configuration B

Distance From Bottom of Fuel (in.)	Beginning of Life				End of Life			
	Clad o.d. Temperature		Clad M.W. Temperature		Clad o.d. Temperature		Clad M.W. Temperature	
	(°F)	(°K)	(°F)	(°K)	(°F)	(°K)	(°F)	(°K)
8.	597	587	598	588	597	587	597	587
16.	614	596	630	605	612	595	626	603
24.	735	664	788	693	719	655	767	681
32.	878	743	939	777	845	725	901	756
40.	1016	820	1071	850	968	793	1018	821
48.	1115	875	1151	895	1055	841	1088	860
56.	1118	876	1120	878	1059	844	1060	844
64.	1118	876	1118	876	1059	844	1059	844
72.	1117	876	1118	876	1058	843	1058	843

TABLE XXXIV. Nominal Cladding Temperature Axial Profiles for Design Limiting Fuel Pin, Configuration B

Distance From Bottom of Fuel (in.)	Beginning of Life				End of Life			
	Clad o.d. Temperature		Clad M.W. Temperature		Clad o.d. Temperature		Clad M.W. Temperature	
	(°F)	(°K)	(°F)	(°K)	(°F)	(°K)	(°F)	(°K)
8.	596	586	597	587	596	586	597	587
16.	606	592	614	596	598	588	599	588
24.	694	641	720	655	682	634	706	648
32.	805	703	836	720	781	689	809	705
40.	918	765	946	781	881	754	906	759
48.	1003	813	1022	823	957	787	974	796
56.	1019	821	1020	822	971	795	972	795
64.	1019	821	1020	822	971	795	971	795
72.	1019	821	1019	821	971	795	971	795

TABLE XXXV. Peak Temperatures in the Assembly with the Hottest Fuel Pin, Configuration A

	Temperature, °F	
	Nominal	2σ
Cladding		
Outer Diameter	1028	1140
Mid Wall	1041	1164
Inner Diameter	1054	1188
Coolant[a]	1016	1114
Duct[a]	877	942

[a]Local peak values within the assembly.

TABLE XXXVI. Fuel Pin and Assembly Data

	Configuration A	Configuration B
FUEL PIN		
Fuel Parameters		
Plutonium Content (Pu fissile/Pu+U)		
Fuel form	----------mixed oxide----------	
Fuel smear density, %TD	--------------88---------------	
Cladding Parameters		
Cladding outside diameter, mm (in.)	6.6 (0.260)	6.1 (0.240)
Cladding wall thickness, mm (in.)	0.33 (0.013)	0.30 (0.012)
Cladding material	----------20% CW316SS----------	
Plenum Parameter		
Location	--------------Top--------------	
Length, mm (in.)	1016 (40.0)	914 (36.0)
Volume, cc and in.^{3}		
Bond Type	------------Helium------------	
FUEL ASSEMBLY		
Pins Per Assembly	271	331
Pin Pitch-to-Diameter Ratio	1.197	1.200
Spacer Description		
Wire wrap diameter mm (in.)	1.29 (0.051)	1.22 (0.048)
Spacer pitch, cm (in.)	30.48 (12.0)	30.48 (12.0)
Edge ratio	1.0	1.0
Overall Bundle Length, cm (in.)	279.4 (110.0)	264.2 (104.0)
Lattice Pitch, cm (in.)	14.36 (5.653)	14.62 (5.757)
Duct Inside Flat-to-Flat, cm (in.)	13.24 (5.212)	13.52 (5.323)
Duct Wall Thickness, mm (in.)	2.87 (0.113)	2.97 (0.117)
Interduct Gap, mm (in.)	5.46 (0.215)	5.08 (0.200)
Duct Material	----------20% CW316SS----------	

TABLE XXXVII. Blanket Pin and Assembly Data

	Configuration A	Configuration B
BLANKET PIN		
Fuel Parameters		
Fuel type	------------depleted U--------------	
Plutonium content, Pu/Pu+U	------------0% at BOL--------------	
Fuel Form	--------------oxide---------------	
Fuel smeared density, %T.D.	----------------90-----------------	
Cladding Parameters		
Cladding outside diameter, mm (in.)	10.80 (0.425)	11.02 (0.434)
Cladding wall thickness, mm (in.)	0.33 (0.013)	0.30 (0.012)
Cladding material	------------20% CW316SS------------	
Plenum Parameters		
Location	----------------Top----------------	
Length, mm (in.)	1016 (40.0)	914 (36.0)
Volume cm^3 and $in.^3$		
Bond Type	-------------Helium---------------	
BLANKET ASSEMBLY		
Pins Per Assembly	----------------127----------------	
Pin Pitch-to-Diameter Ratio	1.070	1.070
Spacer Description		
Wire wrap diameter, mm (in.)	0.76 (0.030)	0.76 (0.030)
Spacer pitch, cm (in.)	15.24 (6.0)	15.24 (6.0)
Edge ratio	1.0	1.0
Overall bundle length, cm (in.)	297.4 (110.0)	264.2 (104.0)
Lattic Pitch, cm (in.)	14.36 (5.653)	14.62 (5.757)
Duct Inside Flat-to-Flat, cm (in.)	13.24 (5.212)	13.52 (5.323)
Duct Wall Thickness, mm (in.)	2.87 (0.113)	2.97 (0.117)
Interduct Gap, mm (in.)	5.46 (0.215)	5.08 (0.200)
Duct Material	------------20% CW316SS------------	

TABLE XXXVIII. Control Assembly Compositions

Control rod full in	
B_4C Pellet	0.3174
Void	0.0216
Coolant	0.3323
Structure	0.3287
Control rod full out	
Coolant	0.8842
Structure	0.1158

TABLE XXXIX. Duct Wall Pressure Differential Profile For Design Limiting Duct

Distance Above Bottom of Active Fuel (in.)	Duct Wall Pressure, psi	
	Configuration A	Configuration B
0	61.7	62.0
2	60.4	60.6
4	59.1	59.2
6	57.8	27.8
8	56.5	56.3
10	55.2	54.9
12	53.9	53.5
14	52.6	52.1
16	51.3	50.7
18	50.0	49.3
20	48.7	47.9
22	47.4	46.5
24	46.1	45.1
26	44.8	43.7
28	43.5	42.3
30	42.2	40.8
32	40.9	39.4
34	39.6	38.0
36	38.3	36.6
38	37.0	
40	35.7	

TABLE XL. Fabrication Cost Breakdown

	Core A	Core B
Fixed Overhead, $	19,945	19,945
Variable Overhead, $	13,235	13,235
Assembly, $	13,397	13,397
Pin, $	24,034	28,956
Heavy Metal, $	1,204	1,125
Fissionable Material, $	10,771	10,118
Pellet, $	1,211	1,442
Steel, $	11,957	13,129
Axial Blanket, $	1,729	1,918
10% Change, $	9,748	10,327
Total Cost, $		
$/Assembly	107,232	113,592
$/kg Heavy Metal	1,675	1,900
$/Pin	396	343

These costs should be used only for comparing cores A and B. Actual costs are expected to be significantly lower.

REF A

TABLE XLI. Fuel Cycle Costs of Configuration A

	RESIDENCE TIME (YRS)	FABRICATION COST ($/KG)	REPROCESSING COST ($/KG)	USAGE FACTOR (KG/KWH)
ZONE 1	0.20002E 01	0.16750E 04	0.59500E 03	0.16596E-02
ZONE 2	0.20002E 01	0.16750E 04	0.59500E 03	0.0
ZONE 3	0.20002E 01	0.16750E 04	0.59500E 03	0.0
ZONE 4	0.20002E 01	0.0	0.59500E 03	0.12810E-02
ZONE 5	0.20002E 01	0.0	0.59500E 03	0.0
ZONE 6	0.20002E 01	0.0	0.59500E 03	0.0
ZONE 7	0.20002E 01	0.25000E 03	0.59500E 03	0.19581E-02
ZONE 8	0.50005E 01	0.25000E 03	0.59500E 03	0.86775E-03
ZONE 9	0.60006E 01	0.25000E 03	0.59500E 03	0.0

	FABRICATION (MILL/KWH)	REPROCESSING (MILL/KWH)	FABRICATION CC (MILL/KWH)	REPROCESSING CC (MILL/KWH)
ZONE 1	0.27799E 01	0.98748E 00	0.43257E 00	-0.70101E-01
ZONE 2	0.0	0.0	0.0	0.0
ZONE 3	0.0	0.0	0.0	0.0
ZONE 4	0.0	0.76222E 00	0.0	-0.54110E-01
ZONE 5	0.0	0.0	0.0	0.0
ZONE 6	0.0	0.0	0.0	0.0
ZONE 7	0.48952E 00	0.11651E 01	0.76173E-01	-0.82707E-01
ZONE 8	0.21694E 00	0.51631E 00	0.61209E-01	-0.87926E-01
ZONE 9	0.0	0.0	0.0	0.0

CARRY CHARGE ON PU INVENTORY	=	0.71846037E 01
REVENUE	=	-0.48222046E 01
CHARGE ON REVENUE	=	0.17434245E 00
LOSSES	=	0.29779458E 00
CARRY CHARGE ON LOSSES	=	-0.51820204E-02
CREDIT FOR SALE AT PLANT EOL	=	-0.62980794E 00
TOTAL FUEL CYCLE COST	=	0.91920710E 01

REF B

TABLE XLII. Fuel Cycle Costs of Configuration B

	RESIDENCE TIME (YRS)	FABRICATION COST ($/KG)	REPROCESSING COST ($/KG)	USAGE FACTOR (KG/KWH)
ZONE 1	0.20002E 01	0.19000E 04	0.59500E 03	0.16078E-02
ZONE 2	0.20002E 01	0.19000E 04	0.59500E 03	0.0
ZONE 3	0.20002E 01	0.19000E 04	0.59500E 03	0.0
ZONE 4	0.20002E 01	0.0	0.59500E 03	0.14735E-02
ZONE 5	0.20002E 01	0.0	0.59500E 03	0.0
ZONE 6	0.20002E 01	0.0	0.59500E 03	0.0
ZONE 7	0.20002E 01	0.25000E 03	0.59500E 03	0.18748E-02
ZONE 8	0.50005E 01	0.25000E 03	0.59500E 03	0.89960E-03
ZONE 9	0.60006E 01	0.25000E 03	0.59500E 03	0.0

	FABRICATION (MILL/KWH)	REPROCESSING (MILL/KWH)	FABRICATION CC (MILL/KWH)	REPROCESSING CC (MILL/KWH)
ZONE 1	0.30548E 01	0.95664E 00	0.47535E 00	-0.67911E-01
ZONE 2	0.0	0.0	0.0	0.0
ZONE 3	0.0	0.0	0.0	0.0
ZONE 4	0.0	0.87672E 00	0.0	-0.62238E-01
ZONE 5	0.0	0.0	0.0	0.0
ZONE 6	0.0	0.0	0.0	0.0
ZONE 7	0.46871E 00	0.11155E 01	0.72935E-01	-0.79191E-01
ZONE 8	0.22495E 00	0.53538E 00	0.63469E-01	-0.91173E-01
ZONE 9	0.0	0.0	0.0	0.0

CARRY CHARGE ON PU INVENTORY	=	0.70920153E 01
REVENUE	=	-0.43552718E 01
CHARGE ON REVENUE	=	0.15073760E 00
LOSSES	=	0.29304630E 00
CARRY CHARGE ON LOSSES	=	-0.50840115E-02
CREDIT FOR SALE AT PLANT EOL	=	-0.81420922E 00
TOTAL FUEL CYCLE COST	=	0.99311924E 01